

POLITECNICO DI TORINO

**DIPARTIMENTO DI
INGEGNERIA MECCANICA E
AEROSPAZIALE**

TESI DI LAUREA MAGISTRALE



**Design and verification of the Thermal Control
System for a CubeSat equipped with a miniaturized
electric propulsion system.**

RELATORI

Prof. Sabrina Corpino

Ing. Fabrizio Stesina

Dott. Daniele Calvi

CANDIDATO

Jacopo Garrone

APRILE 2021

CONTENTS

CONTENTS	3
LIST OF FIGURE	5
LIST OF TABLES	7
ABBREVIATIONS	8
1. INTRODUCTION	10
1.1 CONTEXT	10
1.1.1. <i>Technology Readiness Level</i>	11
1.1.2. <i>Thermal Control System necessity</i>	12
1.2 MOTIVATION AND OBJECTIVES	13
2. THERMAL PROBLEM	14
2.1 SPACECRAFT THERMAL ENVIRONMENT	14
2.1.1 <i>Launch thermal environment</i>	16
2.1.2 <i>In-orbit thermal environment</i>	17
2.1.2.1 Direct sun	17
2.1.2.2 Planetary Albedo	18
2.1.2.3 Planetary IR radiation	19
2.1.3 <i>Interplanetary mission thermal environment</i>	20
3. THERMAL CONTROL SYSTEM FOR CUBESAT	21
3.1 PASSIVE CONTROL	21
3.1.1 <i>Films, Coatings, and Thermal Insulation</i>	22
3.1.2 <i>Thermal straps</i>	23
3.1.3 <i>Thermal louvers</i>	24
3.1.4 <i>Deployable radiators and solar arrays</i>	24
3.1.5 <i>Heat pipes</i>	25
3.1.6 <i>Thermal Storage Units</i>	26
3.2 ACTIVE CONTROL	27
3.2.1 <i>Electrical heaters</i>	28
3.2.2 <i>Pumped fluid loop</i>	28
4. THERMAL ANALYSIS	31
4.1 THERMAL MODELING FUNDAMENTAL	34
4.1.1 <i>Nodes</i>	34
4.1.2 <i>Conductors</i>	36
4.2 THERMAL ANALYSIS CODES	38
4.2.1 <i>Finite-Difference method (FDM)</i>	38
4.2.1.1 SINDA	40
4.2.2 <i>Finite-Element method (FEM)</i>	41
4.2.3 <i>FDM vs. FEM for thermal analysis</i>	42

4.3	MODELING WITH THERMAL DESKTOP	43
5.	CASE STUDY 1: ESAUPROP-2.....	46
5.2	ESA-uPROP 2: PROJECT OVERVIEW	46
5.1.1	<i>Test Platform Architecture</i>	47
5.1.1.1	Service module.....	49
5.1.1.2	Electrical Propulsion System (ePS).....	51
5.1.2	<i>CTP AIV Plan</i>	52
5.2	ESA-uPROP 2 THERMAL MODEL AND SIMULATION	54
5.2.1	<i>CTP Thermal environment</i>	54
5.2.2	<i>Optical and thermophysical properties</i>	57
5.2.3	<i>Thermal Desktop model definition</i>	59
5.2.3.1	Structure	61
5.2.3.2	Avionics.....	62
5.2.3.3	Battery packs.....	63
5.2.3.4	Electrical Propulsion System	64
5.2.3.5	Thermal loads definition	65
5.2.4	<i>Thermal control system</i>	69
5.2.5	<i>Model simulation and validation</i>	74
5.2.5.1	Thermal analysis set-up	74
5.2.5.2	Thermal model validation	76
5.3	RESULTS AND DISCUSSION.....	83
6.	CASE STUDY 2 - ESAUPROP-3 TCS DESIGN	88
6.1	THERMAL MODEL DEFINITION	89
6.1.1	<i>CTP environment, thermophysical and optical properties definition</i>	89
6.1.1	<i>Thermal Desktop model</i>	93
6.2	THERMAL CONTROL SYSTEM DESIGN	97
6.2.1	<i>Thermal parametric analysis</i>	98
	Variable parameters	98
6.2.2	<i>CTP thermal assessment</i>	100
6.2.2.1	Configuration	100
6.2.2.2	Efficiencies	105
6.2.3	<i>Thermal control system analysis</i>	108
6.2.3.1	Thermal strap solution.....	109
6.2.3.2	Thermal gap filler pad solution.....	113
6.3	RESULTS AND DISCUSSION.....	118
7.	CONCLUSION.....	121
8.	REFERENCIES.....	123

LIST OF FIGURE

FIGURE 1:TECNOLOGY READINESS LEVEL SUBDIVISION. CREDIT: NASA.....	11
FIGURE 2: TYPICAL IN-ORBIT THERMAL ENVIRONMENT (CREDITS: DAVID G. GILMORE 2002)	15
FIGURE 3: SOLAR AND ROOM TEMPERATURE BODY SPECTRAL DISTRIBUTION (CREDITS: J. R. WERTZ,).....	17
FIGURE 4: SOLAR FLUX AS A FUNCTION OF DISTANCE FROM THE SUN. (CREDITS: DAVID G. GILMORE, 2002)	18
FIGURE 5: COPPER BRAIDS THERMAL STRAPS	23
FIGURE 6:SCHEMATIC HEAT PIPE (CREDITS: D. G. GILMORE, SPACECRAFT THERMAL CONTROL).....	25
FIGURE 7: FLAT HEAT PIPE FOR CUBESAT	25
FIGURE 8: THERMAL STORAGE UNIT IN SANDWICH TCS SYSTEM (CREDITS: D. G. GILMORE, SPACECRAFT THERMAL CONTROL	27
FIGURE 9: PUMPED FLUID LOOPS SCHEME 1 – HEAT EXCHANGER; 2 – PUMP; 3 – HEAT SOURCE	29
FIGURE 10: THERMAL ANALYSIS IN THE CONTEXT OF A SPACE PROJECT (CREDITS: ECSS-E-HB-31-03A).....	31
FIGURE 11: MODELLING PROCESS (CREDITS: ECSS-E-HB-31-03A).....	32
FIGURE 12: NODALIZATION (CREDITS: NASA, "THERMAL NETWORK MODELLING HANDBOOK").....	35
FIGURE 13:THERMAL NETWORK ELECTRICAL SCHEME (CREDITS: NASA, "THERMAL NETWORK MODELLING HANDBOOK") .	37
FIGURE 14: CONDUCTIVE AND RADIATIVE CONDUCTORS (CREDITS: NASA, "THERMAL NETWORK MODELLING HANDBOOK")	37
FIGURE 15: MODEL BROWSER IN THERMAL DESKTOP	44
FIGURE 16: CTP INTERNAL CONFIGURATION	47
FIGURE 17: CTP AVIONICS MODULE AND BATTERY PACKS	51
FIGURE 18: VACUUM CHAMBER MODEL	56
FIGURE 19:OPTICAL PROPERTIES DATABASE	60
FIGURE 20:THERMOPHYSICAL PROPERTIES DATABASE	60
FIGURE 21: EXTERNAL STRUCTURE AND BULKHEAD MODELS	61
FIGURE 22: CTP PRIMARY AND SECONDARY STRUCTURE	62
FIGURE 23: CTP MODEL WITH STRUCTURE AND AVIONICS MODULE	63
FIGURE 24: CTP MODEL WITH STRUCTURE, AVIONICS AND BATTERY PACKS	64
FIGURE 25: REGULUS EPS MODEL DETAIL	65
FIGURE 26: HPMS BOARD WITH TEMPERATURE SENSOR IN PROXIMITY OF POWER DIODES	67
FIGURE 27: BATTERIES, AVIONICS AND EPS THERMAL LOADS.....	68
FIGURE 28: STRUCTURE THERMAL LOADS.....	69
FIGURE 29: THERMAL DESKTOP SIMULATION OF STEADY STATE.....	70
FIGURE 30: HPMS TEST IN CLEAN ROOM WITH NO TCS	70
FIGURE 31: ESA-UProp 2 THERMAL CONTROL SYSTEM	71
FIGURE 32: HPMS TEST IN CLEAN ROOM.....	72
FIGURE 33: THERMAL CONTROL SYSTEM IN THERMAL DESKTOP	73
FIGURE 34: THERMAL DESKTOP SIMULATION OF STEADY STATE WITH THERMAL CONTROL SYSTEM	74
FIGURE 35: ELECTRICAL MISSION PROFILE	78
FIGURE 36: PS BATTERIES TEMPERATURES.....	79
FIGURE 37: SERVICE MODULE TEMPERATURE	79
FIGURE 38: PS MODULE TEMPERATURE	80
FIGURE 39: BURST PHASE TEST AND SIMULATION DATA	81
FIGURE 42: THERMAL STRAP NODES TEMPERATURE.....	87

FIGURE 40: THERMAL DESKTOP SIMULATION OF WORST-CASE MISSION	87
FIGURE 41: HPMS NODES TEMPERATURE	87
FIGURE 43: VACUUM CHAMBER CONTAINING CTP IN THERMAL DESKTOP	90
FIGURE 44: EPS INTEGRATED IN CTP STRUCTURE	94
FIGURE 45: INTEGRATION OF BATTERY PACKS ON-BOARD CTP	95
FIGURE 46: AVIONICS BOARDS DISPOSITION	96
FIGURE 47: AVIONICS MODULE INTEGRATION	96
FIGURE 48: EPIS POWER IN FR4, EPS IN ALUMINIUM	101
FIGURE 49: TWO-LAYERS ALUMINIUM/FR4 EPS AND EPIS POWER BOARDS	101
FIGURE 50: SINGLE ALUMINIUM POWER BOARD	102
FIGURE 51: TEMPERATURE TREND OF THE DL BOARD AS THE DISTANCE FROM EPIS POWER VARIES	103
FIGURE 52: TEMPERATURE TREND OF THE CDH BOARD AS THE DISTANCE FROM EPS VARIES	104
FIGURE 53: EPS HUB EFFICIENCY VARIATION	105
FIGURE 54: EPIS POWER DCDC EFFICIENCY VARIATION	106
FIGURE 55: BATTERY PACKS TEMPERATURES IN BEST THERMALLY CASE	107
FIGURE 56: BATTERY PACKS TEMPERATURES IN WORST THERMALLY CASE	108
FIGURE 57: COMPARISON OF SIMULATION RESULTS: CTP WITHOUT TSS VS. CTP WITH TSS	110
FIGURE 58: TWO-LAYERS POWER BOARDS WITH THERMAL STRAP SYSTEMS	111
FIGURE 59: WORST HEAT LOAD CONDITION - EPIS POWER TEMPERATURE TREND	112
FIGURE 60: ELECTRONICS POWER BOARDS EPS AND EPIS POWER IN CONTACT WITH STRUCTURE PANEL	114
FIGURE 61: THERMAL GAP FILLER PADS	115
FIGURE 62: AVIONICS BOARDS TEMPERATURES WITH THERMAL PADS IMPLEMENTATION	116
FIGURE 63: WORST CASE SCENARIO WITH 80x80MM, 1.5MM, 1.6W/MK GAP FILLER	118
FIGURE 64: DATA LOGGER AND COMMAND AND DATA HANDLING BOARDS TEMPERATURE TRENDS	118
FIGURE 65: AVIONICS MODULE CONFIGURATION WITH ALUMINIUM PLATE IMPLEMENTATION	120
FIGURE 66: AVIONICS MODULE - BOARDS DISTANCES	120

LIST OF TABLES

TABLE 1: ELECTRICAL-THERMAL ANALOGY.....	34
TABLE 2: REGULUS EPS PERFORMANCE	52
TABLE 3: REGULUS ELECTRICAL PROPULSION SYSTEM BY T4I	52
TABLE 4: ESA-PROP2 MODEL - THERMOPHYSICAL PROPERTIES	58
TABLE 5: ESA-PROP2 MODEL - OPTICAL PROPERTIES	58
TABLE 6: CTP BURST MODE POWER BUDGET	75
TABLE 7: TEST PROCEDURE DESCRIPTION	78
TABLE 8: ESA-UPROP 3 MODEL - THERMOPHYSICAL PROPERTIES.....	92
TABLE 9: ESA-UPROP 3 MODEL - OPTICAL PROPERTIES	93
TABLE 10: VARIABLE PARAMETERS	100

ABBREVIATIONS

- ADC:** Analogue to Digital Converters
- AIV:** Assembly Integration and Verification
- AU:** Astronomical Unit
- AV:** Avionics
- CAD:** Computer Aided Design
- CDS:** CubeSat Design Standard
- COMSYS:** Communication System
- COTS:** Commercial Off The Shelf
- C&DH:** Command and Data Handling
- CPU:** Central Processing Unit
- CTP:** CubeSat Test Platform
- DL:** Data Logger
- ECSS:** European Collaboration for Space Standardization
- EP:** Electric Propulsion
- EPIS:** Electric Propulsion Interface System
- EPL:** Electric Propulsion Laboratory
- EPS:** Electric Power System
- ePS:** Electric Propulsion System
- ESA:** European Space Agency
- ESTEC:** European Space Research and Technology Centre
- FDM:** Finite Difference Method
- FDIR:** Failure Detection Isolation and Recovery
- FEM:** Finite Element Method
- FEP:** Fluorinated Ethylene Propylene
- GF:** Gap Filler
- GEO:** Geostationary Earth Orbit

GMM: Geometric Mathematical Model

GSE: Ground Support Equipment

GSS: Ground Support System

GUI: Graphic User Interface

HPMS: High-Power Management System

IR: Infrared Radiation

LEO: Low Earth Orbit

LISN: Line Impedance Stabilization Network

MLI: Multi-Layer Insulation

MUX: Multiplexer

MWR: weighted residual methods

NASA: National Aeronautics and Space Administration

PCB: Printed Circuit Board

PCM: Phase Change Materials

PFS: Propellant Feed System

PGS: Pyrolytic Graphite Sheets

PPU: Power Processing Unit

PS: Propulsion Systems

RF: Radio Frequency

RSSI: Received Signal Strength Indicator

SINDA: Systems Improved Numerical Differencing Analyzer

SPF: Small Plasma Facility

TCS: Thermal Control System

TMM: Thermal Mathematical Model

TRL: Technology Readiness Level

TS: Thermal Strap

1. INTRODUCTION

1.1 CONTEXT

In recent years, the use of nano-satellites for space missions has been subject to significant growth, with a continuously growing number of launches exceeding 300 per year. Nanosatellites today, in addition to academic educational or technological demonstration missions, are used in numerous other types of space missions with scientific goals, observation of the earth or other planets, or communication purposes. In particular, scientific community and space industry are dedicating more and more interest to CubeSat technology in the last years, due to their low cost and fast delivery. The CubeSats are based on a modular technology, being spacecraft composed of multiples of standardized dimensions units $10 \times 10 \times 10 \text{ cm}$, hence the name "Cube". The main feature of these standard-sized spacecraft is the use of highly integrated and highly modular on-board systems, also thanks to the use of Commercial Off The Shelf (COTS) equipment. The dimensions standardization of these particular nanosatellites also has the advantage of allowing easier accommodation of the CubeSats inside the launcher for placing in orbit. In fact, standard containers are used, which ensure safety for the launcher and other transported payloads. These solutions, called CubeSat Deployer, by reducing the complexity of the accommodation lead to a time reduction and therefore to an increase in launch opportunities. Furthermore, the reduced complexity of developing specific containment systems for the launch phase generates a reduction in the costs of this phase. The performances and operational capabilities of nanosatellites, and in particular of CubeSats, continue to evolve, affecting an increasingly large number of technological aspects such as: pointing, propulsion, and communications. These increasingly performing capabilities have made it possible in recent years to use these satellites for carrying out missions characterized by constellations for communication networks, or by interplanetary missions generally in combination with larger spacecrafts or as stand-alone platforms. The considerable reduction in the design, development, production, and verification times of CubeSat systems generally allows reaching the operational in-flight mission within a couple of years. This unprecedented opportunity, together with the considerably lower entry-level costs, have led to increasing interest from space agencies, universities and private companies [1], [2].

One of the most ambitious challenges, and on which a great interest is pouring into the capabilities of the future generation of CubeSat, is to use miniaturized electric

propulsion systems on board spacecraft. This would allow to provide CubeSats to perform manoeuvres to control the trajectory, orbit and attitude [1].

1.1.1. Technology Readiness Level

Lately, with regard to technologies adopted in nanosatellite missions, considerable progress has been made concerning the level of technological advancement. The greatest challenge has been, and still is, the miniaturization of existing technologies, and in many cases used on board medium / large spacecraft with already high levels of TRL. The margin for improvement in the field of nanosatellites is still wide, although considerable progress has already been made [3]. Through a continuous process of improvement of the technology in use on satellites, and of the confidence to use it, this category of spacecraft will acquire more and more importance, being used for increasingly varied and complex functions.

The ESA-uProp project of the CubeSat Team of the Politecnico di Torino aims to advance the knowledge and technological readiness of miniaturized electric propulsion systems for nanosatellites. These systems are being developed in an increasingly in-depth manner by various entities in the space sector, but their integration and experimentation with satellites in relevant environments is necessary to evaluate the mutual influence with the host spacecraft. The use of CubeSat-like test platforms inside vacuum chambers can lead to a clear improvement in the knowledge of these technologies, allowing to reach a TRL 6, according to the subdivision of the levels shown in the following image [1], [3].

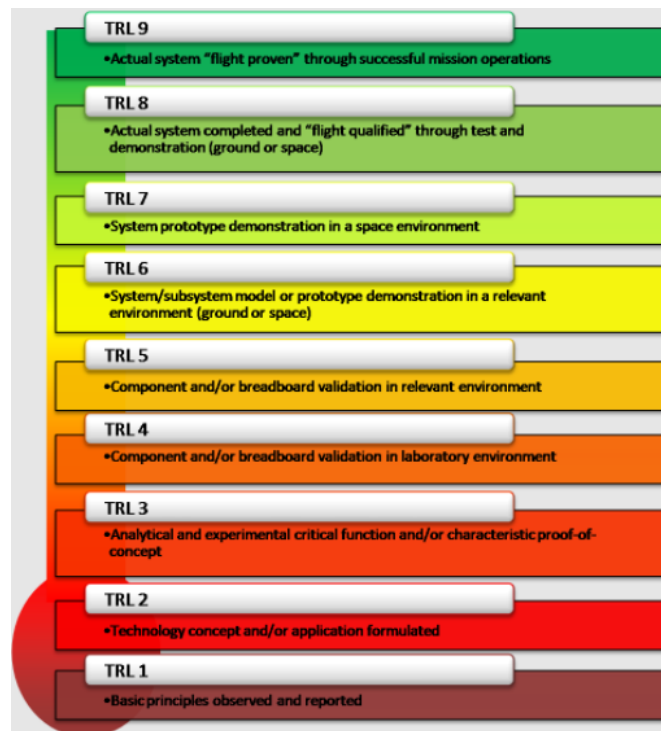


Figure 1:Technology Readiness Level subdivision. Credit: NASA

As a consequence of the attempt to integrate these propulsion systems on CubeSat, the development of thermal control systems suitable for guaranteeing the operation of satellites capable of managing increasing electrical power levels also gains importance. Technologies already widely developed and known for large-scale applications, must be adapted and optimized to work also on small systems, taking into account the most important drivers in these applications: low cost and fast development.

1.1.2. Thermal Control System necessity

Whether in LEO, in an interplanetary mission, or inside a ground test facility, the use of thermal management techniques, passive or active, allow compliance with the operating or survival temperature limits of on-board subsystems and components, especially the most thermally critical ones. The on-board implementation of increasingly performing payloads, including the possibility of integrating electric propulsion systems, has the disadvantage of high heat dissipations inside the spacecraft. These problems, combined with the fact that the nanosatellites external surfaces have small dimensions, makes external heat dissipation complex and limited. Therefore, an adequate development of the thermal control system for maintaining temperatures within the ranges indicated by the requirements is of great importance. To optimize TCS functionality and reduce project times and costs, virtual thermal models are developed, which are necessary to perform more or less detailed thermal analyses, depending on the phase of the project. “The capability of performing effective and reliable thermal analyses represents therefore a fundamental role in the design of the TCS and of the whole satellite” [4].

1.2 MOTIVATION AND OBJECTIVES

The reasons that led to the fulfilment of this thesis derive mainly from the need to define a path for thermal control on board nanosatellite spacecraft, in particular CubeSat, which implement not yet high readiness level technologies, such as miniaturized electric propulsion systems. As part of the ESA-uProp project, the goal is to evaluate the effects that such an electrical power system has on the platform that hosts it, and consequently study a method for managing the heat generated on board, but also from the external environment of the orbit of the spacecraft.

The objectives driving this thesis work were:

- The analysis of the thermal environment in which the CubeSats operate, and of the related criticalities that may arise from it, or from aspects related to the mission to be carried out.
- The collection of information about the state of the art of TCS used on nanosatellites, their peculiarities and the different configurations in which they are used. For both passive and active solutions.
- The development of mathematical thermal models for the analysis of the thermal problem, and the use of these analyses, through commercial software, for the definition of thermal control systems on CubeSats. Verification of both the models and the control solutions adopted, through experimentation in relevant environments.

2. THERMAL PROBLEM

All space missions require the use of techniques and systems dedicated to controlling the thermal environment on board the spacecraft. This is due to the fact that the environments in which the spacecrafts operate, together with the presence of on-board devices that dissipate energy in form of heat, produce thermal conditions that are difficult to tolerate by various components. “Because a generic thermal control system capable of maintaining spacecraft temperatures in all environments would be prohibitively heavy and expensive, it is generally more cost effective and practical to custom-tailor a thermal design to each spacecraft and its mission environment” [5].

CubeSats, typically, are employed in Low Earth Orbit missions, and require a thermal control characterized by simplicity of development, implementation and low cost, suitable for the external environment and their relatively low on-board power. However, the use of on-board systems characterized by ever greater electrical powers, and the use of these particular nanosatellites for missions no longer only in LEO, generates thermal problems that must be solved by managing to reconcile the necessary performance required with the main drivers. of the CubeSat missions.

The thermal engineers who design the spacecraft thermal control system consider the different thermal conditions in which the system is operating during its operational life. In particular, the thermal analysis process, which is iterated in the different mission phases to obtain increasingly reliable and accurate results, is particularly important for the worst cases, hot and cold. In fact, these are the situations that determine the sizing of the TCS and its components. To identify these extreme cases, it is necessary to consider the various operating modes of the spacecraft, and the net between the heat dissipated by the on-board components of the system, the heat flow dissipated towards the outside and the incoming one coming from environmental thermal loads.

2.1 SPACECRAFT THERMAL ENVIRONMENT

When describing the space environment related to a specific mission, it includes all the environmental conditions to which the spacecraft is subjected: starting from the typical ones found on the terrestrial ground, during the initial phases of the project, then passing through the environment characteristic of the launch phase to that of the outer space of the Earth's orbit or of interplanetary missions. Spacecraft must be designed to survive and operate in each of the different environments to which it will

be subjected, whether it is empty space, whether it is in a planetary atmosphere, terrestrial or otherwise [6].

The phases of Assembly, Integration and Verification, performed on the ground, are characterized by the phenomena of convection with the surrounding air, conduction with objects in contact and radiation. Convection is generally only present in these early stages on the ground, unless the mission involves operations within the atmospheres of other planets.

The launch phase requires the spacecraft to be contained in the cargo bay and protected by the launcher's fairing. During the ascent, the strong friction with the atmosphere, together with external compression phenomena, generates a flow of heat which is radiated from the internal fairing wall to the transported systems.

Once placed into orbit, typically the external thermal loads acting on the spacecraft are: sunlight radiated directly from the sun, sunlight reflected from a celestial body (albedo), or it is the energy emitted by the celestial body itself in the form of infrared waves.

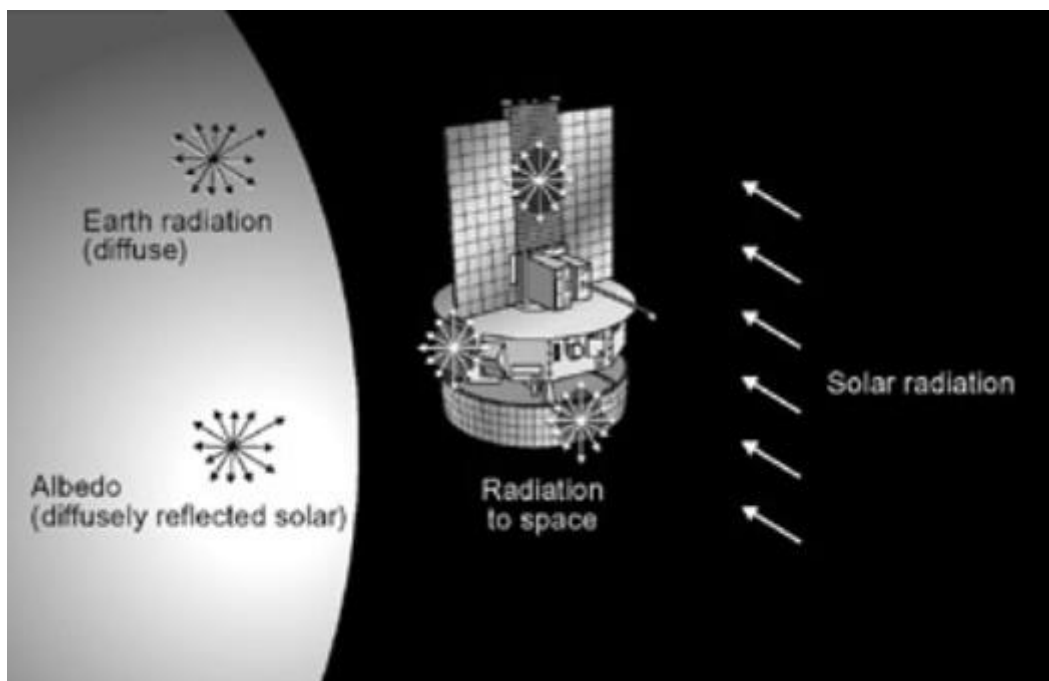


Figure 2: typical in-orbit thermal environment (Credits: David G. Gilmore 2002)

Knowledge of the thermal environment to which the spacecraft is subjected is fundamental for the design of the thermal control system. Generally, once the temperature requirements of the different components and devices of the system have been defined, for the initial mission phases on the ground, which include the integration and test activities, and also for launch phase, compliance with the thermal limits is guaranteed by limiting the exposure of the system and its components to

hazardous environments, which can be particularly severe from a thermal point of view (for example the thermal environment during launch). Another method adopted, especially for ground operations, is to actively control the environment in which the spacecraft operates.

The TCS is designed with the aim of respecting the operating temperature ranges during the phase of longer duration, that is the operational one in orbit. The thermal control provides that the thermal equilibrium, that is generated between the heat absorbed by the spacecraft and that dissipated inside it, and possibly radiated to the outside, allows to respect the temperature limits imposed by the requirements. [5]

2.1.1 Launch thermal environment

As already mentioned, the thermal loads generated during the launch phase are due to aerodynamic effects on the launcher's fairing. At the same speed, these effects are greatest in the lower atmosphere. The heat generated by the external fairing walls is transported inside and diffused to the payloads on board. Once the designated altitude is reached, usually around 115 km of altitude, the fairing releases, allowing a decrease in the mass carried by the launcher. This, however, implies that the spacecraft inside the cargo bay is exposed to atmospheric gas molecules still present at the aforementioned altitude. The high-speed contact with these molecules generates molecular heating, and this must be taken into account for the study of the thermal environment.

Launch is one of the phases with the greatest variation in thermal loads. It can be considered that, during launch, the average thermal load per unit of surface is $250 \frac{W}{m^2}$. Furthermore, it is among the mission phases with the shortest duration, and therefore thermal control solutions are required that do not seriously affect the mass and power budgets and the costs of the entire mission.

Usually, the CubeSats are inserted in standard dispensers that have the function of interface between the satellite and the launcher. In addition to these systems, sometimes, CubeSats can be integrated into large-scale spacecraft and be released only once the desired orbit or spatial position has been reached, or are released directly from the International Space Station. In these cases, the thermal loads to which they are subjected during the launch phase will be lower, with the systems in which they are contained providing adequate thermal protection. [6]

2.1.2 In-orbit thermal environment

The space environment depends on whether the particular mission is Earth-orbiting or deep space. For a spacecraft orbiting the Earth (or any other planet or moon), the main sources of environmental heating are solar radiation, both direct and reflected by the planet, and the infrared energy emitted by the planet itself [6].

2.1.2.1 Direct sun

For spacecraft orbiting the earth or other celestial bodies in the solar system, with the exception of those furthest from the centre, direct solar radiation is among the most intense environmental thermal loads. Since the Earth's orbit around the sun is not circular, but elliptical, the thermal intensity will vary, and it also depends on numerous other factors (such as solar activity) that can influence it. It is estimated that the variation is only about $\pm 3,5\%$ with respect to the average value between the aphelion and the perihelion of the orbit, and therefore as a first approximation we consider a constant average intensity of $1367 \frac{W}{m^2}$ which is the intensity related to the 1 AU distance. This average value is also called the solar constant G_s . The intensity of solar radiation is also a function of the wavelength, and is distributed approximately in 7% ultraviolet, 46% visible, 47% IR with short wavelength [5]. The variation as a function of the wavelength is shown in the following figure.

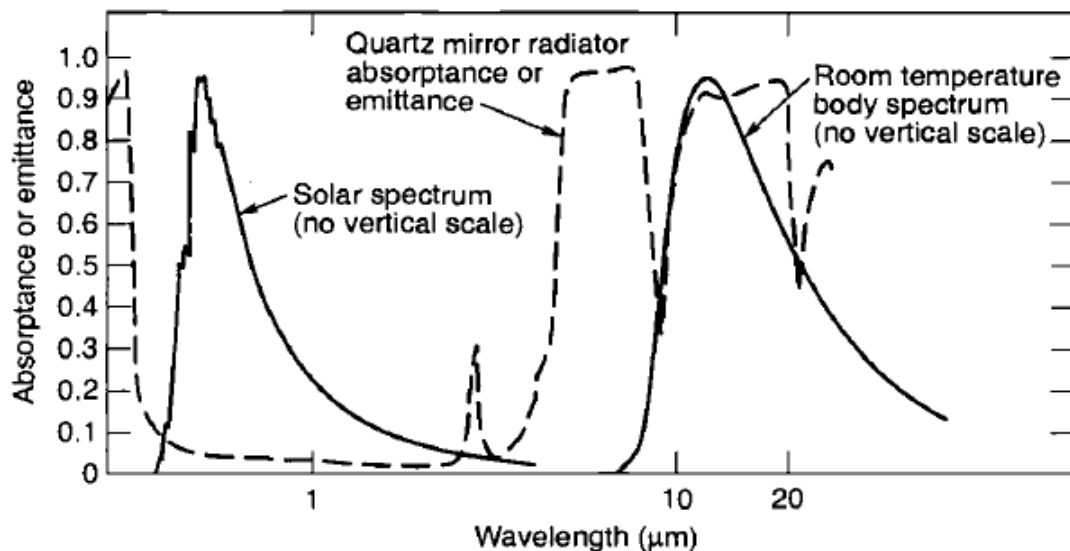


Figure 3: Solar and room temperature body spectral distribution (Credits: J. R. Wertz,)

The fact that the wavelength of the solar infrared spectrum is short is important for the choice of surface treatments, finishes and coatings of the spacecraft external surfaces, which allows to have a high reflectivity in that spectrum range, while

maintaining, in the long-wavelength infrared spectrum (i.e., those emitted by the spacecraft) a high IR emissivity.

Analysing the thermal environment of interplanetary missions, we can see how the intensity of solar radiation decreases considering planets increasingly distant from the sun, as shown in the figure.

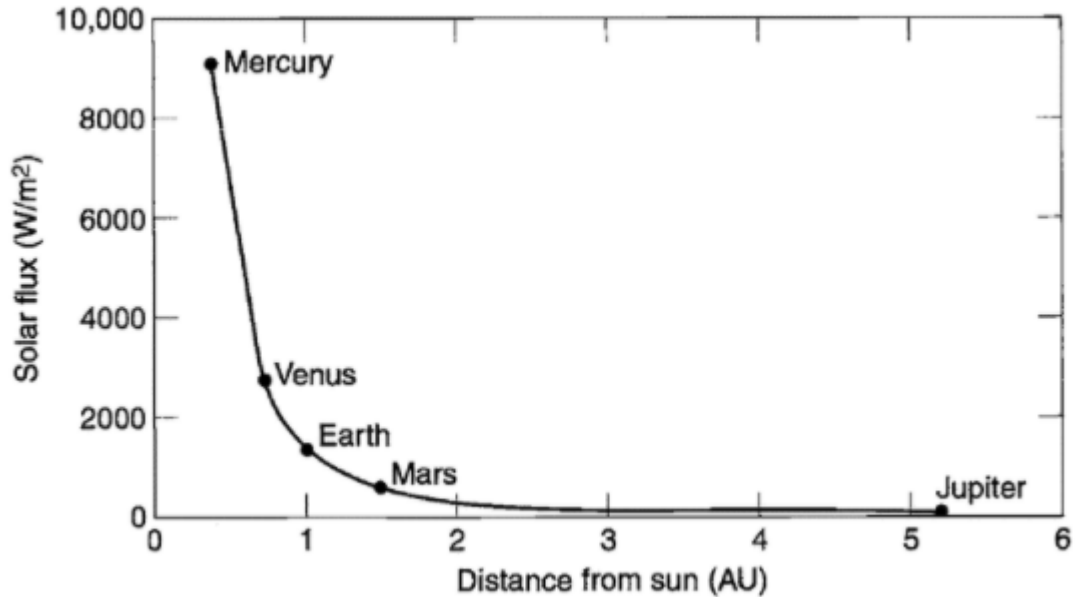


Figure 4: Solar flux as a function of distance from the sun. (Credits: David G. Gilmore, 2002)

2.1.2.2 Planetary Albedo

Another effect that can affect the thermal environment in which a spacecraft orbiting a planet operates is the albedo. Albedo is the part of the solar radiation incident upon the planet which is reflected or scattered by the planet surface and atmosphere (if any) [6]. The albedo coefficient α is defined as the ratio between the light of the sun reflected by the planet and the total light that hits it. Approximating, it can be considered that the reflected radiation has the same spectral distribution as that emitted directly by the sun. This may not be true, as by hitting the planet's surface, some materials can absorb part of the spectrum, reflecting the rest.

According to ECSS-E-ST-10-04C, the average value of the albedo coefficient for the Earth is $\alpha = 0.3$. However, the variability of this value is very high on our planet. In fact, the albedo, due to reflectivity, is greater on continental areas, and is lower above the oceans [0.05 – 0.10]. Cloud coverage of the globe causes an increase in the local albedo coefficient (about 0.8), while the higher the solar elevation angle to the ground, the lower the solar reflection. At the poles, the presence of ice and snow

considerably increases the reflection of sunlight, bringing the albedo coefficient to values around 0.95. The forest areas are characterized by low albedo, as opposed to the desert ones.

As we have seen, albedo is a particularly variable effect on our planet, and depending on the inclination of a satellite's orbit, the mean orbital value can range from 0.24 for equatorial orbits, to 0.42 for polar orbits. This effect, unlike the direct radiation of the sun, is considerable only for spacecraft in LEO (Low Earth Orbit), while for more distant orbits such as GEO the effect is negligible. Typical CubeSat missions in low Earth orbit are therefore affected by albedo.

Within the solar system, celestial bodies have very different albedo levels from each other. For example, the moon has an average albedo of 0.073, while Venus has an average of 0.65 [5].

2.1.2.3 *Planetary IR radiation*

Planetary radiation is the thermal radiation emitted by a planet. It is also called outgoing longwave radiation. It is a combination of the radiation emitted by the planet's surface and by atmospheric gases [6].

This radiation is also called Blackbody Radiation, and depends on the temperature of the body that emits it. The earth has an average temperature of about -18°C , with gases in the atmosphere that heat it, and therefore emit long-wave radiation, compared to that emitted by the sun. Leaving aside the average temperature of the entire planet, also in this case, as for the albedo, the radiation emitted by the planet varies considerably depending on the point on the surface considered, the time of year and the atmospheric conditions in that area. In this case, however, the variation is much less marked than that of the albedo. The higher the surface temperature in a given region, the greater the radiation emitted. This explains why tropical and desert areas have high radiation values, while polar areas emit less. Contrary to the effect they have on the albedo, in this case the clouds tend to decrease the intensity of radiation coming from the area below them. This is due to the fact that clouds absorb some of this radiation and store it in their colder areas.

Since both, the radiation emitted from the earth and that emitted by the spacecraft are long wavelengths similar to each other, the reflection technique used for the solar radiation listed above cannot be used to reflect the terrestrial radiation. As the altitude of the spacecraft's orbit decreases with respect to the earth, or to the celestial body around which it orbits, the effect of radiation emitted by the planet incident on the external surfaces of the system will be greater. Radiative systems for heat dissipation, therefore, find themselves exchanging energy at frequencies of the IR spectrum similar to their own (in the case of the Earth), and this worsens the effectiveness of the

thermal control through radiative dissipation emitted by the spacecraft. However, the heat flux generated by the Earth-satellite binary system acts towards the planet since the latter has an average temperature typically lower than that aboard the space system. "However, for analysis, it is convenient to ignore Earth when calculating radiant heat rejection from the spacecraft to space and to assume that Earth does not block the view to space. Then the difference in IR energy is added back in as an "incoming" heat rate called Earth-emitted IR" [5].

2.1.3 Interplanetary mission thermal environment

Discussing interplanetary missions as a specific possible mission environmental scenario can be reductive since it is a category that encompasses a range of highly varied and theoretically non-limiting thermal environments. On the other hand, this category of space missions is frequently characterized by:

- long mission duration necessary to cover the great distances that separate the Earth from the different celestial bodies of the solar system, and to interplanetary manoeuvres;
- extremely variable thermal environments to which the probes are subjected, whose trajectories can include passages at relatively short distances from the sun (the main source of heat), and at the same time led to zones or orbits characterized by significant distance from the sun or other relevant sources of heat;
- stationary orbits or rapid fly-by manoeuvres around particularly hot celestial bodies, which involve large amounts of heat fluxes in the infrared spectrum, typically difficult to screen for the radiative surfaces of the spacecraft as already mentioned, or around very cold celestial bodies at large distances from the sun, where the intensity of solar radiation, which decreases with the square of the distance from the source, is weak.

Because of these aspects that characterize interplanetary missions, it is necessary that the thermal control systems onboard the spacecraft that deal with them guarantee high performance both in the management of the hottest situations, with high external thermal flows and large internal dissipations, and for the mission phases in which it is necessary to protect the on-board components from the extremely low temperatures generated by the external environment. Especially for long-lasting cold scenarios, a large energy capacity on board is required to ensure prolonged and continuous heating of critical on-board components. [5]

3. THERMAL CONTROL SYSTEM FOR CUBESAT

During the different mission phases, it is necessary that the temperature of all the components inside the satellite varies according to the ranges defined by the requirements. These temperature ranges define the operational and survival limits of the individual components. The former guarantee the performance of the components to which they refer, while the latter are the limits within which functionality is guaranteed.

Several thermal management techniques can be implemented in order to regulate temperatures on board, these techniques are divided into two categories: passive or active. Many of these techniques were born for thermal control aboard medium / large spacecraft, but in recent years there has been increasing interest in their miniaturization, so as to be adapted for use on nanosatellites.

The greatest challenges for the miniaturization and adaptation of these systems, already in use on a large scale, are due to specific typically limited nanosatellites properties, such as:

- external surface area
- volume
- thermal mass
- electrical power

[7]

The typical strategies adopted for passive and active thermal control systems on board nanosatellites are described below.

3.1 PASSIVE CONTROL

Passive thermal control systems require no power consumption to operate. Typically, they are based on different techniques characterized by simplicity, and therefore their use leads to a containment of the weight, volume and cost of the TCS. This simplicity of design, coupled with the absence of complex power lines, implies high reliability. For all these reasons, given the main drivers of CubeSat missions, these systems are among the most used for these types of missions.

Alongside the various solutions that are listed in detail below, thermal control using passive techniques requires a design of the entire spacecraft aimed at managing

thermal flows through the appropriate choice of geometric configurations and materials suitable to facilitate, or limit where it is necessary, the transmission of heat by conduction and radiation [8].

3.1.1 Films, Coatings, and Thermal Insulation

In order to adjust the radiant heat exchange with the external environment, the optical properties of the materials present on the outer surface of the spacecraft can be affected by adding special coatings, surface coatings or tapes with their own specific coatings [7]. Some types of coatings typically used to control the solar absorptivity and IR emissivity of the outer surfaces of nanosatellites are metallized tape coatings and silvered FEP (fluorinated ethylene propylene) tapes. Tape is a widely used coating in the CubeSat industry for thermal control. In fact, it has a relatively low cost compared to other technologies, and is simple to apply on external surfaces, also having the possibility of being removed (before placing the satellite in orbit). As an alternative to the tape, opaque paint can be used to modify the optical properties of the external surfaces in the most appropriate way. Depending on the shade chosen, the paint will have a higher solar absorptivity if it tends to black, or less if it tends to white. Different colour paints can be used on different faces depending on whether they need to be heated or cooled. Paint generally has a shorter lifespan than tape.

“Second-surface silvered FEP tapes have very good performance as a radiant coating, reflecting incident solar energy, while effectively emitting heat from the spacecraft, but these tapes must be handled carefully to maintain optical performance, and they do not always adhere well onto the surface” [7]. Surface coatings must be resistant to both radiation and atomic oxygen to which they are exposed.

In addition to the modification of the optical properties, solutions are adopted for the thermal insulation of the internal and external surfaces of the CubeSats. Typically, MLI (Multi-Layer Insulator) materials, also called thermal blankets, are used for this purpose. The use of MLI is more effective on large surfaces, as at its edges there is a decrease in insulating performance. As they are made up of many very thin layers of reflective shields separated by non-metallic insulating spacers, MLIs are particularly sensitive to compression. In fact, if pressed inadequately, thermal "short circuits" could occur inside. For this reason, their use requires particular attention when the satellite must be integrated into the deployer for the launch phase that involves strong vibrations. These cons mean that in the CubeSat field, the use of MLI is limited, preferring the use of less delicate techniques such as the coatings described above.

“For most small spacecraft projects to date, adhesive tapes (e.g., silver Teflon) or other standard surface finishes (e.g., polishing, anodize, alodine) have been the preferred choices” [7].

3.1.2 Thermal straps

Thermal straps represent a passive thermal control system among the easiest to adapt for small satellites such as CubeSats. In fact, the flexible Thermal straps can be adapted to narrow spaces without particular design efforts, varying the length according to needs. Moreover, having no moving parts or liquids for the transport of heat, they are among the simplest and most reliable solutions for this purpose. This control system allows heat to be transferred from a critical area of the spacecraft to a heat sink or radiator. To do this, highly conductive materials are used, among which the most used are aluminium and copper which has better conductivity, both as thin sheets and as conductive braids.

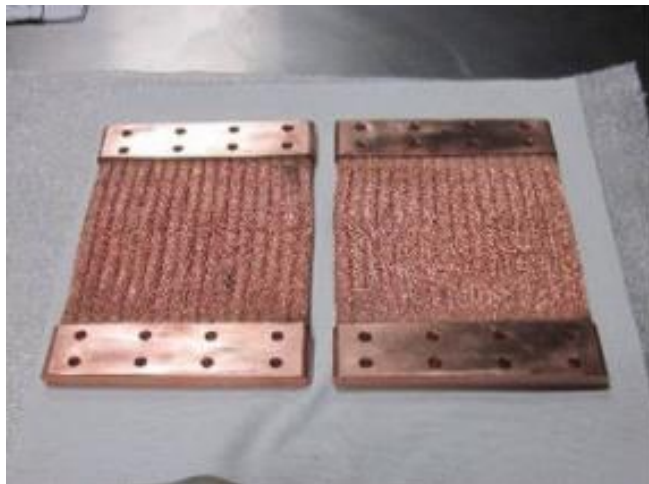


Figure 5: Copper braids thermal straps

The research for the development of this system has led to the use, as an alternative to classical metallic materials, of graphene sheets known as pyrolytic graphite sheets (PGS). This material has a much higher thermal conductivity than that of copper, combined with a lower density which makes it advantageous also from the point of view of containing the weight of the systems. The net improvement of the thermal connection given by the PGS has the high fragility of the material as a disadvantage. The assembly of a PGS thermal strap is a critical action that requires considerable attention, since bending in the plane can lead to sheet tearing as it does not withstand shear forces. Furthermore, the PGS cannot operate at temperatures below 80K, and in case of breakage it risks contaminating the surrounding components

with the release of graphite fibres. Thermal straps made of aluminium or copper are more cost-effective.

[7],[9]

3.1.3 Thermal louvers

Typically, the louvers used in the space field for large spacecraft, represent an active thermal control system, since they require electrical power for their movement, and are characterized by considerable inertia since they are used on large external surfaces. To use these systems on nanosatellites it was necessary to change the principles of this technology, such as to make it a passive thermal control system characterized by a relatively small mass. Thermal louvers are designed that use bimetallic springs, such that the relative stiffnesses of the two metals are different as the temperature varies, determining the movements of the flaps that open and close in a controlled manner. In this way, as in active louvers, when the surface temperature rises the springs expand causing the slits to open, allowing for better heat dissipation. On the contrary, as the temperature decreases, the stiffness of the bimetallic springs causes the system to close, limiting dissipation. This type of TCS has already been used for CubeSat missions in Earth orbit, and is subject to continuous improvement to ease the difficult calibration of the springs, and therefore the system control efficiency.

[7]

3.1.4 Deployable radiators and solar arrays

The radiator has the task of dissipating excess heat outside the spacecraft by radiation, and is one of the most used thermal control systems both on large-scale satellites and on nanosatellites and CubeSat. It functions as a heat sink, collecting the heat carried by other thermal control systems inside the spacecraft, such as heat pipes and thermal straps. While to limit the heating when it is exposed to solar radiation, or to decrease the emissivity, louvers can be mounted on its surface. The power dissipated by the radiator is proportional to the area of the radiative surface, to its emissivity in the infrared frequency band, and to the fourth-degree power of the surface temperature. Therefore, the larger its area, the more thermal power will be dissipated, limiting its use on the external surfaces of CubeSats, characterised by relatively small surface area. In fact, if the amount of heat dissipated by a radiator installed on the face of a CubeSat is not sufficient, by improving its optical properties with suitable paints or coatings is possible to increase its emissivity. If this is still not enough, deployable passive radiators can be used, which allow an increase in the available radiative surface area. An important aspect with simple designed deployable

radiators, is that the conductivity towards the deployed parts is kept good to not compromise radiative performance. This can be achieved with the use of high-conductance hinge for higher system thermal efficiency, or through the implementation of flexible heat pipes for uniform temperature distribution. Research into deployable radiators has resulted in this technology reaching a TRL of 5.

[7],[9]

3.1.5 Heat pipes

The heat pipe is a passive thermal control solution widely used aboard satellites. Generally, heat pipes consist of a working fluid which is liquid at the start of the cycle. By absorbing the heat of the components on which it is mounted, the liquid evaporates and moves thanks to the capillary force within an adiabatic transport section with a wick structure. Finally, the flow ends up in the condenser, where the heat is transferred to a heat sink (it could be a radiator), and the fluid returns to liquid condensing. The use with the ends in contact one with electrical devices and the other with heat sink surfaces is typical.

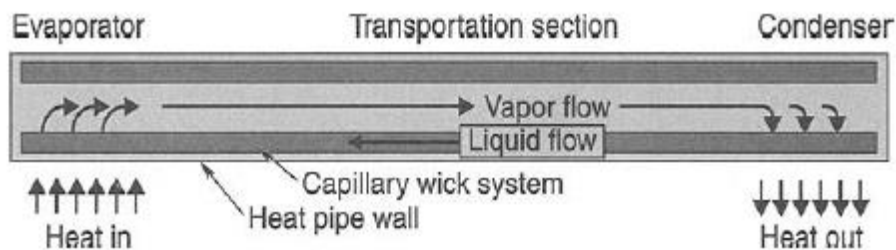


Figure 6: Schematic heat pipe (Credits: D. G. Gilmore, Spacecraft Thermal Control)

The most common heat pipes are cylindrical ones, but flat heat pipes are also developed in the CubeSat field, which are very compact and versatile. The figure shows the application of a flexible flat heat pipe inside a CubeSat 1U.

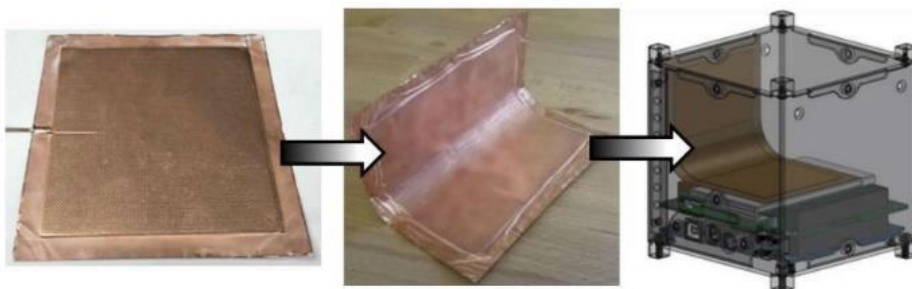


Figure 7: flat heat pipe for CubeSat

These types of heat pipes, used on board nanosatellites, allow for the collection and transport of maximum electrical powers in the order of tens of Watts, making them particularly efficient given the small size.

[7],[9]

3.1.6 Thermal Storage Units

Whether the goal is to keep the temperature of a device on board stable, whether is to control temperature peaks or to take advantage of the energy storage technique, the implementation of thermal storage units can fulfil the required function. This solution is characterized by the use of phase change materials (PCM), which absorb the dissipated heat, or the external heat flux deriving from the orbit, through their latent heat of fusion. By changing their state of aggregation during heat absorption or release, PCMs keep their temperature approximately constant during transformations. The transformation from solid to liquid, and vice versa, is the most common in the space field, as it is characterized by relatively limited volume variations. Liquid-gas, solid-gas or solid-solid transformations are also employed. It is important that the PCMs operate at temperatures close to those of fusion to effectively exploit the latent heat of fusion.

The container in which the phase change material is contained can be located in the centre between a heat source (it could be an electronic device), and a heat sink or a radiative surface. In this way, the thermal storage unit absorbs the heat dissipated by the source during the power consumption phase, changes its state of aggregation keeping the temperature stable, and subsequently, during a cooling phase, the inverse transformation occurs with the transfer of heat to the radiator. This sandwich structure is shown in the next figure.

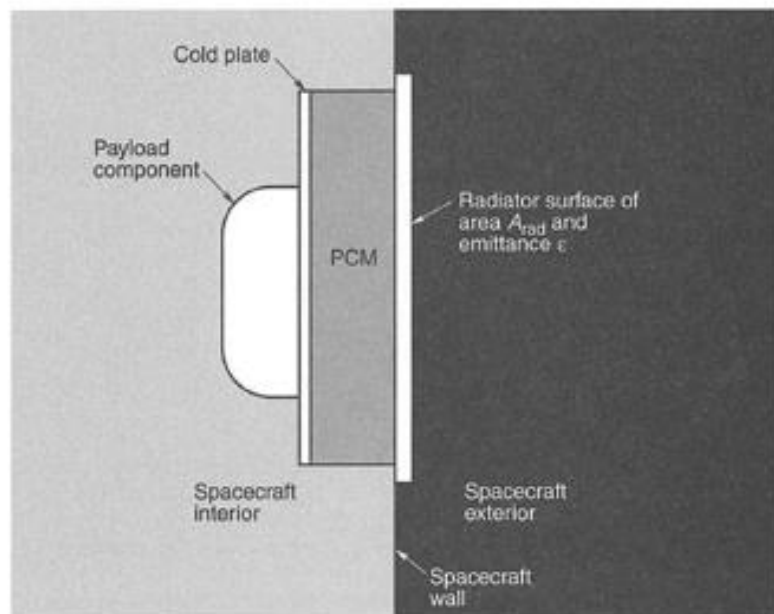


Figure 8: Thermal storage unit in sandwich TCS system (Credits: D. G. Gilmore, *Spacecraft Thermal Control*)

One of the elements with a high latent heat that can be used as a PCM is water. It allows to absorb a considerable amount of heat for a certain time (about 20W for 16 minutes) using a small mass (about 60g) and using a small volume.

In addition to having a high latent heat of fusion, and a high specific mass for the reduction of the occupied volume, it is also necessary that the PCM has a good thermal conduction. In case the PCM does not conduct heat adequately well, it is possible to use fillers or thermal conductivity enhancers to improve this aspect and avoid high temperature gradients within the thermal control system.

[7],[8],[9]

3.2 ACTIVE CONTROL

When through the use of passive thermal control systems combined with each other it is not possible to meet the requirements regarding the thermal environment of the spacecraft, it is necessary to employ active control methods. These technologies rely on the supply of electrical power, and are therefore typically more complex, expensive, heavier and less reliable. However, they have the advantage of allowing a more precise and effective temperature regulation and control, thus managing to keep the temperatures of particular devices within very narrow ranges, and satisfying even the most limiting requirements, or by providing adequate cooling when heat flows are very strong.

The use of active thermal control devices in the field of nanosatellites, and in particular of CubeSats, is still limited today, as the miniaturization of the technologies used and the reduction of the electrical power necessary for their operation represent a challenge that is not easy to overcome.

Alongside the active control systems presented below, another method to actively control the temperatures on board without using systems dedicated exclusively to this purpose, is to use the attitude control of the spacecraft during orbit to regulate heat flows in and out.

3.2.1 Electrical heaters

Electric heaters are typically used where an internal generation of heat is required in the spacecraft in order to protect devices such as batteries from low temperatures, or to heat others so as to bring them to a temperature that falls within the operational range. These active systems are controlled by a closed loop technique, equipped with temperature sensors or thermostats, which provide the feedback temperature signal necessary for thermal control.

The operation of electric heaters is based on the exploitation of the Joule effect, that is the production of thermal energy through the use of a resistance passed through by current. To exploit this technology, it is important that an adequate amount of electricity is available on board, both collected by solar panels during the phases of solar exposure, and accumulated in the batteries on board the satellite for the eclipses phases.

This thermal control method is well known and widely used on board spacecraft of all sizes.

[7] [8]

3.2.2 Pumped fluid loop

A pumped fluid loop is an active system that exploits the recirculation of a refrigerant fluid, within a closed circuit, which extracts heat from the heat sources through forced convection. The basic operating scheme is shown in the figure below.

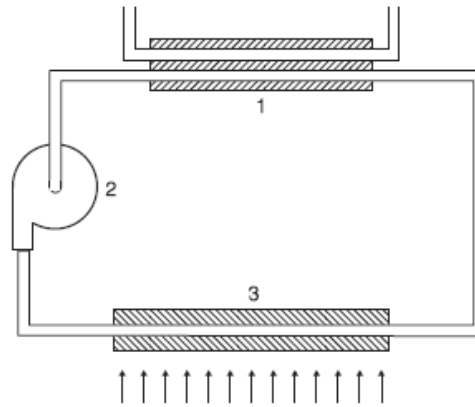


Figure 9: Pumped fluid loops scheme
 1 – heat exchanger; 2 – pump; 3 – heat source

To keep the fluid in circulation it is necessary to use a circulator pump to compensate for the pressure losses caused by the viscous effects and by the shape of the circuit.

This technology, widely used on large-scale spacecraft, allows to manage thermal loads up to $10kW$, keeping the temperatures of particular instruments within very low limits and narrow ranges. Regarding the on-board use on nanosatellites, in particular CubeSat, this technique has not had numerous employments. In fact, the necessary presence of an electro-mechanical organ such as the pump makes it difficult to use it on platforms characterized by limited mass, volume and electrical power. In addition, the pump produces vibrations that are difficult to manage in a CubeSat.

“Nevertheless, Lockheed Martin Corporation is working on a circulator pump which has a mass of 0.2 kg and a power consumption of 1.2 W ” [7], managing up to $40W$ of spacecraft heat power. The development of this system has reached a technology readiness level of 4.

Designing a fluid pumped loop system for a CubeSat requires particular attention to the shape and length of the tubes of the circuit in which the fluid flows, as an unnecessary increase in length, or the presence of an extra bend in the tube, leads to an increase in pressure losses, and therefore the need for a pump with a larger diameter and power.

An alternative system for CubeSat to fluid pumped loops that use electro-mechanical pumps is the magnetocaloric heat pump. This solution employs a ferrofluid, which contains particles with a single magnetic domain, with magnetic attraction that varies with temperature, which allow it to move by pressure gradients when subjected to a magnetic field and temperature gradient. So, when the fluid is near the heat source it heats up, its magnetic attraction decreases, and is replaced by colder fluid.

This is a system still at an early stage of development, and needs a solution for the magnetic field it generates inside the satellite, and which can lead to disturbances for other onboard devices [8].

4. THERMAL ANALYSIS

“The use of computational analysis to support the development of products is standard in modern industry. Thermal analysis is an important method of verification during the development of space systems” [10]. It aims to improve design capabilities and decrease the need for testing and analysis in the following stages to require designers to check certain design decisions and therefore reiterate the design stage. The system requirements for weight reduction, cost reduction, and test complexity are usually accomplished by keeping the thermal design as simple as possible. To be effective, thermal analysis must be applied transversely from the preliminary stages of the project to the operational stages of the mission. Thermal analysis is performed in the order of alternative design selection and supporting analysis.

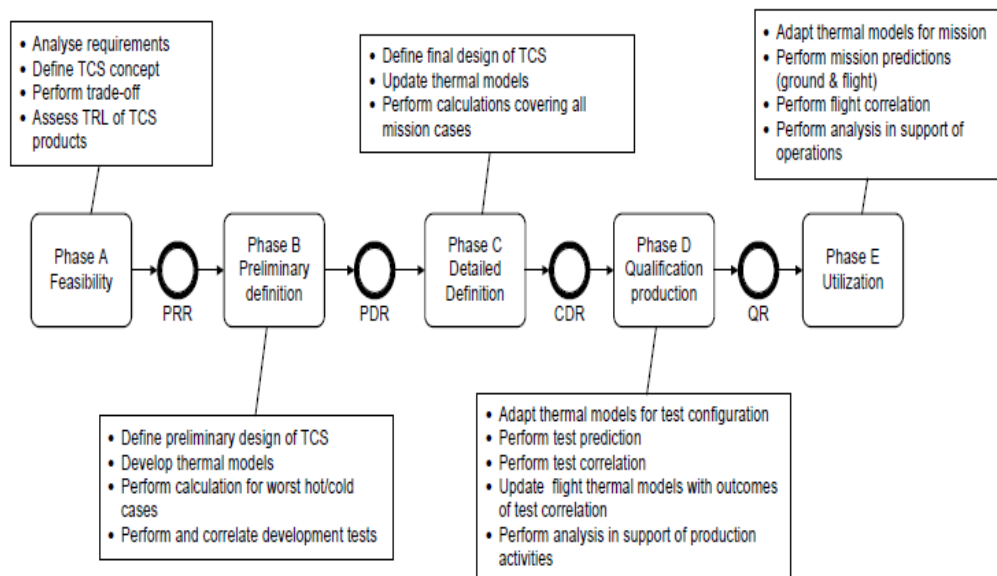


Figure 10: Thermal analysis in the context of a space project (Credits: ECSS-E-HB-31-03A)

From the flow chart above it is possible to see how the thermal analysis activity through the use of thermal models goes through all the phases of the space project, and in each phase, it serves to support various activities. Starting from phase 0 / A, through the definition of the TCS concept, the development of the preliminary thermal models begins to support the design and development of the thermal control system. Although specific tests are planned to validate the thermal models of the systems, not all thermal tests can be performed on the ground for economic reasons or due to the impossibility of recreating some external

environmental conditions. Therefore, some requirements can only be verified through the use of analysis as a verification method. This aspect leads to the need for thermal models of high quality and accuracy.

“Historically the analysis process typically started with the construction of a GMM (Geometric Mathematical Model) which was used to compute the radiative couplings and environmental heat exchanges, which drive the thermal behaviour of a spacecraft. The results of the radiative analysis computed with the GMM were then fed into the TMM (Thermal Mathematical Model) which was used to compute temperatures and heat flows. As the tools develop, the tendency is towards integrated modelling environments where the TMM and GMM merge into a single entity; with most thermal couplings generated automatically by the tool. Thus, the construction of the GMM/TMM becomes a single activity; although the actual analysis sequence necessarily starts with the radiative part, before running the thermal solution” [10].

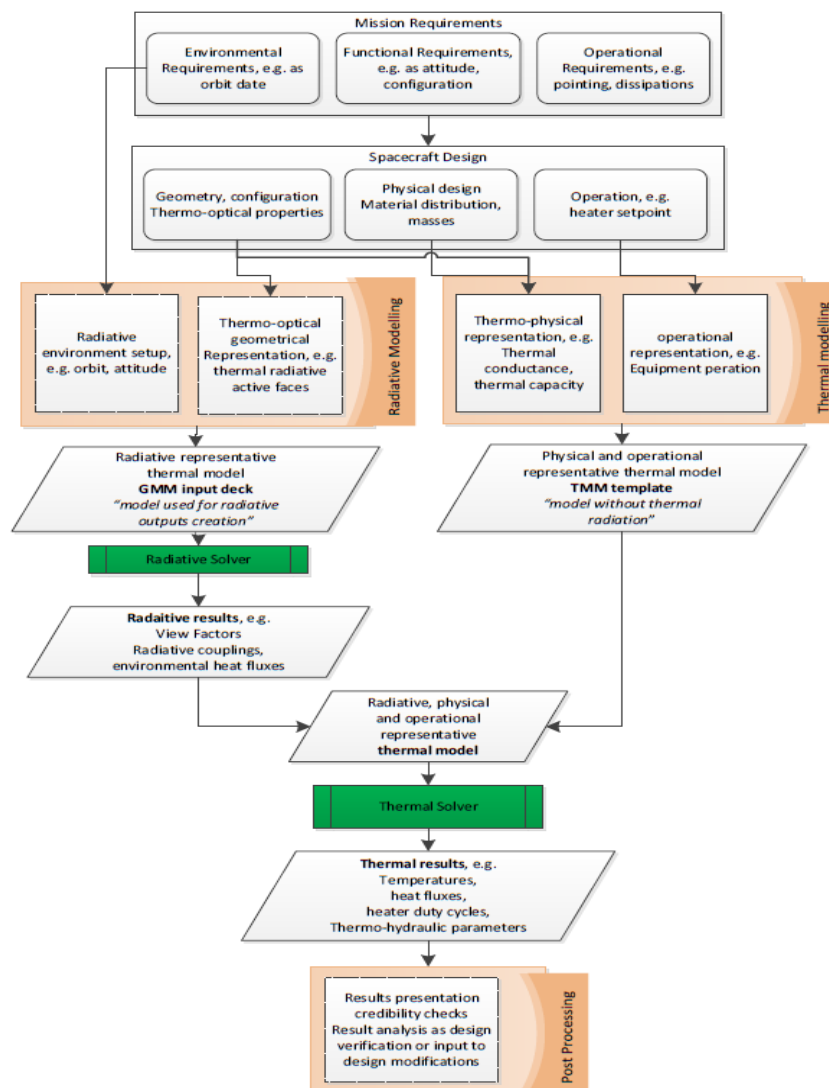


Figure 11: Modelling process (Credits: ECSS-E-HB-31-03A)

The modelling process described by the graphic above derives, like the other aspects of the project, from the mission requirements identified in the preliminary phases. From these high-level requirements, through the use of functional analysis tools, requirements and information on the system to be developed are obtained. These data concern different fields of the project: starting from possible configurations of the system hardware developed through CAD modelling, the more or less detailed specifications of the subsystems and components of the spacecraft with thermophysical and optical characteristics of the materials used, and through the development of the Concept of Operation mission information is obtained such as the orbital parameters and operating modes of the system, from which the thermal conditions of the external environment and on board the spacecraft are determined. In the initial phases of the project, each of this information can be accompanied by one or more possible alternatives, and only in the subsequent development phases are choices made towards a single type of solution as a consequence of analysis and trade-off processes. These information are essential for defining preliminary thermal design methods and building thermal models.

“Using the data gathered as stated previously, the analyst can start to construct the thermal models: a geometric model for the calculation of radiation view factors and a thermal model for predicting temperatures, obtained using a mix of computer aided design (CAD) technologies and calculations. Once the model is completed and debugged it is run to predict hardware temperatures under worst hot and worst cold condition cases. It could be necessary to also perform a certain number of parametric runs to close in on optimum sizing of TCS devices. The analysis must also be rerun to reflect changes in design or updates to new analysis inputs. The final step of the analysis is the documentation, that have to include the complete description of the geometry, the thermal model and the tests.” [8].

The work described by this thesis concerns the development of two thermal models within the ESA-uProp projects. With regard to the collection of information and the definition of the requisites necessary for the correct development of the thermal model (both geometric and mathematical), the definition of the specifications of the electric propulsion system integrated on board the CubeSat played a leading role. Thermal Desktop software was used for the development of thermal models, a fluid and thermal dynamics analysis software that works as an add-on for AutoCAD. This tool made it possible to carry out thermal analysis of the "worst case hot / cold" type, but also a parametric analysis campaign for the definition of the TCS. A more detailed description of Thermal Desktop features will be given later in this chapter.

4.1 THERMAL MODELING FUNDAMENTAL

The goal of the thermal engineer who develops the thermal model is to achieve the best possible accuracy with the relative lower cost. The cost can be divided into two different aspects: the cost of developing the model, and subsequently the cost of using it for analysis.

The thermal model is a network, of variable complexity and dependent on various factors, from which the distribution of temperatures and thermal gradients are derived.

The laws governing the dynamics within thermal models derive from the fundamental laws of electrical systems: Ohm's law and Kirchhoff's law. This characteristic is called electrical-thermal analogy, and allows to adapt the partial differential equations that numerically regulate electrical phenomena, to the resolution of thermal numerical problems simply by replacing the electrical variables with the appropriate thermal ones, as listed in the table.

Quantity	Electrical variable	Thermal variable
Potential	E	T
Flow	I	\dot{Q}
Resistance	R	R
Conductance	$1/R$	G
Capacitance	C	C

Table 1: Electrical-Thermal analogy

These correlations between the variables allow the analogy for Ohm's law in the electrical and in the thermal form:

$$I = E/R$$

$$\dot{Q} = G \cdot T$$

4.1.1 Nodes

The construction of a thermal network, at the basis of a model for solving numerical problems, begins with the subdivision of the system to be analysed into

finite-sized sub-volumes called nodes. The subdivision is called Nodalization, and it allows to concentrate the thermal characteristics at the centre of the nodal volume, generating a lumped parameters model. These characteristics are temperature and capacitance.

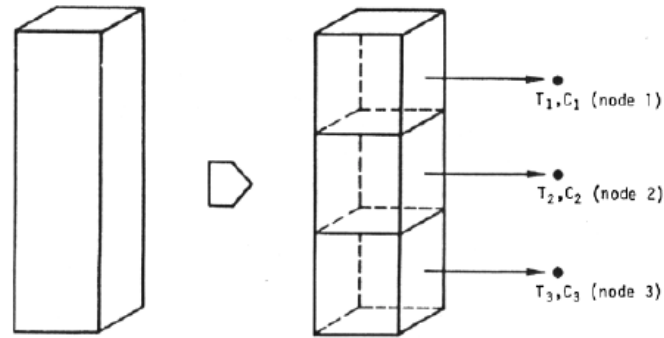


Figure 12: Nodalization (Credits: NASA, "Thermal Network Modelling Handbook")

By concentrating the thermal potential (temperature) and the thermal mass (capacitance) at the central point of the sub-volume, a linear distribution of the temperature between adjacent nodes can be considered. By interpolation, the temperature at an intermediate point with two nodes is known.

Generally, software dedicated to thermal analysis allows the use of three different types of nodes for the construction of a model. The nodes classification is described below:

- *Diffusion nodes*: characterized by a finite and non-zero capacitance, they are the most commonly used nodes, as they describe the thermal behaviour of any type of material that is employed. The temperature of these nodes depends on the incoming and outgoing heat flows involving it, the time of exposure to the flows, and the heat capacity of the material. The thermal behaviour is described by the following equation:

$$\Sigma \dot{Q} - \frac{C \Delta T}{t} = 0$$

- *Arithmetic nodes*: they are nodes that are found in small numbers within the models. They do not represent real elements, but are a mathematical artifice which, representing a node with zero thermal capacitance, allows to facilitate and speed up the thermal simulation of some real elements of the system. For example, in the case in which there is an element characterized

by a very small thermal capacitance compared to that of the other elements of the system, modelling it with arithmetic nodes with zero capacitance avoids having to solve a Stiff numerical problem, significantly saving on resolution times of the problem. Mathematically, an arithmetic node is described by the following expression:

$$\Sigma \dot{Q} = 0$$

- *Boundary nodes*: Unlike arithmetic nodes, boundary nodes are characterized by an infinite thermal mass. This allows them to be used for the modelling of elements whose temperature does not vary under the influence of thermal loads, for the duration of the phase to be simulated. In space applications, typically the deep space temperature sink is modelled by a boundary node, since its temperature is constant regardless of the loads related to the analysed spacecraft. It follows that the law that characterizes these nodes is:

$$T = \text{const}$$

Nodes and their associated sub-volume usually have simple shapes, such as rectangular-shaped nodes, for ease of calculation. The size and therefore the number of nodes that make up a network depend on how accurate the model is to be, considering the performance of the computer solving the thermal problem. The more nodes there are, the greater the accuracy, the computation time and the dedicated memory space.

4.1.2 Conductors

A conductor is a network element of the thermal mathematical model, which implements a heat flow path through which heat flows from one node to another. Once the conductors have been introduced, it is possible to make a schematic representation of the thermal network in analogy with electrical systems.

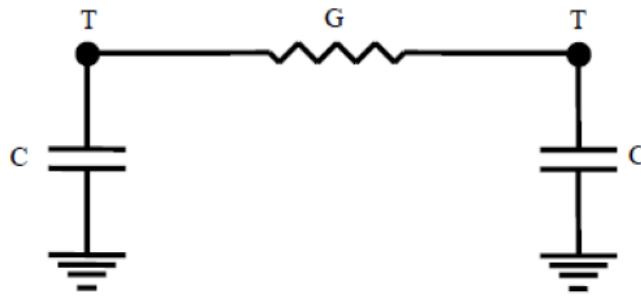


Figure 13: Thermal Network electrical scheme (Credits: NASA, "Thermal Network Modelling Handbook")

The scheme generically represents the conductor element that allows the transmission of heat from the element with a higher temperature to that with a lower temperature. More specifically, there are three types of heat transmission and therefore of conductor: conduction, convection and radiation. The first and the last are typical phenomena of heat transport present in space systems operating outside the atmosphere, while convection is not characteristic in thermal problems concerning space, as it implies the presence of a fluid that transports the heat while moving. The following figure represents the schematic of conductive and radiative type conductors.

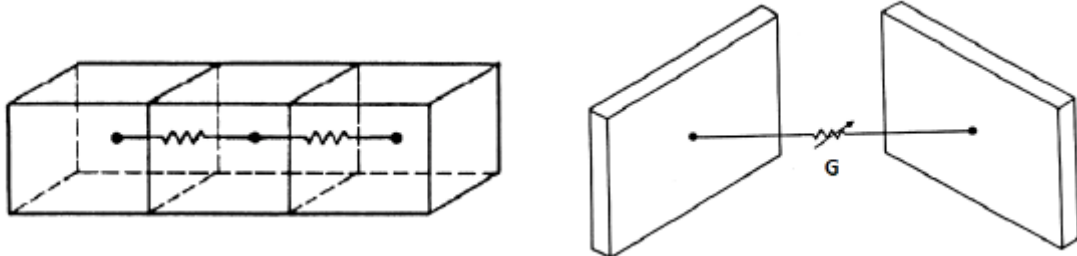


Figure 14: Conductive and radiative conductors (Credits: NASA, "Thermal Network Modelling Handbook")

While the heat flow between two nodes by conductive or convective way is a linear function of the temperatures of the two nodes i and j :

$$\dot{Q} = G_{ij}(T_i - T_j)$$

In the case of radiative heat transport, it is no longer linear, but depends on the fourth order power of the two temperatures:

$$\dot{Q} = G_{ij}(T_i^4 - T_j^4)$$

Most thermal analysis computer programs linearize the radiation term before performing thermal equilibrium at each time step.

4.2 THERMAL ANALYSIS CODES

The constituent elements of the thermal networks described in the previous section constitute the Thermal Mathematical Models (TMMs). The thermal analysis codes allow to create TMMs of different complexity and size, and are developed with the main objective of solving the general equation of heat transfer. The general partial differential equation of heat conduction (energy rate per volume unit) with source term for a stationary heterogeneous anisotropic solid is:

$$\rho C_p \frac{\partial T}{\partial t} = \nabla(K \cdot \nabla T) + Q(T, t)$$

where ρ is density [kg/m^3], C_p is specific heat [J/kgC], ∇ is gradient operator [$1/m$], K is conductivity tensor [W/mC], T is temperature [C], t is time [sec] and Q is the source term [W/m^3].

The general equation of heat conduction generates a thermal problem determined by systems of equations that can be solved by various mathematical and numerical methods. TMMs often use the finite difference method (FDM) as a solver of the thermal mathematical problem, while the finite element method (FEM) is less frequently implemented, derived from applications in typically structural problems, but still suitable for use in the field of thermal analysis. The peculiarities of the two methods, their strengths, and weaknesses with regard to thermal analysis are then presented, and finally, a comparison is made.

4.2.1 Finite-Difference method (FDM)

“Finite-difference codes generate meshes as lumped-parameter. The nodes or sub-volumes are assumed to be isothermal and physical properties are assumed to be constant within a node. The nodes are linked by conduction and/or radiation. The governing partial differential equation is converted into a system of finite-difference equations by constructing an FDM mesh” [11]. The finite-difference technique exploits the Taylor series approximation to transform the general partial differential equation, in the three spatial dimensions, in a system of finite-difference equations that can be solved with numerical methods.

“In constructing a thermal model, the analyst chooses how many nodes to utilize, how to distribute them and how to link them by radiation, conduction or convection. The resulting model network provides a system of finite difference equations with either constant or variable coefficients. The number of equations to be solved is function of the number of nodes decided by the user in the thermal model minus any boundary

nodes, which have a defined temperature history. To convert the finite-difference equations to a set of algebraic equations that are then solved by the code, the time derivative has to be approximated, just as the spatial derivatives” [8].

$$\begin{aligned}
& C_n \frac{T_n(t + \Delta t) - T_n(t)}{\Delta t} \\
&= \theta \cdot \left[\sum_{j=1}^N G_{jn}(T_j - T_n) + \sigma \cdot \sum_{j=1}^N \xi_{jn} A_n (T_j^4 - T_n^4) + Q_n(T_n, t) \right]_{t^* + \Delta t} \\
&+ (1 - \theta) \cdot \left[\sum_{j=1}^N G_{jn}(T_j - T_n) + \sigma \cdot \sum_{j=1}^N \xi_{jn} A_n (T_j^4 - T_n^4) + Q_n(T_n, t) \right]_{t^*}
\end{aligned}$$

The algebraic equations resulting from the finite difference approximation can constitute an explicit numerical problem with forward differences, or an implicit one with backward differences. This difference is related to the value assumed for the θ factor within the equations. As will be detailed later, each type of method has its advantages and disadvantages, and in each case, it should be evaluated which of the two best meets the requirements of the TMM.

By setting the parameter $\theta = 0$, the explicit solution to the finite-difference method is obtained. “This method needs that the calculation of T_i at $t^* + \Delta t$ are based on values of T_i that are known at t^* , the previous time. The forward differencing assumption is explicit and the solution can be unstable if the time step, t , is too large” [11].

The resolution of the explicit equation is not complex from a numerical point of view, but the stability criterion means that the time step Δt cannot be imposed a priori, but is limited by the node of the model having the lowest time constant. CPU performance problems can arise when the thermal model involves nodes with particularly short time constants, so much so as to lead to unreasonably long simulation execution times.

The solution of the thermal problem can alternatively be approached with a backwards finite difference method, setting $\theta = 1$. The backwards finite difference method leads to a system of n equations, where n is the total number of finite-difference nodes whose temperatures are computed at each time step. This is an implicit formulation of the problem, and as such, it is intrinsically stable regardless of the time step adopted which is no longer limited. By adopting a too high time step, the problem of truncation error occurs.

The ability to vary the Δt parameter during simulation can make the backward difference method more convenient to use. In fact, during the simulation, depending on whether the boundary conditions of the thermal problem are varying quickly or slowly, it is possible to act on the time step respectively by decreasing it or increasing it, in order to reduce the execution times. Therefore, the backward difference method is generally considered to be a faster numerical tool than the forward difference method. This may not be correct as setting a higher Δt still results in a higher number of iterations for numerical resolution, so the implicit method is not always faster than the explicit one.

The three most common errors related to finite difference methods applied to thermal problems are:

1. “The truncation error, which is the difference between the differential equation and the approximating difference equations. The temperature T in the analytical solution is a continuous function. The truncation error is determined from the finite-difference node spacing (mesh size) and the size of the time step. As the number of finite-difference nodes is increased and the time step decreased, the error associated with the Taylor series approximation (truncation) decreases and approaches zero in the limit. However, as the number of nodes in the network expands, the corresponding number of difference equations to be solved increases. This, in turn, increases execution time” [11].
2. The instability of the numerical solution derived from the resolution of the thermal problem can lead to errors in the solution. It is important that the error decreases as the resolution of the problem progresses. Otherwise, the solution is considered as unstable.
3. In addition to the truncation error there is also the computer rounding error, which derives from a truncation done by the computer during numerical resolution, and is the difference between the exact numerical result and the one actually found at the end of the calculation process.

4.2.1.1 *SINDA*

One of the commercial programs used for thermal analysis is SINDA/FLUINT, where SINDA stands for Systems Improved Numerical Differencing Analyzer. Is possible, therefore, deduce that SINDA solves TMM by means of finite difference methods. “It has fluid-network analysis capability for evaluating various types of thermal networks,

including incompressible, compressible, two-phase flow, and others, moreover it also allows the analyst to build a thermal model from separate submodels” [11].

Regarding the implementation of the explicit method of forward differences, in SINDA is defined the stability factor called CSGMIN, which is the smallest time constant in the thermal network at each time step. GSMIN can change at each Δt time step. The sufficient condition for the solution to remain stable during execution is that the time step is less than the GSMIN parameter. This happens in cases where the solution could become unstable (explicit methods), and to ensure the stability condition it is required that:

$$\Delta t = 0,95 \frac{GSMIN}{GSGFAC}$$

were $GSGFAC = 1$ generally.

This condition is valid for methods that can be unstable, while for intrinsically stable ones (implicit methods) this condition is not imposed, therefore Δt is not limited.

An aspect that characterizes implicit methods is the need for one or more convergence criteria, as they are based on iterative calculation processes. The SINDA solver requires two convergence parameters for implicit methods since the thermal network is composed of both diffusion and arithmetic nodes. These two parameters are: DRLXCA necessary for the diffusion nodes, while ARLXCA is for the arithmetic ones.

4.2.2 Finite-Element method (FEM)

The other category of heat transport problem solving methods is that of FEM methods. This type of numerical approach was born and is mainly applied for solving problems of structural nature. FEMs can be solved through the use of different approaches. The most commonly used for this purpose is the Galerkin method, which falls into the family of weighted residual methods (MWRs).

“The FEM is based on using elements that are one-, two-, or three-dimensional, depending on the problem being solved. Each element has element nodes at its corners. Parameter values, for example temperatures, are usually specified or calculated at element nodes. Modification within the element are calculated by using interpolation (basis) functions within the element. So, the properties and temperature can differ across the element. The Galerkin MWR is commonly utilized to develop the algebraic equations that define the element-node temperatures” [11].

Unlike the FDM in which it was possible to estimate the error given by the approximation made with the expansion of the Taylor series, for the FEM it is not

possible to have an a priori estimation of the error. The two techniques used to decrease the error and increase the accuracy of the method include the use of higher order basis functions, or the refinement of the mesh as its elements increase.

Several software born with the intent to be applied for structural analysis, based on FEM, are available today for problems of heat transport in the aerospace industry.

4.2.3 FDM vs. FEM for thermal analysis

The FDM is the most used method for the resolution of thermal models, and more generally it is particularly appreciated for the models of spacecraft systems. Being able to easily implement the basic geometry surfaces, the FDMs are extremely compatible with the radiation codes for heat transport problems. The solution has its own accuracy that derives from the truncation of the Taylor series expansion, and therefore from the order of the error.

The FEM is widely used in structural analysis. The method is very effective for solving thermal/stress problems. Commonly the structural model needs conspicuously more detail than the equivalent thermal model. The finite-element codes have the equivalent to diffusion (nodes with mass) and boundary nodes. They do not use arithmetic (zero-mass) nodes. Because of this the resulting algebraic equations can be very stiff and lead to excessive computational costs. Moreover, the finite-element codes cannot use just one node for an electronics box simulation, as finite-difference codes can. For normal thermal analysis, finite element models will always be larger than necessary. The real strengths of finite-element techniques are the mesh-generation schemes. These techniques can easily manage irregular surface shapes and the interface between two different mesh schemes [8].

The thermal problems that include the solution of the radiative heat exchange between the different surfaces of the system are characterized by a non-linear phenomenon. For this type of problem it is not possible to derive an exact analytical solution, and therefore they do not allow to compare the accuracy of FDM methods with respect to FEM ones.

The calculation codes dedicated to thermal analysis are mainly based on FDM. SINDA falls into this category. The Monte Carlo method or the grey-diffuse assumption are the techniques most used for the calculation programs of the radiative heat exchanges.

4.3 MODELING WITH THERMAL DESKTOP

The information presented in this section comes from the user manual of the SINDA/FLUINT code, relative to the reference [12].

C&R Thermal Desktop is a program that allows the user to quickly build, analyse, and postprocess sophisticated thermal models. Thermal Desktop takes advantage of abstract network, finite difference, and finite element modelling methods. RadCAD, a subset of Thermal Desktop, is a module to calculate radiation exchange factors and orbital heating rates. FloCAD, another module of Thermal Desktop, generates flow networks and calculates convective heat transfer factors. The title “Thermal Desktop” is commonly used to refer to Thermal Desktop and its integrated modules.

The output of Thermal Desktop, RadCAD and FloCAD is automatically combined in order to create inputs for SINDA/FLUINT, CRTech’s industry standard thermal/fluid analyser.

Thermal Desktop is also parametric. Input fields for surface parameters, assembly positioning, optical and material properties, network elements, and orbital data will accept either numerical values or expressions using arbitrary user-defined variables. Parametric trade studies and optimizations are easily executed, especially when managed using Case Sets. A dynamic link between SINDA/FLUINT and Thermal Desktop allows SINDA/FLUINT to command Thermal Desktop to recompute radks, heating rates, conduction, and capacitance data on the fly from within a SINDA/FLUINT execution: SINDA/FLUINT can be used as a scripting language for controlling Thermal Desktop execution, and any recalculations of radiation, contact, convection, etc. required of Thermal Desktop by SINDA/ FLUINT can be made to support the execution of parametric runs.

Using the SINDA/FLUINT Solver, optimizations may now be performed that include optical properties and geometric sizing as design variables. Thermal models may be automatically correlated to test data, varying all aspects of the model including capacitance, conduction and radiation values.

A feature with which the user will want to become immediately familiar is the Model Browser. This feature allows the thermal model to be viewed in a hierarchically arranged tree, organized by many different categories, such as node id, surface type, property usage, tracker and assembly groupings, etc. The browser also contains features for editing and isolating the display of selected objects, as well as listing useful information.

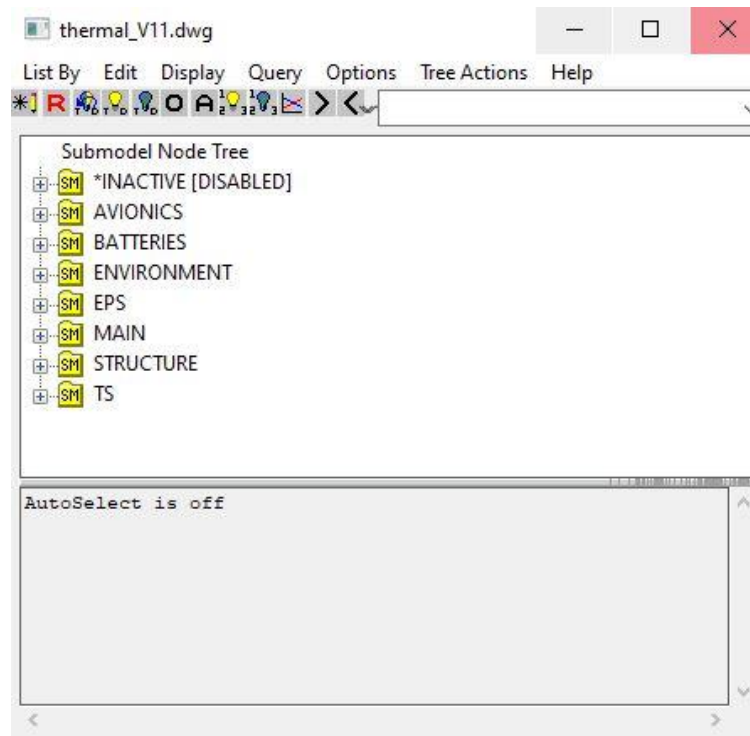


Figure 15: Model Browser in Thermal Desktop

Thermal Desktop runs as an AutoCAD application, fully integrated within an AutoCAD drawing session. Powerful CAD techniques for generating geometry can be used for generating thermal models. Custom menus, toolbars, and dialog boxes permit the construction and analysis of thermal models directly within the AutoCAD environment. Thermal Desktop can analyse thermal models consisting of AutoCAD 3D faces, regular MxN meshes, and arbitrary polyface meshes. These surfaces may be created directly, or by using various AutoCAD mesh generation commands such as surfaces of revolution, ruled surfaces, and edge defined patches. Thermal Desktop is not limited to just conic surfaces.

RadCAD is the radiation analyser module for Thermal Desktop. An ultra-fast, oct-tree accelerated, Monte-Carlo ray-tracing algorithm is used by RadCAD to compute radiation exchange factors and view factors. Innovations by CRTech to the ray-tracing process have resulted in an extremely efficient radiation analyser. A unique progressive radiosity algorithm has also been incorporated to compute radiation exchange factors from view factor data. RadCAD has also incorporated the progressive radiosity algorithm into heating rate calculations, resulting in even faster performance.

FloCAD is a Thermal Desktop module that allows a user to develop and integrate both fluid and thermal systems within a CAD based environment. FloCAD adds the capability of modelling flow circuits, including fans and convective heat transfer,

attached directly to the surfaces and solids representing PCB boards, chips, heat fins, etc.

Geometry is created using thermal-specific custom conic surface types (e.g., plates, disks, cylinders), or from geometry created using the built-in CAD construction techniques. Models may be built from scratch, imported from existing thermal models, or based on geometry from a CAD design database.

Arbitrary (non-geometric) network elements such as nodes and conductors may be created. A thermal model may consist of FD surfaces, FEM elements, and schematic representations using arbitrary nodes and conductors. Nodes may be boundaries, arithmetic (zero mass), or diffusion (finite mass), with the latter optionally including temperature-dependent thermal capacitance (i.e., variable specific heat).

[12]

5. CASE STUDY 1: ESAuProp-2

5.2 ESA-uPROP 2: PROJECT OVERVIEW

ESA-Prop is a project developed by CubeSat Team of Politecnico di Torino in collaboration with the European Space Agency with the aim of design a CubeSat test platform for miniaturized electric propulsion systems to be tested at the ESA-ESTEC Electric Propulsion Laboratory (EPL).

The ESA-uProp 2 project is about the design, development and verification of a 6U CubeSat test platform (CTP) wich host a miniaturized electric propulsion system REGULUS, with the final goal of assessing the effects of operations and interactions between the propulsion system and the platform.

To date, very few CubeSats have flown in space featuring propulsion systems, thus very few data are available on propulsion systems performance in the operative conditions. Electric Propulsion (EP) systems are gaining interest for application in nanosatellite, especially for beyond LEO missions, and many developments are ongoing on this technology. Consequently, a growing need exists for mission and satellite designers and engineers to understand the interactions between EP systems and the host spacecraft.

Interactions between Propulsion Systems (PS) and other onboard subsystems are hard to be modelled and analysed through simulation, but the effects of operations of EP systems within a small platform must be assessed in order to validate the spacecraft design and mission operations. Moreover, the TRL of miniaturised EP systems is still low and need to be raised to enable future nanosatellite missions. One of the goals of this thesis work is to improve the knowledge about the EP systems for nano satellites when they are integrated inside their hosting platforms. In fact, after deep studies and researches of miniaturized EP system information and performance data, one of the output is the lack of information about the real efficiency of these devices, and how to manage heat fluxes dissipated by them. Many electric thrusters developed in the last years, so far have been tested individually, without being integrated into satellites. This did not allow to assess with the desired accuracy the effects and the performances that they can actually have under the expected operating conditions.

The two main objectives of ESA-uProp project are:

- To design and build a prototype CubeSat Test Platform (CTP) based on COTS technology suitable for hosting and handling miniaturised EP systems

- To define a procedure for testing the integrated CTP/EP-system in a relevant environment (@ESA/ESTEC EPL)

In particular, the phase 2 of the project aims at:

- assess the mutual effects of EP system and CTP
- integrate and verify in vacuum CTP with a selected EP system
- identify of a set of procedures for the AIV of an all-electric CubeSat

Main drivers for the platform design are: flexibility/adaptability of interfaces (mechanical, electrical, and data) towards propulsion system, accessibility, simple manufacturing and assembly, low-cost development. Platform requirements have been drawn through functional analysis developed from system-level up to component-level functions.

5.1.1 Test Platform Architecture

The platform features an Al-alloy 6U structure. As can be seen in the next figure a Propulsion Box (4U) hosts the propulsion system, and a Service Module contains the on-board avionics (1U), and battery packs (1U). A bulkhead is fixed to separate the propulsion box from the rest of the platform. The PS thruster is mounted with the thrust axis along the X geometrical axis of the satellite.

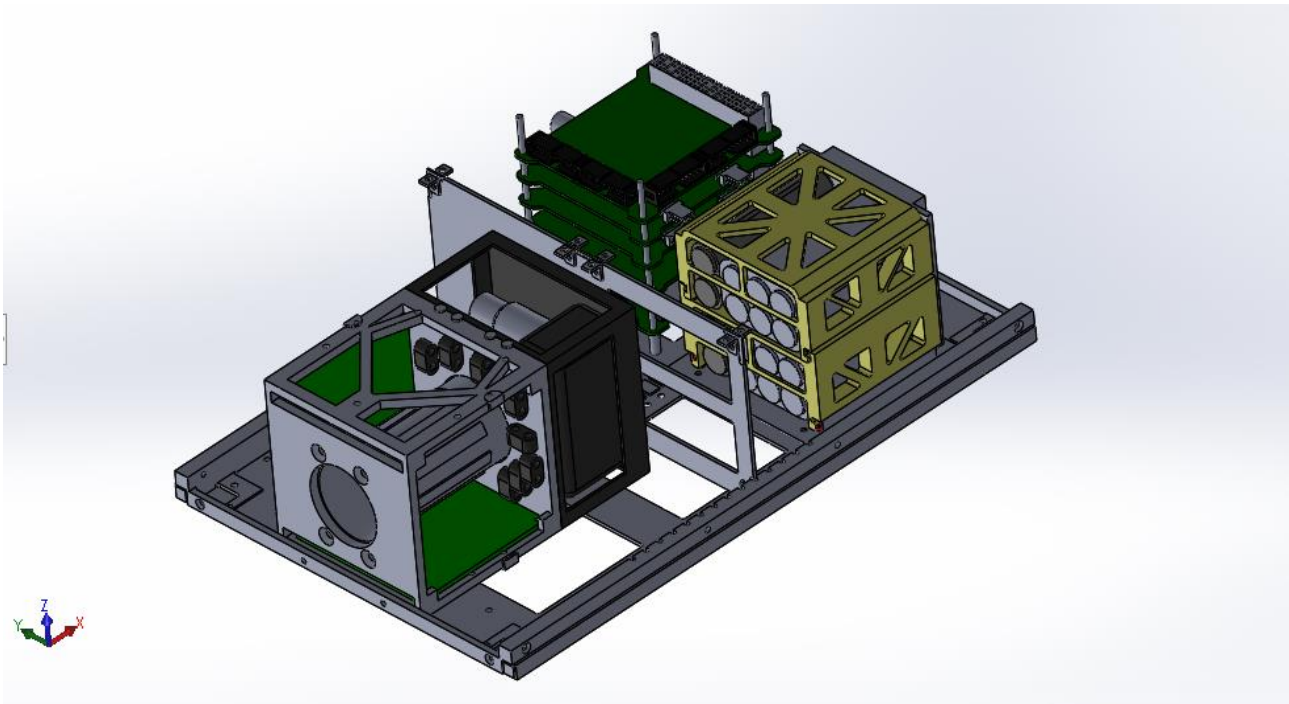


Figure 16: CTP internal configuration

The Propulsion System includes the Thruster, the Power Processing Unit (PPU) and the Propellant Feed System (PFS), and the propellant tank.

The avionics is constituted by the on-board computer for command and data handling functions, the electrical power system (PCDU and battery), and the communication module (UHF for housekeeping and experiment data) and two boards that constitutes the Electric Propulsion Interface System (EPIS). EPIS provides the interfaces of CTP towards the EP system and the instruments and devices to measure the parameters for assessing the mutual interactions between CTP and EP system. Two main parts constitute EPIS: the Data Logger (DL) and the High-Power Management System (HPMS).

The avionics boards are in-house developed electronic boards resulting representative of the basic Cubesat technology. Data Logger gathers all the information about the radiation and thermal environment and the power consumption of the EP system. The HPMS supplies electrical power at a regulated voltage to the EP system using the energy of two dedicated battery packs; battery packs are recharged thanks to an external source and recharging control circuits. Two lines guarantee communications between the platform and EPL operators: a RF link in UHF band and a wired serial line that directly connect the on-board computer with the Ground Support System. Command & Data Handling is based on ARM-9 microcontroller that manages data and commands time, operations and on-board failures. Sensors and acquisition circuits provide the information (e.g., voltages, currents, temperatures, magnetic fields, and electrical fields). Electrical Power System is constituted by a board that controls and distributes power to the other subsystems and manages the avionics battery packs recharging.

The five avionics boards are stacked on top of each other, mounted on four brackets screwed to primary structure.

Batteries (both the Avionic Battery packs and the Propulsion Battery packs) are installed in the second unit of the Service module and can be recharged during the test thanks to an external line connected to GSE through SPF Chamber umbilicals.

The structure is fully compliant with the CDS in terms of external geometrical interface and material (apart from surface coatings and treatments). The primary structure is constituted by two truss-like parts joined together through four brackets. The primary structure is built through metal additive manufacturing. The secondary structure includes external panels for protection of onboard systems from external environment, and internal mounting elements (screwed to the primary structure) for installation of avionics and the propulsion system. The internal layout can be adapted depending on the specific test.

5.1.1.1 Service module

Command and data handling - (C&DH)

CDH subsystem main functions are to monitor, control and command the onboard systems.

- The board performs the acquisition of the measurements of the on-board parameters through the conditioning of the sensing signals, their serialization and conversion of signals from analogue to digital.
- CDH manage the data extracting, processing, and formatting them. In addition to data, the subsystem also manages commands through the reception, validation and decoding of them. Tasks management requires time counting, tasks organization and synchronization. Failure Detection Isolation and Recovery (FDIR) functions are also integrated.
- To command the onboard systems consist of activate/deactivate tasks and change the tasks sequence, driving the platform between different operating modes.

A sensing unit, constituted by sensing circuits for voltages and current, temperature sensors for temperatures in different points of CTP, and magnetometer the magnetic field with respect to the three body axes, provides the physical and electrical parameters of CTP. RC filter and amplifiers adapt the sensing level for micro-controller reading, and multiplexers (MUX) and Analogue to Digital Converters (ADC) serialize the conditioned data and convert the signals of analogue sensors, if required. Processing unit is the brain of the platform that handles data and commands, manages time and synchronization, saves and loads data in/from EPROM and SD card memory, manages own failures (through a software watchdog) and CTP failures through FDIR procedures. Clock allows counting the time. Data bus distributes information among C&DH components and with the other subsystems: different communication protocols are implemented giving a good flexibility to the CTP that can connect a wide range of analogue and digital components.

High power management system - (HPMS)

The HPMS board is dedicated to supply electrical power to the propulsion system. To do that HPMS has to:

- obtain electrical power from an external source of the GSE.
- store electrical energy received from the external source into the dedicated PS batteries, regulating the charging process
- provide the EP system with electrical power regulated at 12V, connecting the batteries to the power bus, and protecting the EP system from over-voltages.

The energy is delivered by an external power supplier, passes through a charge regulation circuit which control the recharging phase and is stored in PS battery packs. The distribution is controlled by switches and the regulation is guaranteed by Boost regulator circuit which contains the Step-up circuit that takes the power from the battery and regulates the output to 12 V.

Data Logger – (DL)

Data Logger function is to assess the mutual interaction between the CTP and the EP system. To do that through different sensing units the board measures various onboard parameters.

The electromagnetic field is measured gathering data of: RSSI (Received Signal Strength Indicator) of the radio-module, RF emissions strength and current ripple on the electrical interfaces between CTP and EP system.

The assessment of the thermal environment is characterized by a wide set of measurements of the temperatures in different points of the CTP.

DL also measures the power consumption of EP system, measuring the voltage and current output of HPMS power bus.

All the signal provided by the sensing circuits of the DL pass through conditioning circuits that adapt signals levels, and then through an ADC and a Multiplexer which convert the signals of analogue sensors and serialise data. The data are sent to CDH processor.

Communication system - (COMSYS)

The highest-level function of COMSYS is the exchange of information between CTP and GSS. Two communication channels are used to do this:

- a wired link called Hard-line directly connects CDH board with GSS, using a serial cable that transfer data along the hard-line using the RS232 protocol. The hard-line required a level adapter unit.
- A RF link which uses a TNC/MODEM unit connected to a Transceiver which receives and sends data to a dipole antenna. radio module operates at 437 MHz frequency.

Electrical power system – (EPS)

The EPS has similar functions as the HPMS except that this subsystem is dedicated to the power distribution through the other avionic onboard systems, instead of the EP system as the HPMS. EPS has to take energy from an external power (e.g. a power supplier), to store the energy in dedicated AV batteries that shall be recharged using a battery charge regulator, to regulate the battery and external voltages (3.3V and 5V) to

supply the avionic loads, to control the power distribution and to protect the system from over-voltages.

Battery packs unit

All onboard batteries are mounted in a dedicated unit of the service module. Battery packs (PS and Avionics) are sized based on power peaks derived by the power budget analysis, adding a 20% of margin. This requires batteries that provide 60W for the PS and about 3,3W for the avionics peak. Both the battery pack for the avionics and the one for the propulsive system have been redundant, so there are four battery packs. The two of the PS contain each six cylindrical AA-size Li-Ion cells, 12V and 5,2 Ah (total 62.4 W). Avionics battery pack are constituted by two packs each one with two AA-size Li-Ion cells, 7,4V and 2,2Ah. Battery packs are mounted and contained in an aluminium structure.

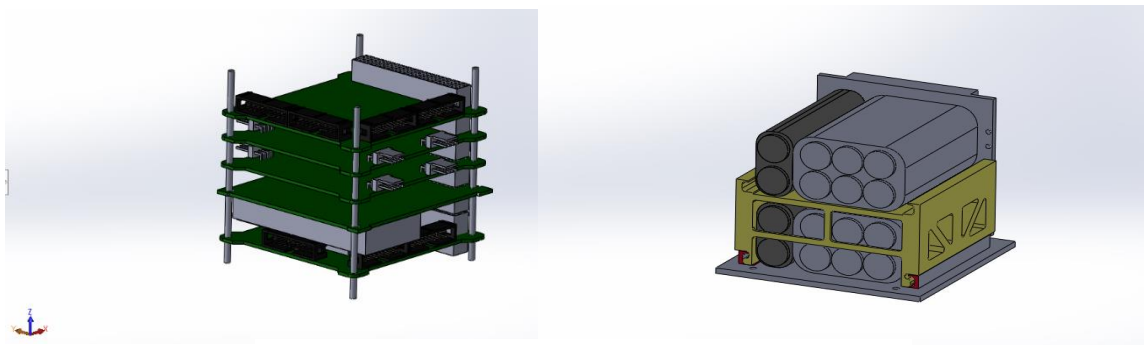


Figure 17: CTP Avionics module and battery packs

5.1.1.2 Electrical Propulsion System (ePS)

The miniaturized electric propulsion system is the REGULUS helicon plasma thruster provided by T4I. The main specification of Regulus system are reported in the following table.

Thrust	0.5 mN @30W (0.2 – 0.7) mN
Specific Impulse	600 s @30W (220 – 900) s
Total impulse	3000 – 11000 (up to unlimited) Ns
Required power	[20 – 60] W
Mass flow	0.1 mg/s

Propellant	Iodine (I_2)
Volume	1,5 U @3000 Ns; 2 U @11000 Ns
Weight	2.4 kg @3000 Ns

Table 2: Regulus ePS performance

“REGULUS is compatible with thermal, mechanical, and electrical interfaces of the CubeSat platforms available in the market, and it relies on COTS components. It is equipped with a passive thermal control system. The main framework of application of the REGULUS platform is the propulsion of medium-to-large CubeSats (from 6U up to 27U). It was designed to address various mission objectives and mission scenarios as drag compensation and constellation deployment. The REGULUS platform can compensate the effects of atmospheric drag on a 6U CubeSat in a 400 km altitude orbit for years. Besides, a CubeSat constellation can be deployed through several planes in some months employing small fractions of the onboard propellant” [13].

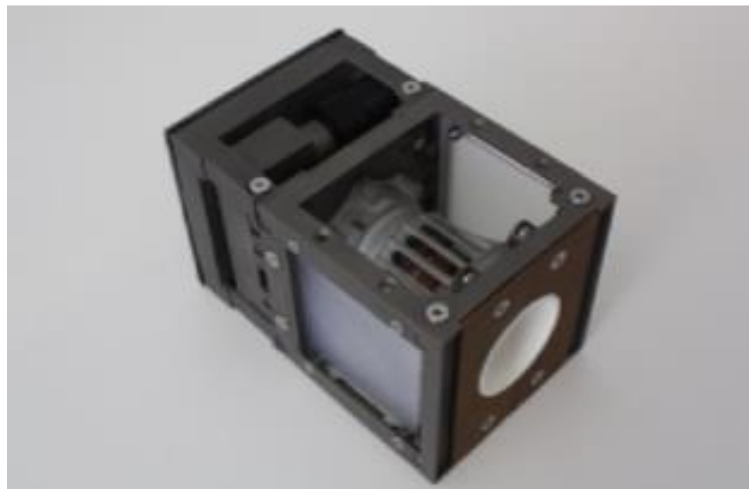


Table 3: REGULUS electrical propulsion system by T4i

5.1.2 CTP AIV Plan

Following the execution of the initial verifications on the subsystems of the CTP, necessary for the verification of the requirements of the service module and the assessment of its performance, a Test Plan was developed dedicated to the test necessary for the integration of the EPS with the CTP, verification of system requirements and the plan for future mission tests. The Test plan describes the AIT

programme for the CTP from the integration of the propulsion system up to verifications in the Small Plasma Facility (SPF) at ESA-ESTEC.

The verification campaign is performed through a step-by-step approach at the different level of product decomposition. ESA- μ Prop product requires verification at equipment, subsystem, and system level.

The verification process is addressed through different stages, each with its own objectives. The verification stages implemented in the test plan are:

- *Development stage*: aims at support the design feasibility and to assist in the evolution of the design. Development verifications are used to validate the design concepts using appropriate models.
- *Pre-qualification stage*: with the purpose of demonstrate that the items function satisfactorily in the laboratory environment and prepare it for future verification in the intended environment. Most part of the pre-qualification activity is done by testing through a step-by-step verification campaign that confirms the capability of the single interfaces between CTP and ePS.
- *Qualification stage*: aims at demonstrating that the items perform satisfactorily in the vacuum chamber environment, which is the intended environment to operate the CTP with the ePS integrated.

Through the definition of a model philosophy, it was possible to establish the optimum number and the characteristics of virtual and physical models required to achieve confidence in the product verification with the shortest planning and a suitable weighing of costs and risks.

5.2 ESA-uPROP 2 THERMAL MODEL AND SIMULATION

One of the most interesting aspect to be studied within ESA-uProp project is how to manage the heat generated by the electrical propulsion system, and by relative subsystems. This is a critical aspect that need an accurate investigation to allow, in the future, to design and develop in a short time and at low cost CubeSats with electric thrusters on board. The small dimensions of nano-satellites, and in particular of CubeSats, makes it difficult to manage and dissipate large heat flows internal to the satellite.

As mentioned above, the test campaign of ESA-uProp2 CTP was divided into three distinct verification stages, according to the AIV Plan of the project and following the indications of the ECSS standards: *Development*, *Pre-qualification* e *Qualification*. The *Development* stage aims to support the design feasibility and to assist in the evolution of the design, and also to validate the design concepts. In this first stage, frequently, since it is a preliminary phase of the project, physical components of the system could be not yet available, just because they may not have been defined in detail, therefore virtual models and simulations are used with the analysis verification method to support its development. One of the objectives of ESA-uProp2 project is “to develop tools and competences enabling a better, faster and more efficient design of CubeSats with propulsion systems” [3]. For this purpose, a thermal model of the CTP was developed, using Thermal Desktop. Thanks to this model, in the preliminary phases of the project it will be possible to simulate the behaviour of the satellite, with a rather good accuracy, under different operating conditions, with different configurations and above all with different ePS models, without the need to physically test them. This early-stage process may allow to steer the project towards some better options of thrusters, avionics, or batteries for example, speeding up system development.

After an initial definition and development of the thermal model, a validation and improvement phase of the latter was necessary, thanks to the empirical data resulting from the tests of the CTP qualification stage. In this way the accuracy of the model has been increased making it more reliable for future simulations.

5.2.1 CTP Thermal environment

During its life-cycle, a generic spacecraft shall withstand a wide variety of thermal environments, both from the point of view of thermal loads and their duration. Spacecraft is normally subjected to ground test, integration and transport, characterized by heat exchange by convection with ambient air, conduction and irradiation, and by the specific environmental conditions of the tests to which it is

subjected. Then follows the launch phase, in which the fairing that protects the payload is subjected to thermal loads, even very large, partly transferred by radiation of its inner faces to spacecraft. Once reached the orbit, usually the external thermal loads that act on the spacecraft are of radiative type, and derive from: solar radiation, albedo of the earth or other celestial bodies, infrared radiation emitted by celestial bodies.

The thermal control system is usually designed to maintain within the range of temperature limit for operation or for survival spacecraft components in the operational phase of the mission (typically the one with the longest duration). Thermal loads coming from the external environment and the internal components are considered, the conditions of greater heating and cooling are identified and on these two the TCS is dimensioned. For the other mission phases, expedients are used to maintain spacecraft and its components in the limit conditions [5].

Through the use of Thermal Desktop for the development and simulation of thermal models, it is possible to define models subjected to different thermal conditions, and in particular, it is possible to set the orbit of spacecraft so that the external loads in the operating condition are defined. Since the ESA-uProp mission does not foresee the launch of the CubeSat, but is used as a ground test platform for testing electric propulsion systems for nano-satellites, this function has not been implemented in the thermal model. Therefore, the model developed with Thermal Desktop provides environmental and geometric modelling of the facilities in which the CTP mission tests are performed.

Actually, the test campaign to be conducted at ESA/ESTEC EPL, and in the laboratories of T4i/Padua University, is to replicate as nearly as possible potential CubeSat orbit conditions. This is made possible by the use of vacuum chambers that aim to recreate the vacuum conditions typical of the space environment, with the main consequence of eliminating the phenomenon of convection for the heat transport. In addition, electric thrusters typically work better (or work exclusively) in vacuum conditions.

The attempt to emulate the space environment through the use of vacuum chambers involves limits. Radiative effects such as solar radiation, albedo of planets and their IR emissions are not simulated. In this way, important external thermal loads, that characterize the orbit of spacecraft, are not considered, including the radiative effect of deep space, with an absolute temperature in the range $3 - 4 K$. Instead, the spacecraft inside the vacuum chamber exchanges heat through radiation with the inner walls of the chamber surrounding it. These walls can be at room temperature, or in some more complex and performing vacuum chambers, they are cooled to temperatures around $80 - 100 K$, reducing heat exchange. Solar radiation could be

simulated using a sun simulator. This tool allows to recreate the heat load that the sun generates on spacecraft, using powerful infrared lamps that provide intensity and spectral composition similar to sunlight [3].

The tests are carried out in different facilities through the different verification stages, as described in the AIV Plan of CTP these are the T4I/UNI-PD facilities and the Small Plasma Facility at ESA-ESTEC. In order to model the thermal environment of the vacuum chamber on Thermal Desktop, a parameterized cylindrical geometry has been built, in order to adapt its dimensions depending on the different facility to be simulated.

The model consists of a thin shell cylindrical element divided into ten boundary nodes. By setting the fixed temperature of the nodes, it is possible to simulate a vacuum chamber with walls at constant room temperature, or one with cooled walls.

In addition, still using boundary nodes, some simulations were performed by varying the temperature of the chamber walls with time. This allowed to consider that the chamber does not have an infinite thermal inertia, such as to have invariant temperature with respect to the thermal loads to which it is subjected, but especially in the case of uncooled walls, the thermal loads produced by the spacecraft inside it can warm up the walls during a test.

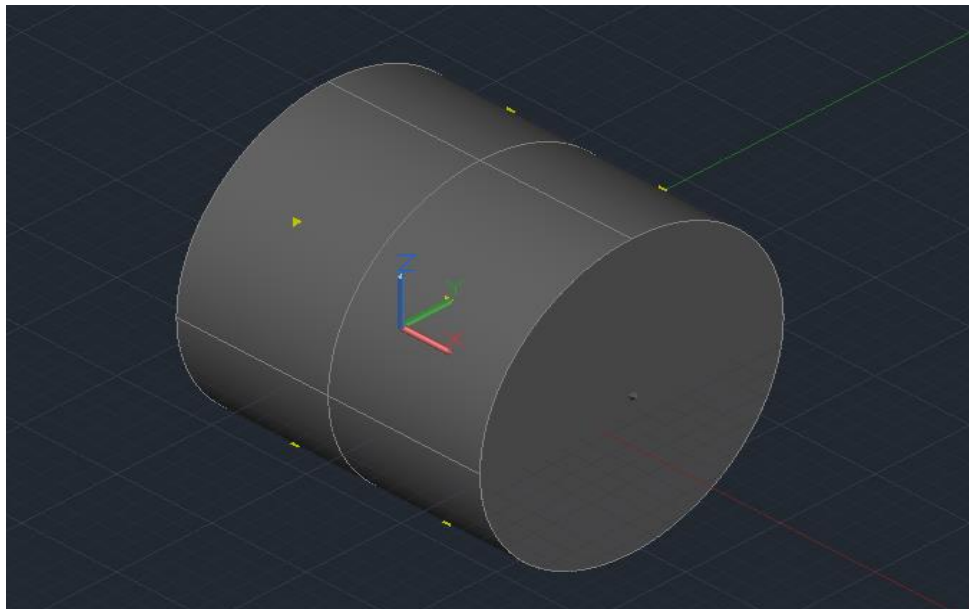


Figure 18: Vacuum chamber model

5.2.2 Optical and thermophysical properties

This thesis work was born following the design of version 2 of the CTP, and therefore the choice of the materials and their thermal and optical properties used, is previous the beginning of this work. The research focused not in particular on what were the best materials to use for the different components of the platform and its surfaces, given that these had already been chosen, but rather on how to make the thermal model of the platform as faithful as possible, adequately reproducing the types of chosen materials. This work led to the study of several documents containing characteristics of different materials and various methods for their modelling, and subsequently to the use of empirical data deriving from the qualification tests of the CTP, used to enrich the validity of the same model. Naturally, this path, as in general the attempt to create a thermal model of the CTP, required simplifications and more or less wide approximations, depending on the confidence and the need for accuracy required by the model.

Since the CTP had already been developed and built, it was not possible to change the thermal and optical properties of its systems, but there was still the possibility of inserting elements of simple addition such as insulating materials, or other elements. With regard to this, the model was useful in defining a system for the thermal protection of onboard avionics, the Thermal Strap, which was not initially envisaged by the project.

The following tables indicate the materials used and their thermophysical and optical characteristics.

Thermophysical properties			
Material	Conductivity $\frac{W}{m K}$	Density $\frac{kg}{m^3}$	Specific Heat $\frac{J}{K m^3}$
Al5005	201	2700	900
Al6082	17	2700	900
Batteries	65,8	2118	795
Board	17,5	3937	1192
Copper	39,8	8930	385

Stainless steel	16,2	8000	500
Chamber	34,3	9000	850

Table 4: ESA-Prop2 model - Thermophysical properties

Optical properties		
Material	Solar Absorptivity	IR Emissivity
Aluminium	0,25	0,10
Aluminium anodized	0,25	0,77
Aluminium alodine	0,45	0,15
FR4	0,49	0,88
Copper	0,64	0,15
Solder mask blue	0,7	0,88
Steel	1	0,70

Table 5: ESA-Prop2 model - Optical properties

The primary structure components are made of Al6082, while the other aluminium alloy Al5005 is used for the secondary structure. Since the structure panels are modelled by thin shell elements, they represent both the primary and secondary structure, and therefore, the properties of both aluminium alloys were used. The Al6082 is used also for battery packs drawer and for the bulkhead. The ePS is also made of Al6082 in the model, but this feature is to be considered linked to the specific propulsion system type to be simulated.

For the modelling of the batteries, the study previously carried out for the first version of the CTP was considered, together with the collection of information on the composition of lithium-ion cells. Batteries of this type are anisotropic in nature, and therefore it was decided to use average characteristics that would allow the average temperature of these components to be simulated with good accuracy, without having to spend excessive time and tests to achieve greater accuracy. Furthermore, for the optical properties, it was considered that the batteries are enclosed in plastic material: the blue solder mask. The optical properties therefore correspond to those of the latter material.

The modelling of the avionics boards material was more complex, and subsequently required the use of data derived from the tests to improve the accuracy of the property correctness. In fact, the electronic boards are anisotropic multilayer elements, in which there is FR4, a plastic laminate material, with printed copper circuits on top. This implies that in the directions drawn by the copper tracks the heat is conducted much better than in the other directions of the board, in particular the one perpendicular to the surface. Furthermore, various electronic components are mounted on the boards, often small in size and difficult to be modelled, each one with its thermal properties.

Copper is used to model the thermal strap, the component dedicated to absorbing and transfer heat from the electronic boards to the CTP structure, in order to avoid overheating.

The four brackets that support the avionics unit are made of stainless steel, which is used also for the connectors that represent screws and fileted bars.

5.2.3 Thermal Desktop model definition

As mentioned above, the thermal model was developed using Thermal Desktop. The basis from which the work started was the model of the previous phase of the project, with limited accuracy due to the fact that it has never been validated through tests in a vacuum chamber.

For the development of the model, it was decided to employ a strategy aimed at keeping the use of the model as simple as possible, thanks also to the modularity that was used to model the different subsystems and components of the CTP. In this way it was easy to work on different parts of the model separately, and it will also be easier for a user who did not participate in the development, to use the model for simulations, modifying it appropriately to best represent the object of study (like a new ePS).

The first step in defining the model was the creation of the database with the thermophysical properties of the materials used and that of the optical properties, both already analysed previously. This was an iterative process, as some of the initially entered materials and their properties were replaced or changed during the model definition, in order to make it more faithful to the system. Using the *Edit optical properties* and *Edit thermophysical properties* tools, shown in the following images, the databases were built and subsequently modified.

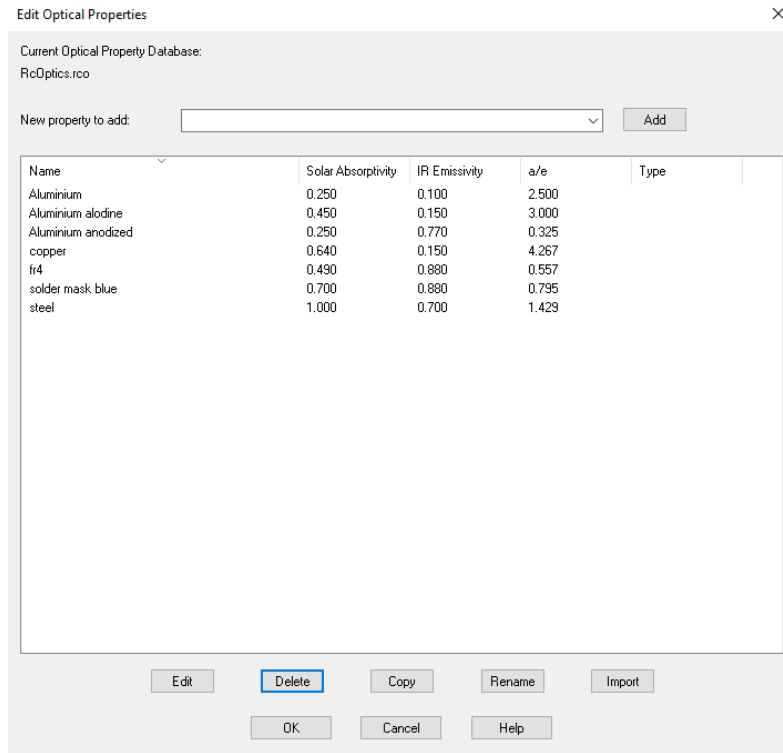


Figure 19: Optical properties database

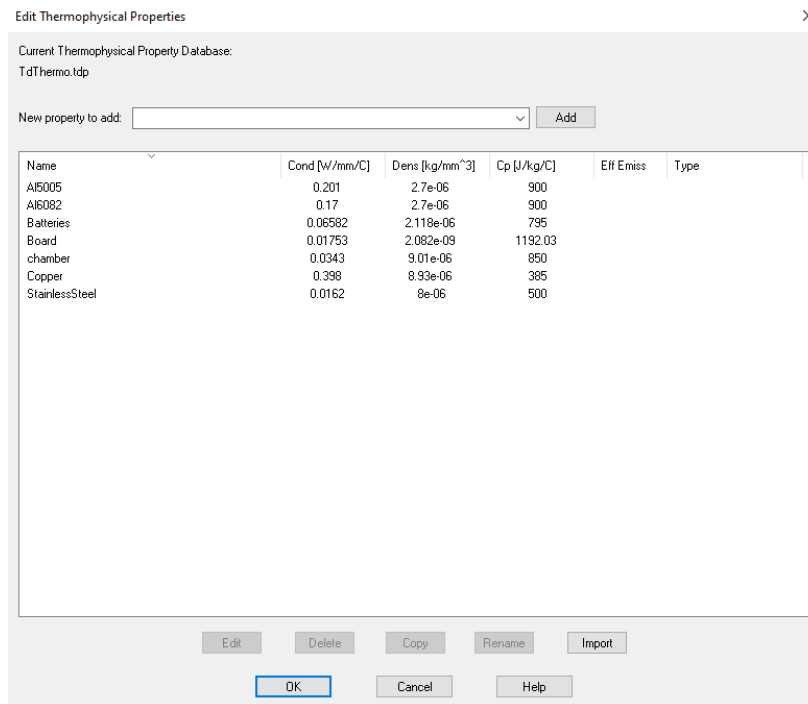


Figure 20: Thermophysical properties database

5.2.3.1 Structure

In order not to make the model too complex it was decided to adopt a simplification in the modelling of the structure. The two truss-like parts joined together by four brackets of the primary structure, and the external panels of the secondary structure were merged together, modelled by aluminium plate as thin shell elements, forming a box with the CTP dimensions. In order to maintain the simplicity of the model, an average of the different plates thicknesses has been set. The bulkhead was also modelled from a thin aluminium plate and positioned inside the platform to separate the service module with that of the electric propulsion system. Each plate of the external structure has been divided in 10 edges nodes for each unit of the side, leading to a number of external plates plus the bulkhead nodes of 2041. To give continuity to the external panels of the structure it was decided to join the coincident nodes to the intersections of the different panels. The bulkhead instead was connected to the top and bottom plates of the structure through the use of contactors. In this way the connection is more accurately simulated.

Top plate, Bottom plates and bulkhead materials implemented are Al6082 while lateral plates are made of Al5005.

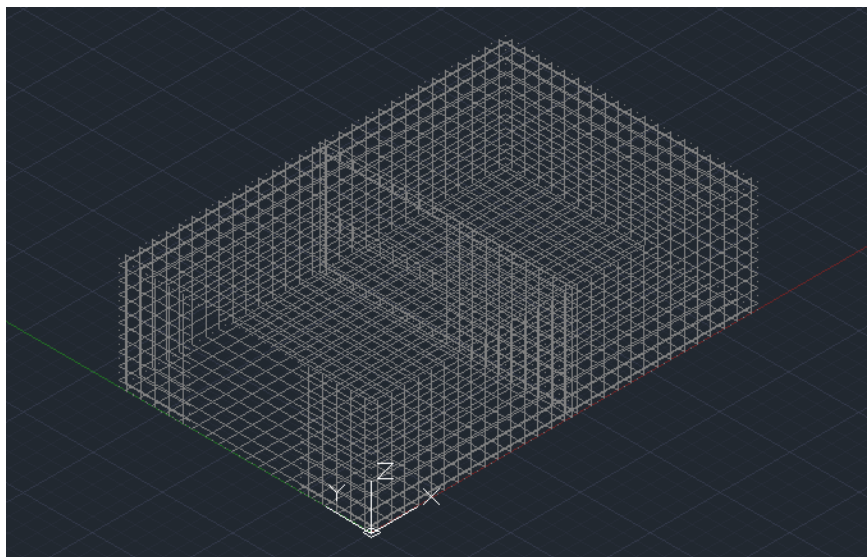


Figure 21: external structure and bulkhead models

The other two components of the secondary structure that have been modelled are: the battery packs drawer and the fileted bars on which the avionics cards are inserted.

The first one, is represented by a cube consisting of thin shell elements panels divided into its interior to accommodate the two battery packs, and designed in Al6082.

While the fileted bars are built with solid cylindrical elements divided into 10 nodes

along the longitudinal direction. As mentioned above, they are made of stainless steel. The following image shows the structure of the CTP with the secondary elements described above.

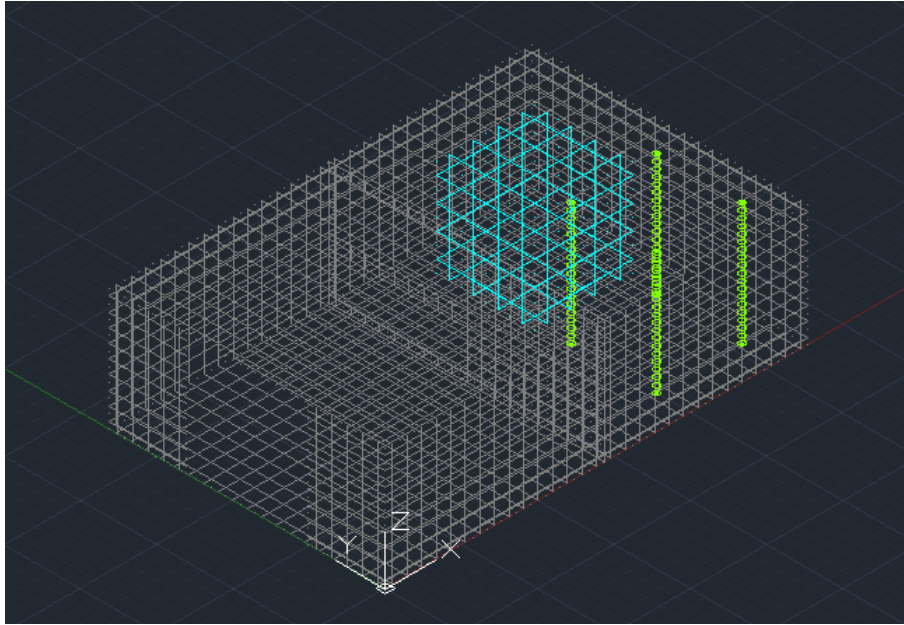


Figure 22: CTP primary and secondary structure

5.2.3.2 Avionics

The ESA-uProp 2 project foresees that the avionics occupy a dedicated unit, inside the service module. Therefore, the three electronic boards dedicated to the management of the electrical power for avionics, to the platform control and command and to the communication with the outside (EPS, C&DH and COMSYS), are stacked in series with the two boards dedicated to the interface with the propulsion system (HPMS and DL). The five boards, as already mentioned, are mounted on four stainless steel fileted rods. Each electronic board was modelled using a thin shell element divided into 64 nodes, and with a thickness of 2 mm. The material used is FR4. The connection between avionic boards and fileted bars was made by merging coincident nodes. Therefore, with this model, the physical differences between the different boards have been neglected (not in size, but in components mounted on the boards). This is partly true, because as will be explained later, with the insertion and modelling of thermal loads, particular components were considered such as to have specific thermal effects (for example, high power diodes, radio modules, etc.).

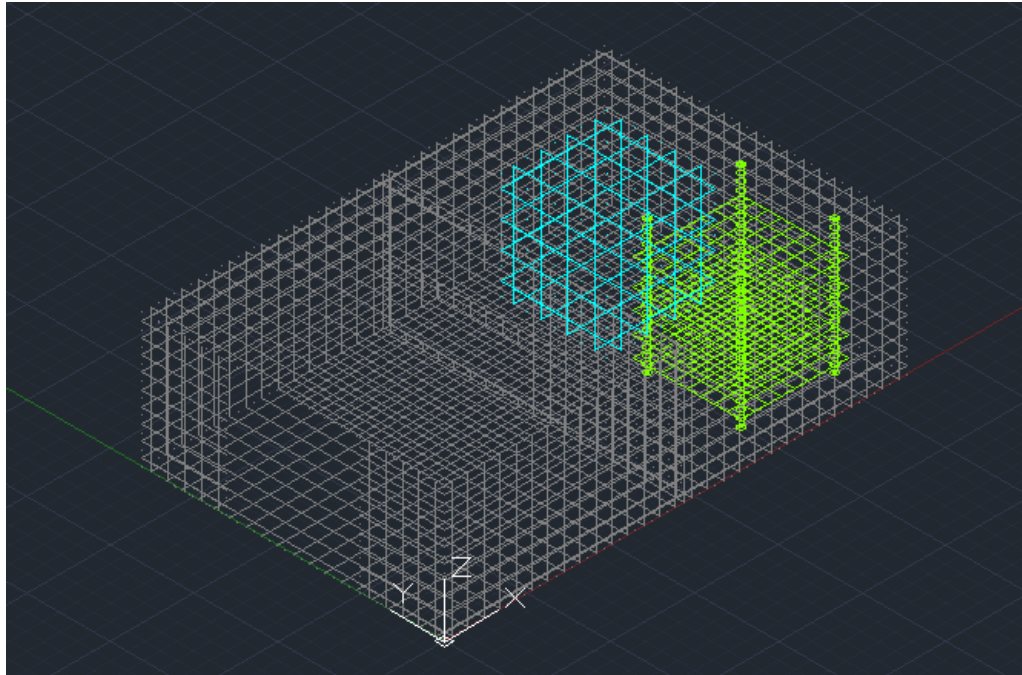


Figure 23: CTP model with structure and avionics module

5.2.3.3 Battery packs

Just like for avionics, the batteries are also placed in a dedicated unit, both those for avionics and those dedicated to PS. The battery drawer, the modelling of which has already been discussed, is divided into two compartments one above the other. Each compartment contains two battery cells for the avionics and six of those for the ePS. Although there are differences between the two types of batteries, it was decided to neglect the latter and create two solid brick elements in the two compartments of the battery drawer, each representing eight cells per compartment. This choice is due to the fact that the physical differences between the two types are minimal, and therefore for simplicity of modelling, also because in subsequent versions there will probably be a solution with the same batteries, it was decided to unify them. Battery packs are connected to battery drawer via contactors.

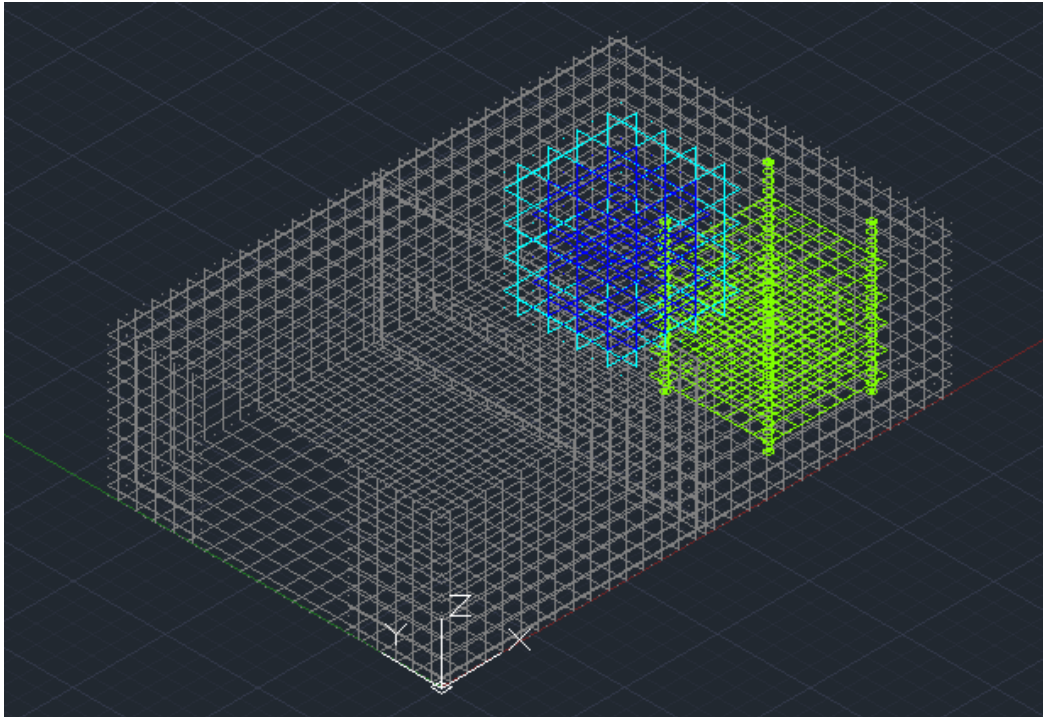


Figure 24: CTP model with structure, avionics and battery packs

5.2.3.4 Electrical Propulsion System

Unlike the modelling of the service module, of which almost all the information necessary for a faithful reconstruction were known, that of the ePS was more complex. This complexity is due to the fact that it is not always possible to know in detail the specifications of the PS, which is developed by an external company, and therefore, except for the interface requirements with the platform, it may not be completely transparent. Another reason is that having to make the model easily accessible for the simulation of different propulsion systems, the goal was to implement an adaptable model in a simple way, focusing on reproducing the aspects that influence the thermal environment of the platform faithful.

The model refers to the REGULUS propulsion system developed by the T4i company of Padua, which has a size of $15 \times 10 \times 10$ cm. Through the use of thin shell elements, the cylindrical external structure of the EPS was recreated. Furthermore, thanks to the information on the internal design provided by T4i, the volume dedicated to the tank has been added, and the cylindrical burst chamber belonging to the thrust section separated from the first by a vertical wall. In particular, the study focused on defining the contact between the ePS and the upper and lower panels of the structure. The ePS is fixed to both panels by 6×2.5 mm stainless steel screws on each side, which therefore generate a conduction coefficient of approximately 137 mm .

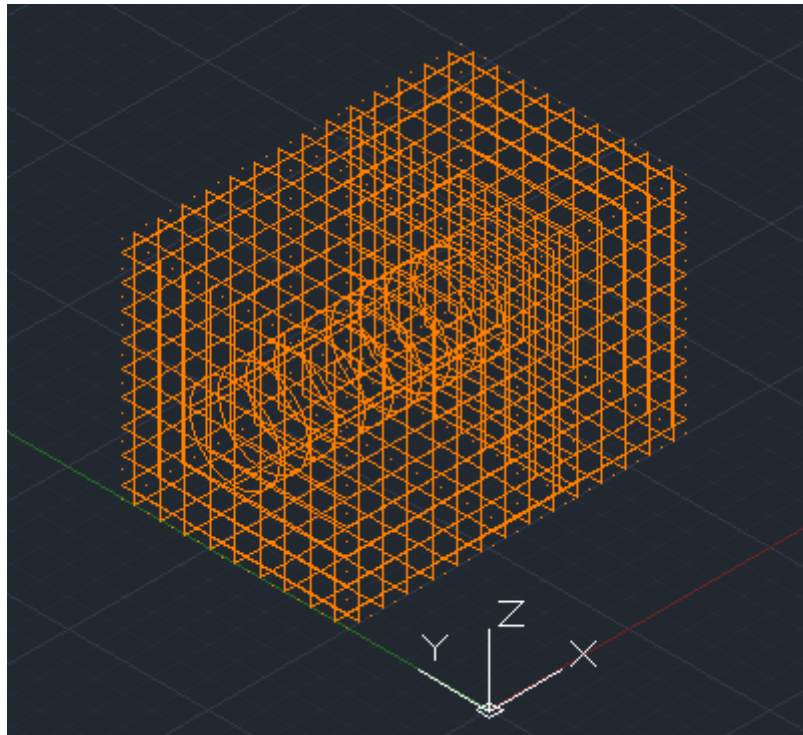


Figure 25: REGULUS ePS model detail

According to ECSS-E-HB-31-03A, in order to manage model complexity, a breakdown of the overall system thermal model into individual submodels has been made. A submodel represents an element, subsystem or equipment which can be treated as a separate entity. Also, the different submodels have been divided into layers, to facilitate their visualization and make their modelling easier.

5.2.3.5 Thermal loads definition

An accurate modelling of the thermal loads acting inside the platform, in terms of intensity, correct positioning and trend over time, is one of the most important aspects to be able to faithfully simulate parts of a mission or entire test sessions in a vacuum chamber. First of all, this task required an in-depth study of the different components on board the platform, in order to define which of them dissipated heat during their operation, whether they did so constantly or in a variable manner with time and with the operating mode of the CTP, and moreover, if the dissipations were punctual, concentrated in relatively small areas, or if they were uniformly distributed in a certain space.

In the first phase of model development, the focus was on the definition of the loads, through the estimation of components efficiency, and then their positioning within the model. Only in a second phase, which involved the first thermal simulations

and the validation of the model through the emulation of tests carried out in a vacuum chamber, the precise modelling of thermal loads has been made such that they reflected the mission profile of the tests, in terms of intensity and time variation. This phase will be described in detail in the *Model simulations and validation* section.

One of the first steps taken to determine the thermal loads to be included in the model was to estimate the thermal efficiencies of the various items on board. In this way it was possible to evaluate, according to the operating conditions of the CTP, the intensity of the different heat dissipations, based on the power budget of the platform.

Since the avionics and PS battery packs contain lithium-ion cells, the study of their efficiency has been generalized. The batteries were analysed both by studying the datasheets provided by the manufacturer and by collecting data on batteries based on the same technology as those implemented, and by tests carried out in the clean room of the Politecnico di Torino. A variable efficiency was estimated in the range [92 – 95] %, with lower values during the charging phase. The thermal dissipation generated by the batteries is to be considered proportional to the electrical power supplied by them during operations. The proportionality is not linear due to the slight variability of the efficiency, also dependent on other factors such as the operating temperature of the lithium ion cells.

Avionics is the main source of heat by thermal dissipation of the service module. Each of the five electronic boards dissipates heat in different ways and intensities. Analysing them in order of arrangement from top to bottom, the COMSYS board is first encountered. The radio module of the COMSYS has consumption peaks of about 1W in the transmission phase lasting 2 seconds every 30 seconds. In the model, for simplicity, it was decided to insert a constant average value of 0.05W as a thermal load distributed on the board near the radio module. The component of the CDH board that requires the greatest consumption of electrical power for operation is the microprocessor, which at full operation absorbs 1.75W. Data Logger is the subsystem with the lowest power consumption, as its function is only to collect the data coming from the sensors and send them to CDH for processing. Therefore, its heat dissipation, compared to that of the other electronic boards is negligible. The EPS is the system dedicated to the distribution and regulation of electrical power for the operation of avionics systems, and manages a peak power of approximately 3.3W. Considering an overall efficiency of the board slightly higher than 90%, a maximum heat dissipation of about 0.4W will be obtained.

The High-Power Management System is the avionics board with the highest power consumption, as it is dedicated to the regulation and distribution of the electrical power necessary for the operation of the PS. In ESA-uProp 2 there is a maximum supply of 60W to the propulsor, and therefore considering an efficiency of the board

of about 92%, dissipated power peaks of 5W are obtained. In addition, a margin of 20% dissipated power is added to the critical components for thermal analysis, bringing the peak to 6W. The greatest dissipation occurs in the Step-up DC / DC circuit which regulates the output voltage towards the PS at constant 12V with variable current up to 5A. Another area of the electronic board which is critical from the thermal point of view is where there are two power diodes (under the Kapton tape in the next figure), in which the dissipation is considerable.



Figure 26: HPMS board with temperature sensor in proximity of power diodes

The greatest thermal load when the platform is in operation is that generated by the electric propulsor. As the model must be adaptable to different electric thrusters, a standard heat dissipation configuration is not defined for each, but it can vary according to the PS implemented.

Taking into consideration the REGULUS ePS used for the development of the model, a distributed load was inserted into the thrust chamber to simulate the high internal temperatures, while the dissipated thermal power was distributed to the external faces, considering the ePS as a black box whose walls are heated from the inside and then diffuse heat inside the CTP. In particular, a thermal load has been inserted in correspondence with the twelve screws that fix the PS to the top and bottom plate, because these are the points where the heat is transmitted most to the structure of the spacecraft and then spreads to the other components.

The dissipated thermal power is proportional to the PS burst power and varies

according to the platform operating modes. In case of absence or uncertainty of data on the thermal efficiency of the tested PS, it is difficult to establish it a priori, and as in the case of REGULUS a test in the vacuum chamber was necessary to define in more detail the dissipated thermal load.

The following images show the thermal loads applied to the components of the CTP, the ePS and the structure.

The thermal dissipation of the batteries is considered uniform within their volume, and therefore a distributed volumetric load has been applied.

The COMSYS and HPMS electronic boards have surface thermal loads, distributed over certain areas of the boards: in the first one, the distributed load is faithful to the position of the radio module on the board, while on the HPMS the areas listed above are subjected to the thermal loads (step-up circuit, diodes) on which there are the greatest thermal dissipations. The remaining electronic boards have thermal loads concentrated in a central node for modelling simplicity.

On the structure there are the thermal loads in correspondence with the fixing screws of the PS, while four distributed loads of very small intensity $0.1W$ on the bulkhead have also been added, to simulate the dissipations of the LISN boards mounted on this part of the structure.

Finally, it is possible to view the thermal loads distributed on the external faces of the propulsion system.

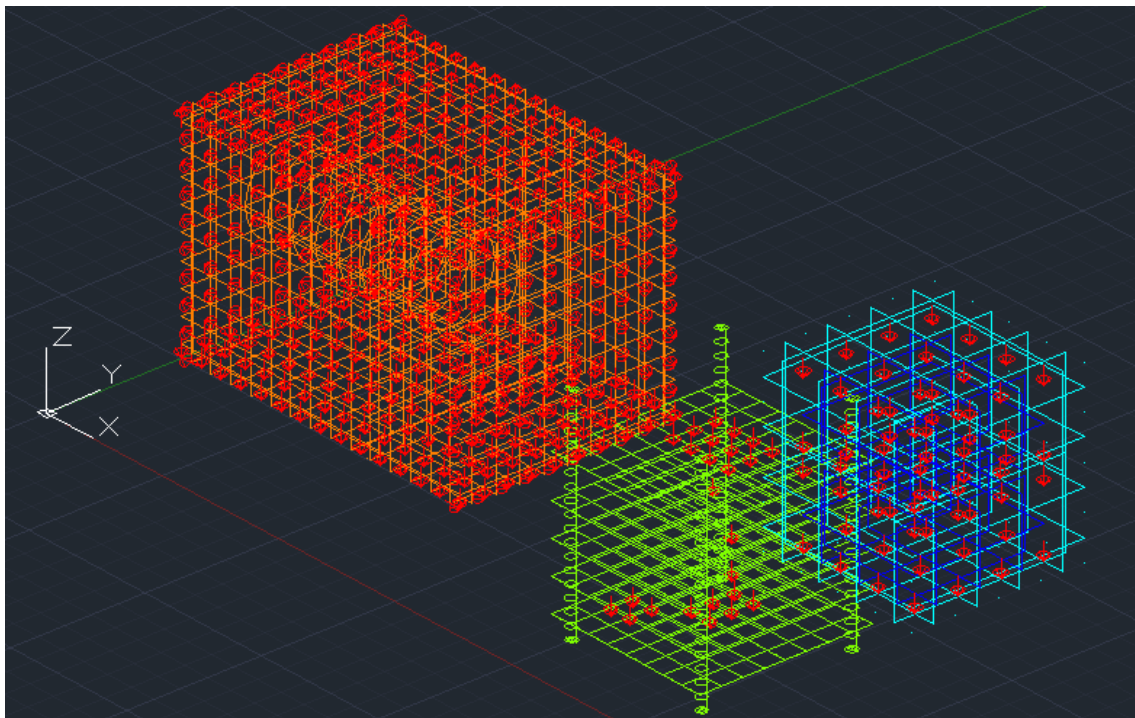


Figure 27: Batteries, avionics and ePS thermal loads

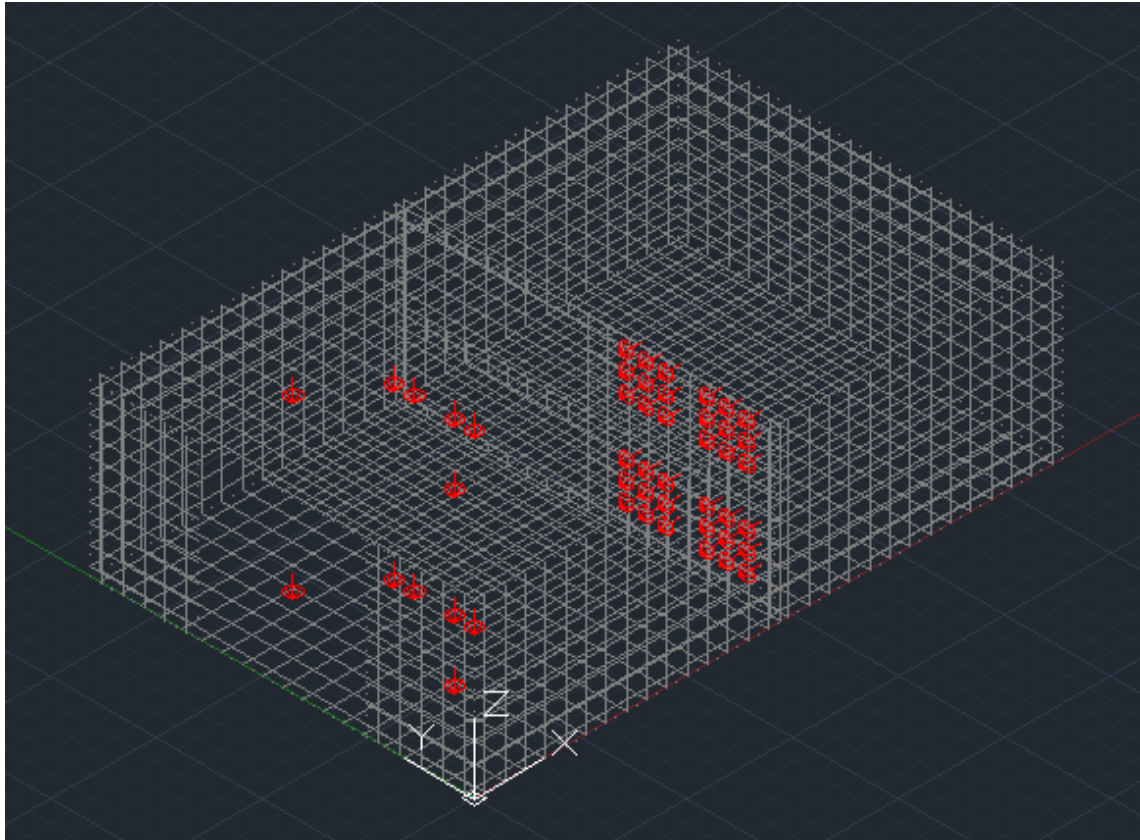


Figure 28: Structure thermal loads

5.2.4 Thermal control system

Once the thermal model was defined on Thermal Desktop, the first phase of thermal analysis through simulations began. Since, at this level of advancement, the model did not yet have the accuracy necessary to faithfully simulate the entire course of a test in a vacuum chamber, it was used to study the critical components from the thermal point of view, simulating the temperature conditions in the worst case in steady state, omitting for the moment the thermal transients.

As it had been guessed during the evaluation of the efficiencies and thermal dissipations of the various components, the highest temperature peaks were found on the HPMS electronic board, which manages the electrical power for the propulsion system. The image below is the result of a Thermal Desktop simulation in which the peak power of $6W$ is dissipated on the HPMS, and represents the stationarity condition at the end of the transient.

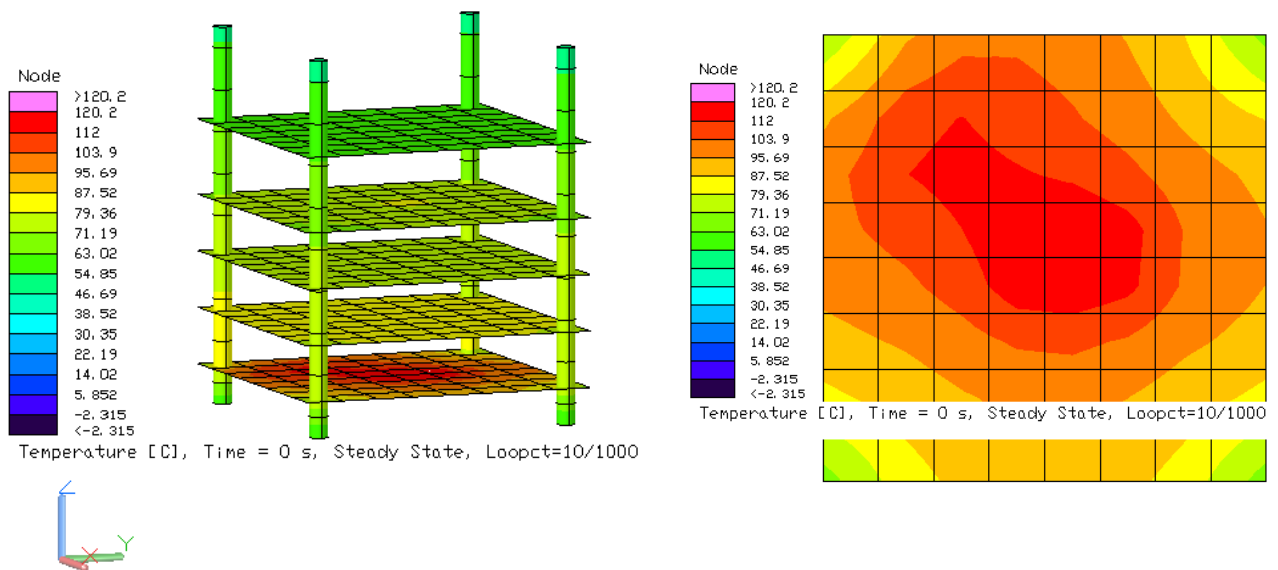


Figure 29: Thermal Desktop simulation of steady state

It can be seen how particularly high temperatures are reached on the whole board, but especially in correspondence with the thermal loads. The upper limit of the operating temperature range of the HPMS electronic board is about 100°C , it can be deduced that in such operating conditions the subsystem would undergo a degradation of performance, but most likely, due to such high temperatures, it would irreversibly damage.

Also, from the tests of development stage in the StarLab of the Politecnico di Torino, high temperatures were noticed on some components of the HPMS board, although in the clean room the phenomenon of convection with air has led to a thermal equilibrium around 70°C .

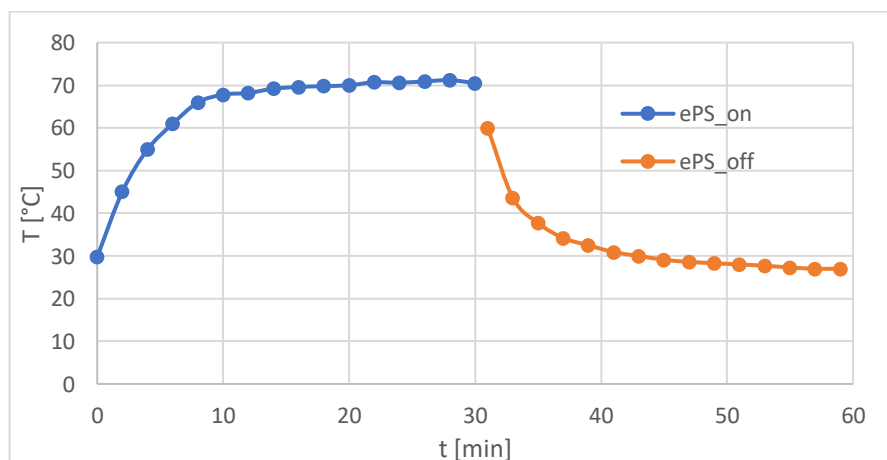


Figure 30: HPMS test in clean room with no TCS

The problem of heat dissipation on small components, and the problem of heat dissipation to avoid reaching too high temperatures for the on-board items, is a problem common to nanosatellites and in particular to CubeSats, especially when trying to implement in small-scale technologies such as electric thrusters, which require high power levels relative to the size of the spacecraft.

Furthermore, once these problems have been encountered, and control and thermal control systems implementation to mitigate the critical problems are needed, one of the fundamental aspects that characterize the CubeSat missions must be taken into account: low costs. This essential aspect means that more technologically advanced and attractive solutions, such as miniaturized active thermal control systems, must be abandoned in order not to exceed the project budget, falling back on solutions characterized by low costs and simplicity of design and implementation, but nevertheless, adequately effective and reliable.

Based on these assumptions and on the thermal problems encountered through the analysis with the thermal model, the solution adopted was to use as a passive thermal control system for the HPMS, a copper Thermal Strap connected to an heatsink attached to the board through a highly conductive rubber material, which allows to reduce the gap between the board and the dissipative surface. The thermal strap is connected at the other end to a copper plate attached to the structure panel on which the heat is dissipated.

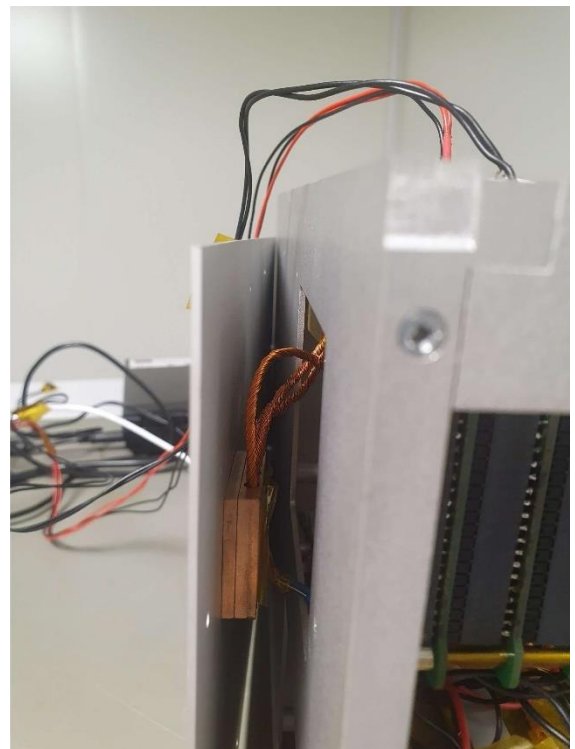
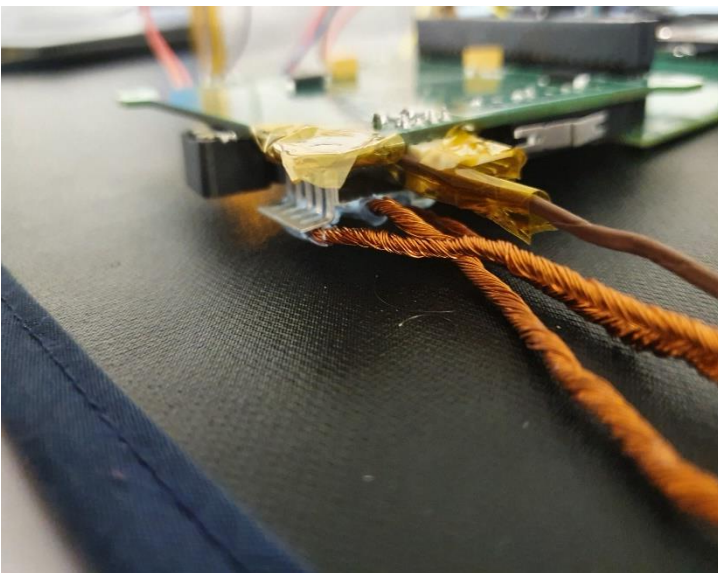


Figure 31: ESA-uProp 2 thermal control system

In this way, unlike the use of only the heatsink without gap filler, the maximum temperature drop reached by the electronic board was consistent, both from the data collected with the tests in the clean room, and with those of the simulations carried out on Thermal Desktop.

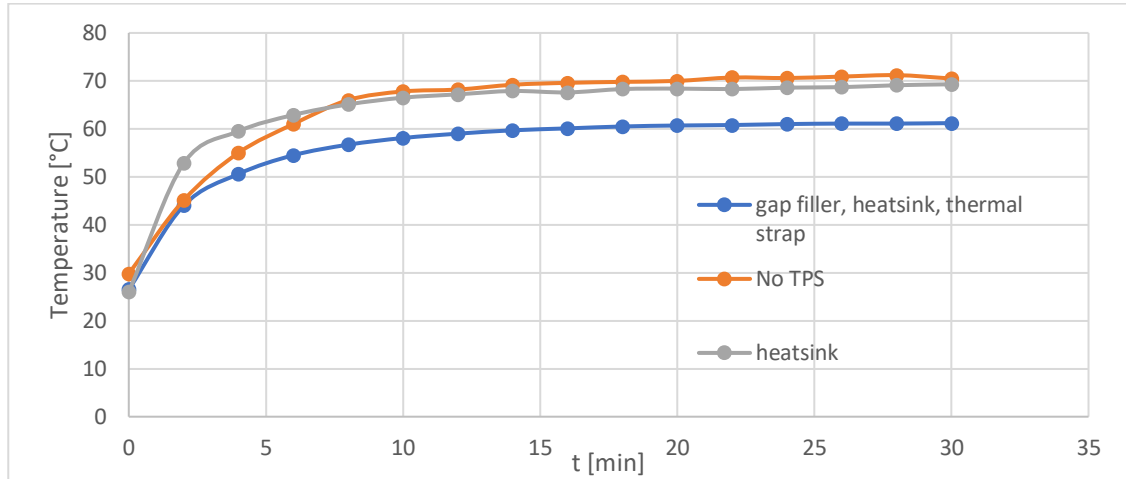


Figure 32: HPMS test in clean room

The Thermal Strap to perform its primary function *to provide thermal protection of the critical subsystems*, provides two other functions that derive from the first:

- To extract heat from HPMS equipments
- To transfer heat toward external components

The thermal control system was modelled on Thermal Desktop thanks to the use of the tools conductor, contactor and a solid brick element. The conductor simulates the behaviour of the heatsink connected to the HPMS and to the three copper cables of the thermal strap, which connect it to the copper plate. Therefore, in modelling this conductor, the contact surfaces and the length of the thermal strap of 5 cm were taken into account. The conductor acts on the area of the electronic board in which the thermal loads due to the diodes are present, and ends in the central node of the solid brick just as in reality the copper cables are inserted in the centre of the plate. In turn, the thermal plate is connected to the structure panel by 4x2,5 mm stainless steel screws.

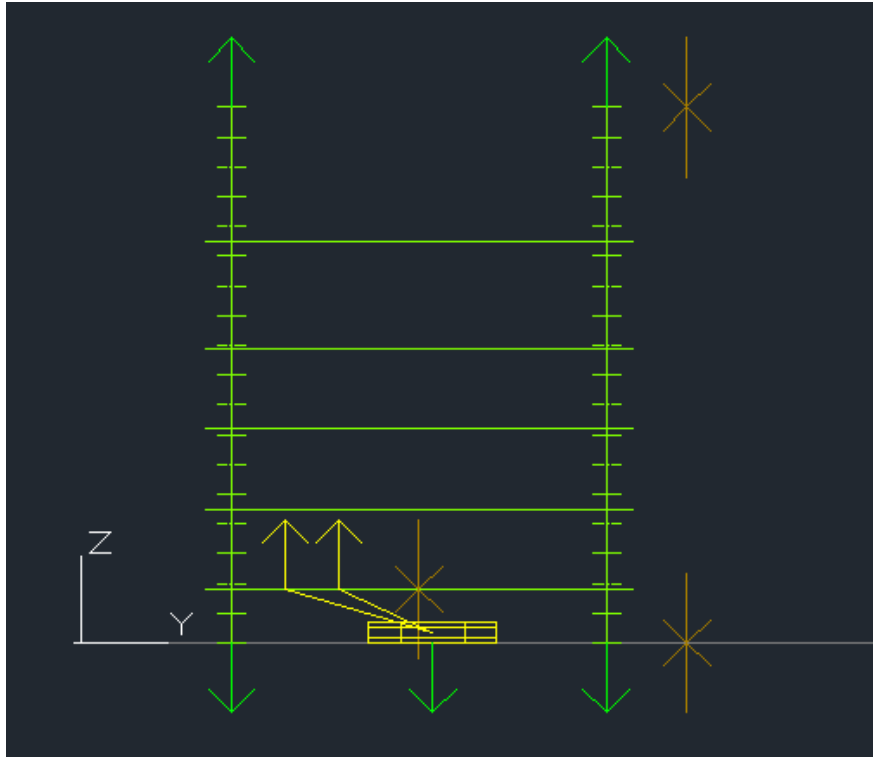


Figure 33: Thermal control system in Thermal Desktop

The implementation of this system in the Thermal Desktop model allowed to analyze its effectiveness through simulations of the stationary condition of the platform thermal equilibrium and in particular of the HPMS subsystem. The result of the simulations is shown in the following images. It is noted that there was a decrease of about $20\text{ }^{\circ}\text{C}$ in the peak temperatures on the electronic board, and how the use of the thermal strap brings benefits from a thermal point of view, particularly in the critical area where there was a strong dissipation due to in the presence of the two power diodes.

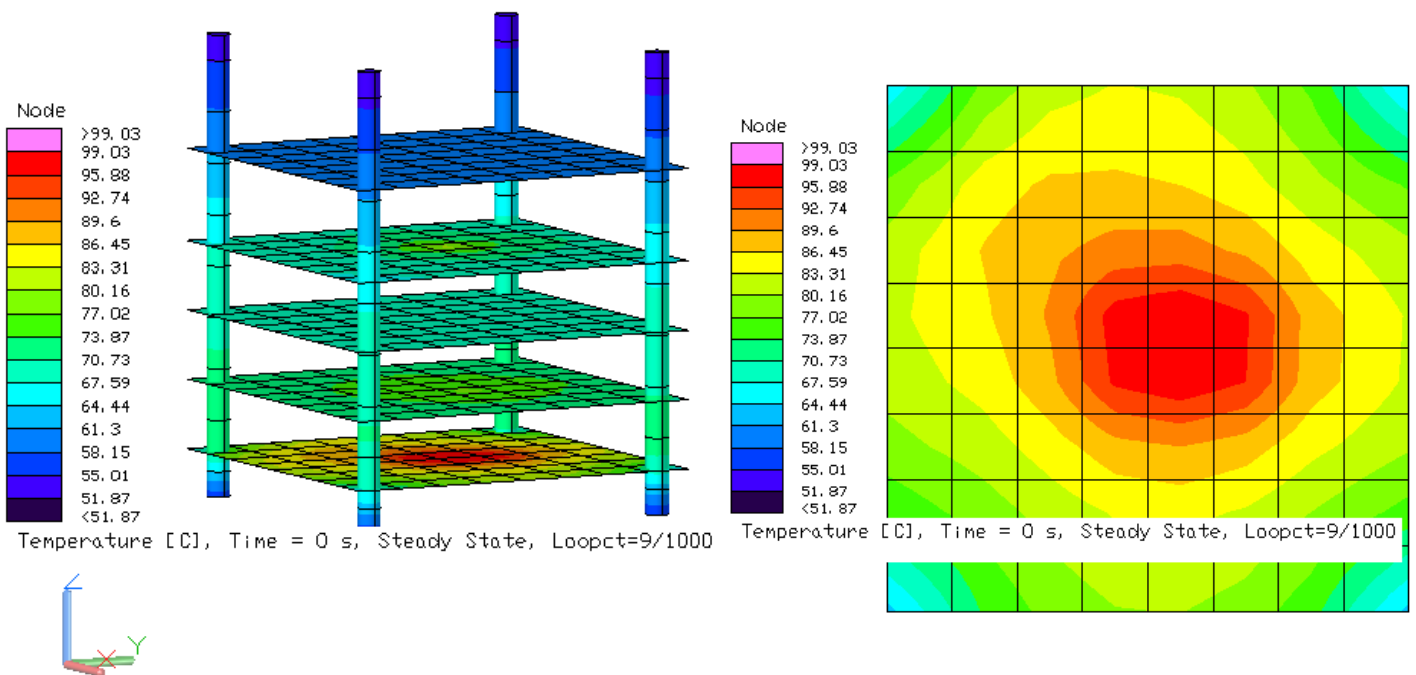


Figure 34: Thermal Desktop simulation of steady state with thermal control system

The simulations of the steady state in which the maximum power is dissipated, including the additional margins, are to be considered as the worst case from the point of view of the thermal stress to which the components are subjected. Frequently, in the reality of the mission, the state of thermal equilibrium is never reached, because this requires very long times in the same load conditions. Therefore, the fact that the maximum temperature reached by the HPMS board is below the 100°C limit of the subsystem is positively evaluated.

5.2.5 Model simulation and validation

5.2.5.1 Thermal analysis set-up

The first simulations carried out with Thermal Desktop seen in the previous section were made with the aim of studying the most critical elements of the platform, using the steady state mode. This made it possible to design and implement a thermal control system, necessary to protect the most overheated electronic boards. Parallel and iteratively to this process, the thermal analysis phase of the mission scenarios envisaged by the Test Plan and by the requests of the developers of the ePS was carried out.

As prescribed by the ECSS-E-ST-35C, about the Propulsion general requirements, The duration of the firing phase to be tested shall be as the same of the highest

duration manoeuvre considered for the mission. Since the CTP must be able to repeat its mission for different types of ePS, the flexibility of the platform must allow in the best way to be subjected to firing phases as long as specified by the developer of the propulsion system [3].

According to the will of the T4i company, manufacturer of the REGULUS micro-electric propulsor, the maximum duration of the burst mode to be tested is two hours. To this must be added a phase of pre-heating of the engine, necessary to bring the fuel to the desired temperature of 90 ° C.

The worst mission scenario from a thermal point of view for the CTP is therefore the one in which the burst phase of two hours is carried out in a vacuum chamber with unheated walls, but at room temperature.

The power budget of the CTP Burst mode, derived from TN02 – *Test Platform Design Report*, is detailed in the following table.

S/S Burst mode	ePS	HPMS	CDH	COMSYS	LD	TOT.
Power Consumption [mW]	50000	5196	720	672	120	56708

Table 6:CTP Burst mode power budget

The simulation of the CTP mission scenario was performed considering the end of the warm-up phase and the start of the burst phase as the initial time. The modelling of the loads acting in the pre-heating phase and the related simulations were subsequently developed with the support of the empirical data of the tests performed in the vacuum chamber. Therefore, for setting the initial temperature of the various onboard components, an ambient temperature of 20 °C prior to pre-heating was considered, to which the dissipation effect of the ePS, avionics and batteries was added, brought the components to an initial temperature in the interval [25 – 30] °C depending on the component considered.

Through the Case set manager tool, the simulation to be performed, to analyse the desired mission, was set. Contrary to those seen previously, this analysis is made on the transient condition of the different components temperatures of the CTP, and how they vary over time in this thermal condition of greater stress. Therefore, a duration of the transient condition of 7200s has been set, corresponding to the two hours of the burst phase. The integration time step chosen is variable, in this way the simulation is

optimized, reducing the times and avoiding problems of numerical instability that could occur with a fixed step.

This worst-case thermal simulation was repeated numerous times during the iterative process that involved model development, refinement, and later validation. Initially the results of the analysis were not very accurate and had considerable uncertainties, while with the improvement of the model and the use of the results of the tests in the vacuum chamber the accuracy of the results has become increasingly greater. The results are presented in the *Results and discussion* section.

5.2.5.2 Thermal model validation

“Validation is the process of determining the degree to which a computational model is an accurate representation of the real world from the perspective of the intended uses of the model” [7].

Accuracy indicates the correlation of the analysis results with real data, usually obtained from physical tests. “The purpose of the verification and validation effort is thus to improve and quantify modelling accuracy.

In the analytical process of temperature prediction with a thermal mathematical model, a number of inaccuracies due to the depth of modelling, available physical data and lack of precise definition of the item and its environment are present. All these different inaccuracies lead to temperature uncertainties

Generally, the uncertainties reduce during the course of a project as a consequence of the use of more detailed models and improved knowledge of the properties usually obtained by tests” [7].

[7]

As prescribed by ECSS-E-ST-31C, in order to provide data for the validation and verification of thermal model, a thermal test (called Thermal Balance Test) shall be performed. The correlation between the results of the analyses and those of the test must be successful in both transient and steady state conditions. Through this thermal test the functionality and performance of the components that make up the thermal control system are also checked [14].

“According to ECSS-E-HB-31-03A, typical temperature uncertainty values, together with a short definition of the TCS activities and models relevant to the C and D phase project, are:

1. TCS detailed design with detailed overall TMM, where all items are modelled explicitly.
2. Typical uncertainty: ± 8 K before thermal balance tests.

3. Typical uncertainty: ± 5 K after thermal balance test and TMM correlation”
[7]

As defined in the Test Plan, following the tests carried out in the clean room of the StarLab at the Turin Polytechnic, the CTP was brought to Padua for mission tests in the vacuum chamber of the T4i company, manufacturer of the ePS REGULUS.

During the test campaign in Padua, on the 25th of September 2020, the test that allowed to improve and validate the results of the thermal model of the CTP created on Thermal Desktop was performed. This was a mission simulation test, also considered as a thermal test dedicated to the correlation between thermal model and thermal behaviour of the CTP. The test lasting just over 100 *min*, with a 45 *min* burst phase.

After a first short cooling phase (about 5 *min*), which was necessary since the platform had previously been subjected to tests that had raised the temperature of the various components, the test was divided into three phases:

Test phase	Description	Duration
Initialization	In this phase the recharging of the PS batteries is completed, then the ePS is switched on and the pre-heating is carried out to bring the propellant to a suitable temperature. CTP exchanges data with the propulsion system to check its condition. HPMS regulates the voltage of the ePS at constant 12V.	25 <i>min</i>
Burst	The CTP goes into <i>Burst on</i> mode. The propulsor generates thrust with a power of 20W. The current supplied to the propulsion system varies	45 <i>min</i>

	in the range $[4.5 - 3.5]$ A. Meanwhile, the power supplied by the battery PS varies in the range $[55 - 42]$ W.	
Controlled cooling	At the end of the burst phase, the current supplied to the thruster is reduced to less than 2A. In this phase, data are collected on the cooling trend of the ePS and the CTP.	15 min

Table 7: Test procedure description

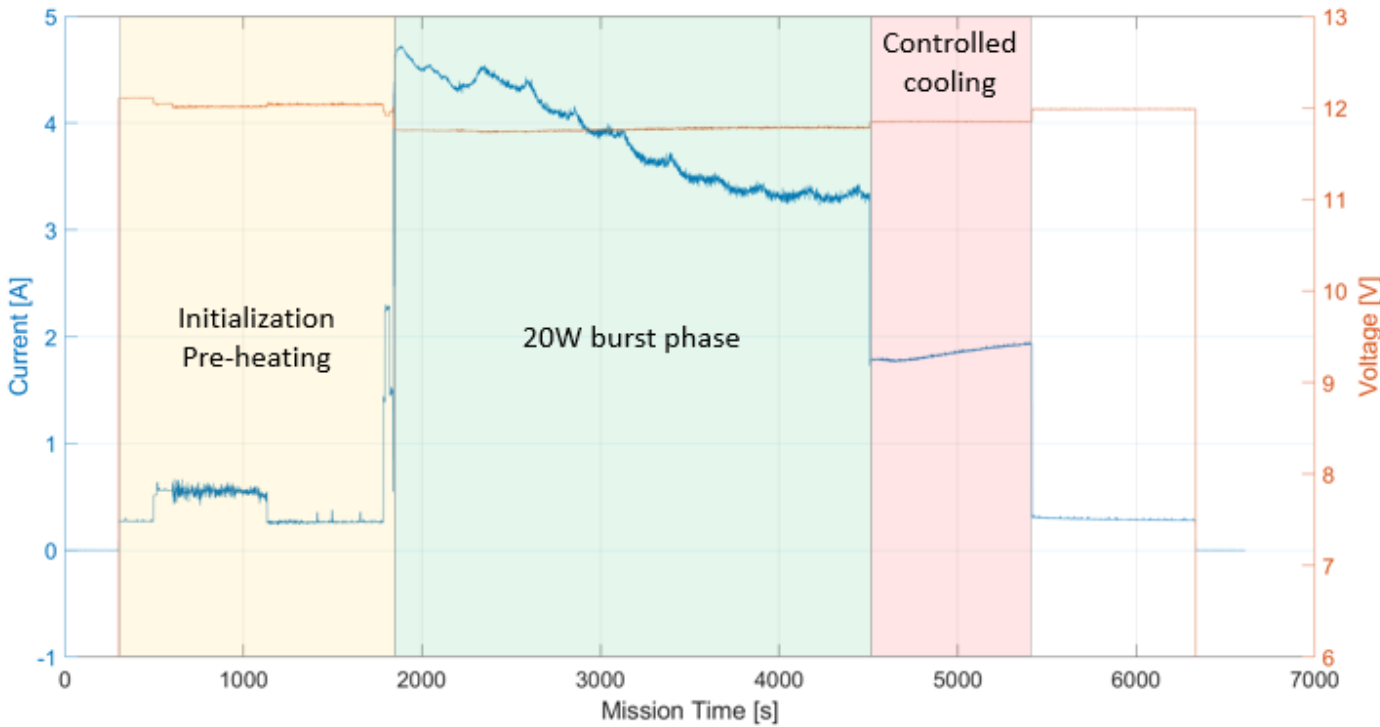


Figure 35: electrical mission profile

Thanks to the various sensors on board, it was possible to collect numerous data on different measured quantities. For thermal performance data, eight temperature sensors were used in the service module, and seven more to monitor temperatures on the structure bottom panel in the PS module. The data collected by the sensors are

processed by the Data Logger and the Command and Data Handling, collected in the SD memory and, after the test, post-processed in *MATLAB*. The following temperature trends are obtained during the test.

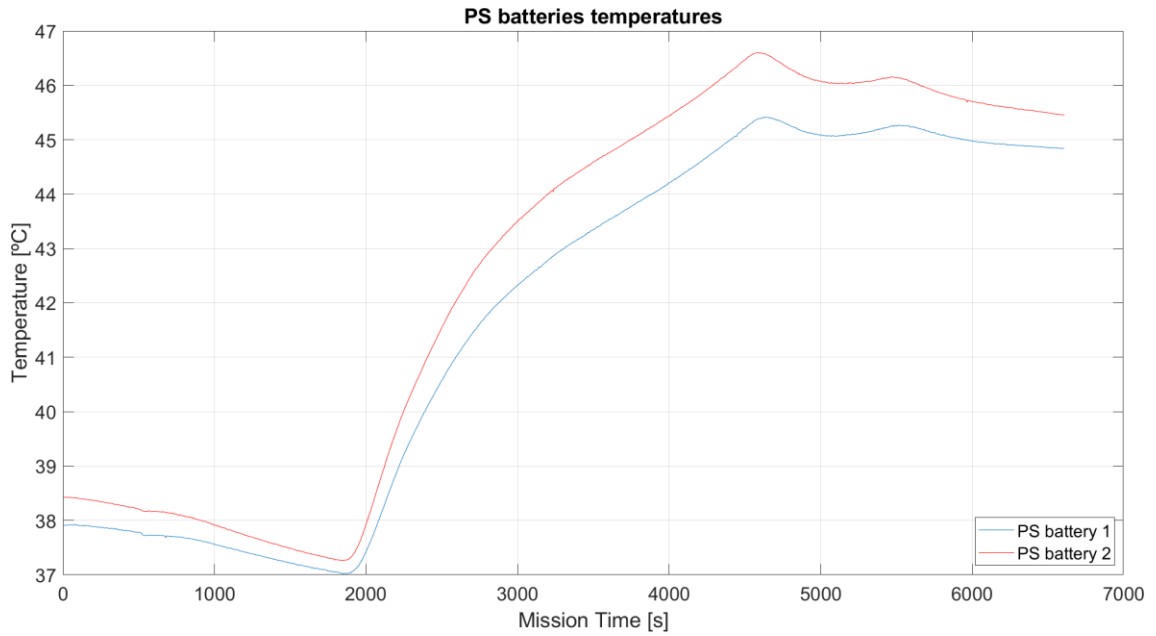


Figure 36: PS batteries temperatures

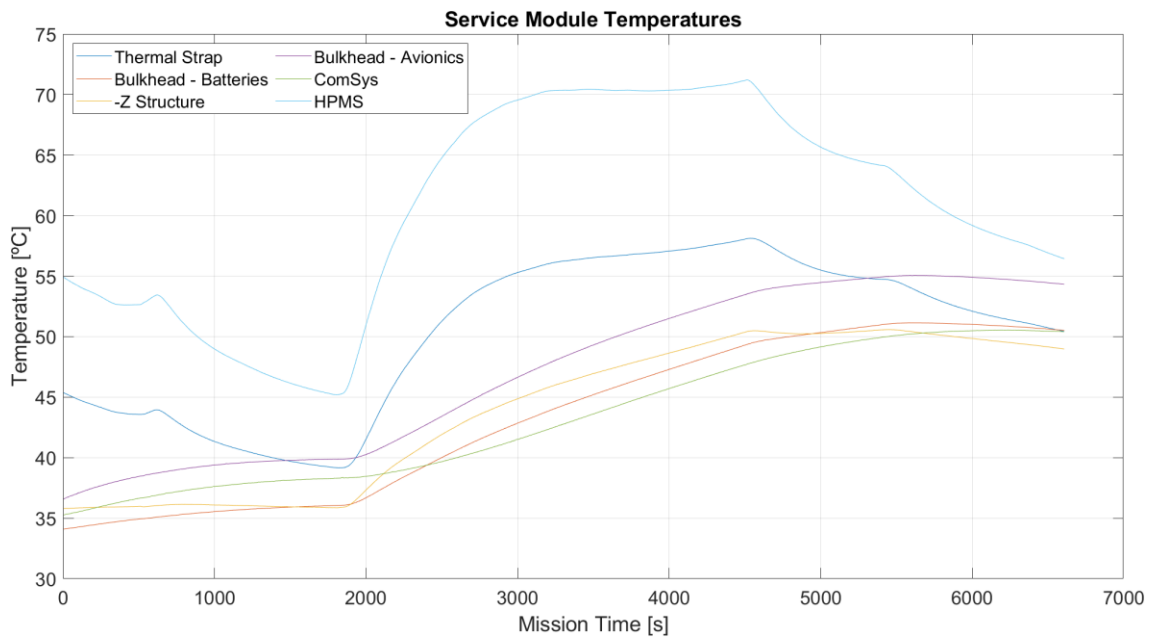


Figure 37: Service module temperature

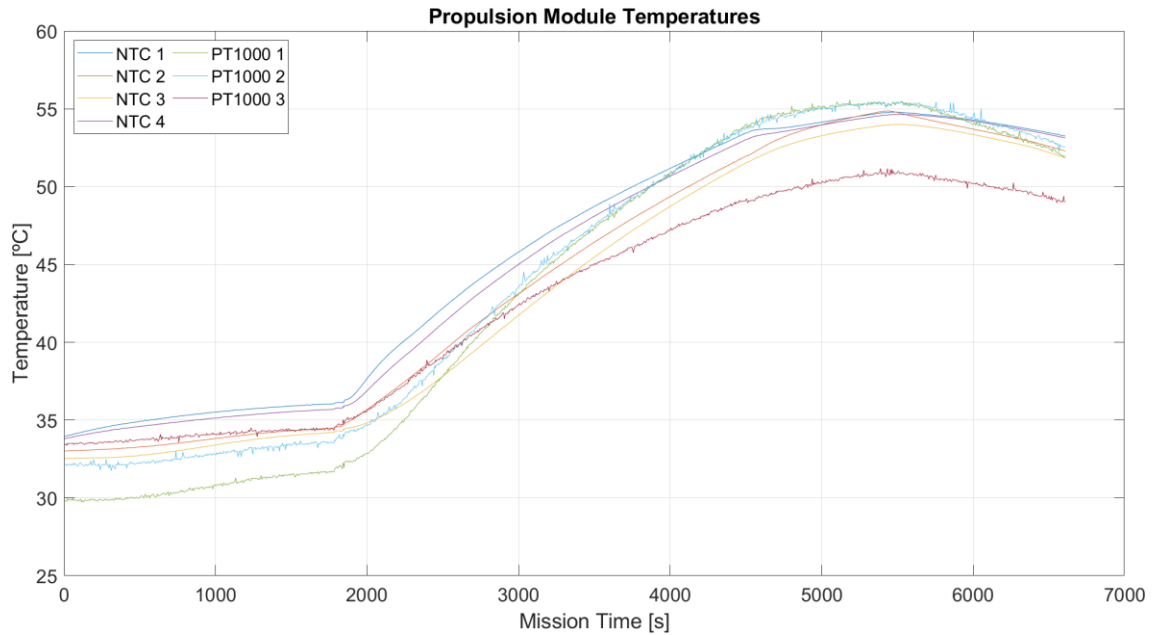


Figure 38: PS module temperature

It can be seen how, at the end of the firing phase (about 4500s), only the HPMS board and the TCS plate connected to the Thermal Strap have reached a temperature of thermal equilibrium, while it is clear how the temperatures of the other elements are still in a phase of transitory with increasing values.

To simulate the test performed in the vacuum chamber on Thermal Desktop, the burst phase and the initialization phase were modelled individually, then the entire test was simulated. This mode allowed a more in-depth study on the operating conditions of the platform in the different phases of the test, and therefore it was possible to adequately analyse and model the loads acting on the various items in each operating condition.

Starting from the burst phase, the most important for analysing the transient thermal dynamics of the different components of the CTP subjected to a thermal load close to the maximum, the power of about 50W supplied by the PS batteries to the propulsion system through the HPMS, has been divided between the electronic board and the ePS, excluding the 20W used by the latter for the production of thrust. After setting the constant loads for the 45 min firing both on the batteries and on the HPMS and ePS, the model has been refined considering the current variation supplied in this phase (see figure 35) which reduces the power supplied from 55W to 42W. The decrease of about a quarter of the power supplied to the ePS results in a proportional decrease of the thermal loads acting on the various components involved.

The results obtained with the simulations of this phase were satisfactory. The comparison of the data on the critical component HPMS and the TCS plate, relative to the burst phase, is shown below.

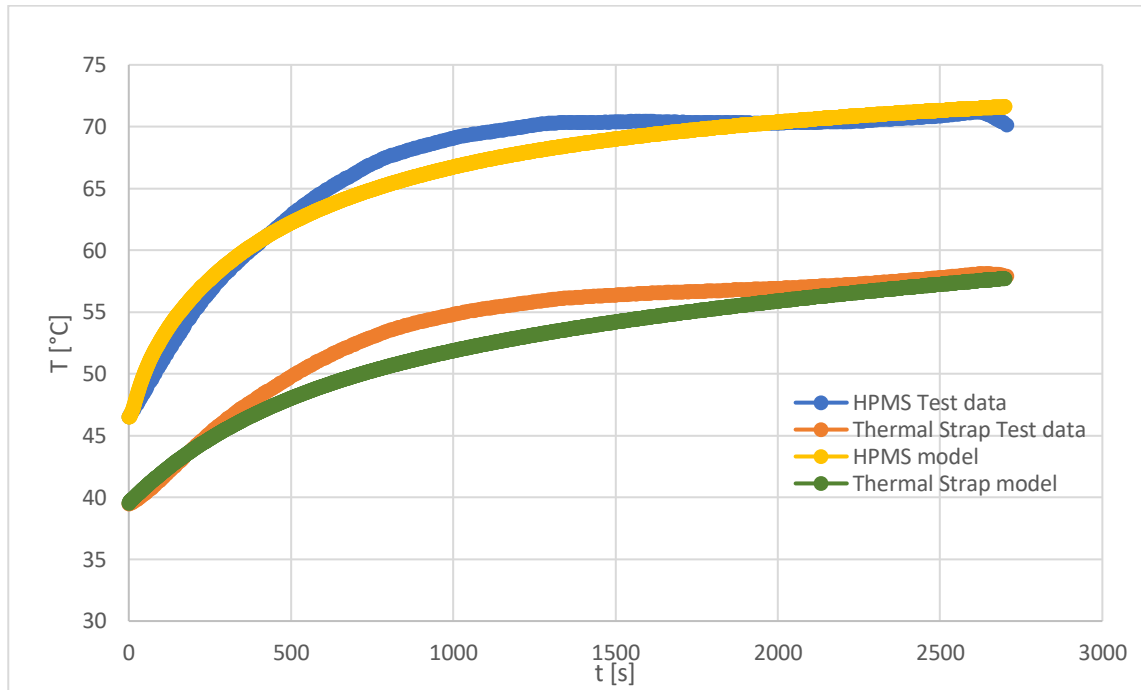


Figure 39: Burst phase test and simulation data

$$ERR_{HPMS} = \frac{|T_{HPMS_{test}} - T_{HPMS_{model}}|}{T_{HPMS_{test}}} \cdot 100 = 4,0\%$$

$$ERR_{TS} = \frac{|T_{TS_{test}} - T_{TS_{model}}|}{T_{TS_{test}}} \cdot 100 = 5,3\%$$

After demonstrating that the model faithfully simulated the response of the platform to the thermal loads of the burst phase, the first phase of CTP cooling, battery charging, and pre-heating of the ePS was modelled.

The modelling of the loads for this phase was more complex than the previous one, since instead of considering linearly decreasing peak loads, it was necessary to analyse in detail the different processes carried out by the various components of the platform, such as the initial charging process of the battery packs, the pre-heating phase of the EPS, or the approximately constant consumption of the avionics subsystems (excluding the HPMS).

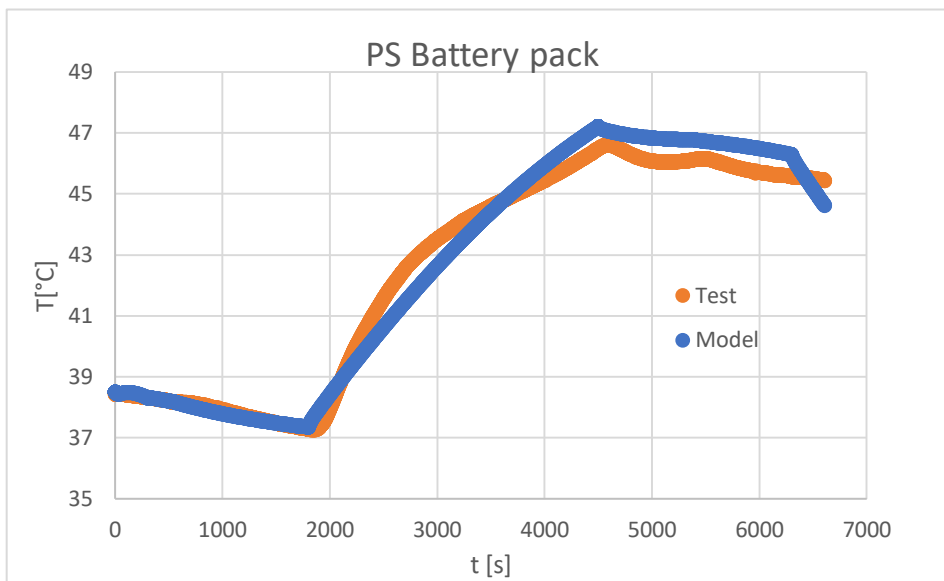
This in-depth study has allowed, in addition to the modelling of thermal loads, the improvement of the entire thermal model, improving the realization of different elements such as the contacts, the characterization of the materials, the definition of the thermal inertias of the components.

Finally, the entire test performed in a vacuum chamber was simulated, allowing to evaluate the validity of the model for each operating condition performed. The results and related assessments are presented in the next section.

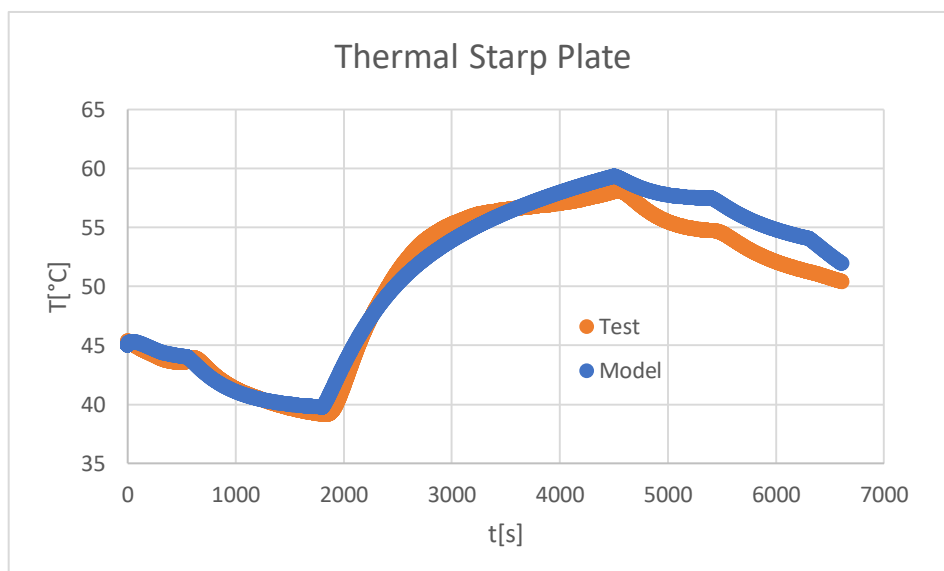
5.3 Results and discussion

In order to study the deviations of the simulations compared to the thermal tests in the vacuum chamber, the test data was plotted and compared with the output data of Thermal Desktop by post-processing. The data, relating to the different elements and subsystems, refer to the nodes corresponding to the positions of the temperature sensors used during the test.

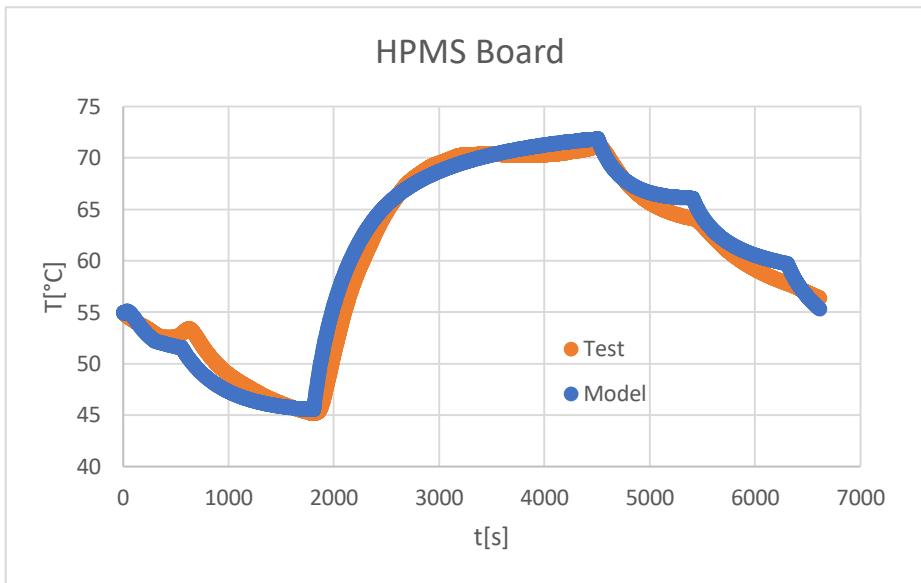
The results of the test correlation are presented below.



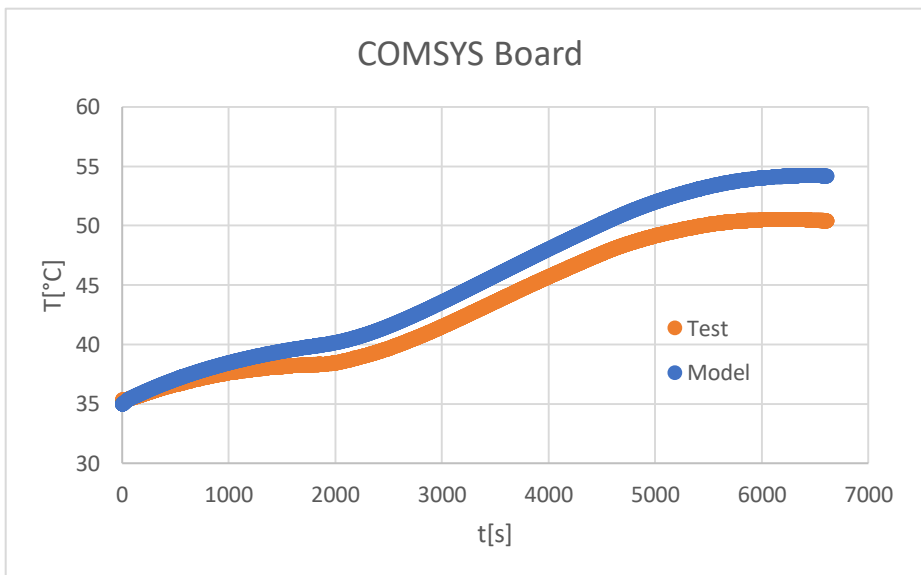
- $ERR_{MAX} = 2,8\%$
- $\Delta T_{MAX} = 1,2^{\circ}C$



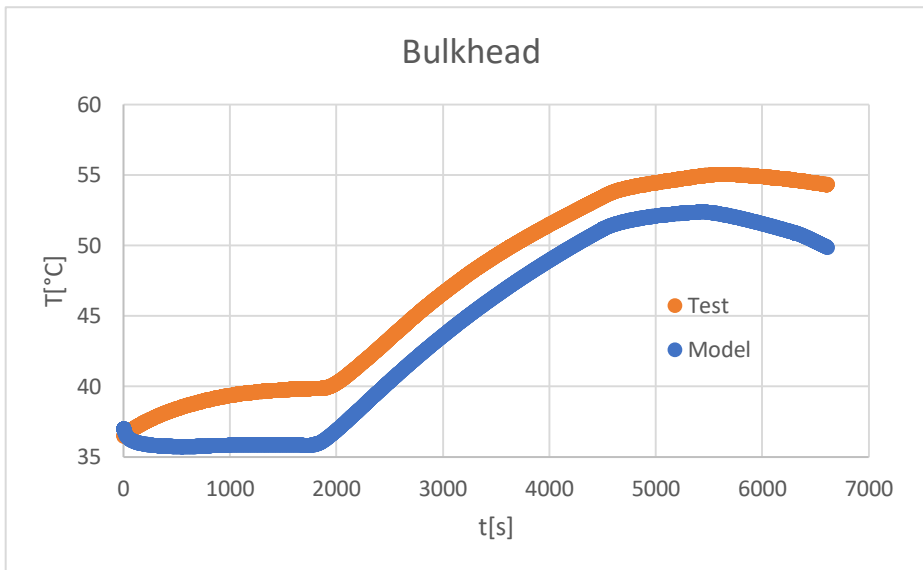
- $ERR_{MAX} = 4,7\%$
- $\Delta T_{MAX} = 2,6^{\circ}C$



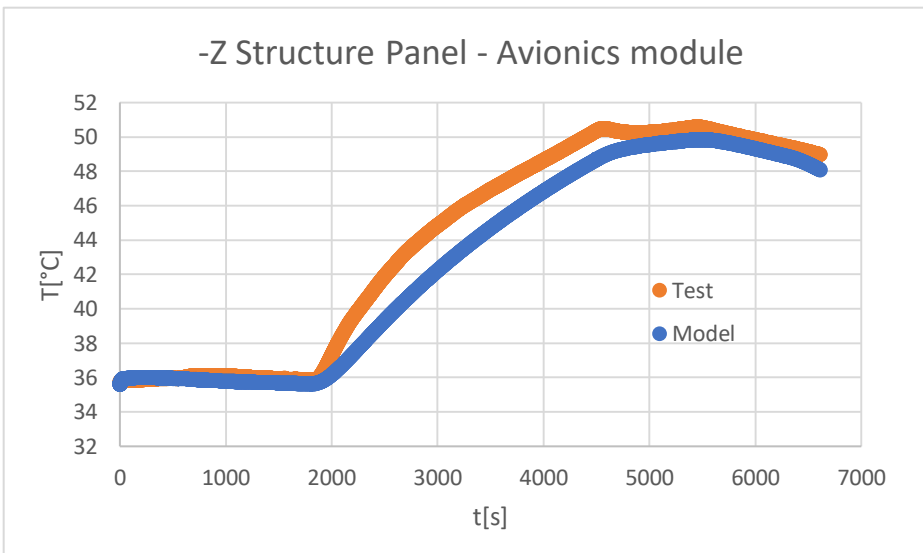
- $ERR_{MAX} = 4,0\%$
- $\Delta T_{MAX} = 2,7^{\circ}C$



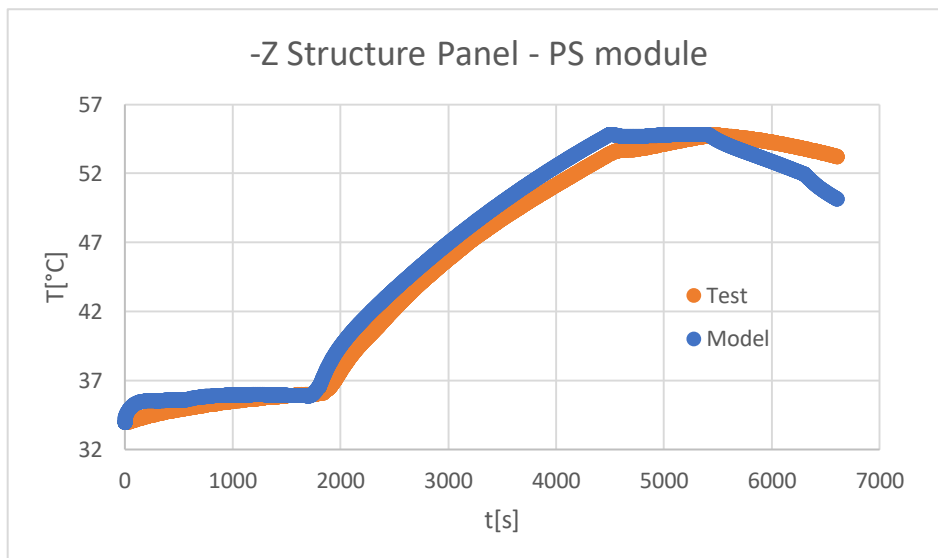
- $ERR_{MAX} = 7,5\%$
- $\Delta T_{MAX} = 3,8^{\circ}C$



- $ERR_{MAX} = 9,5\%$
- $\Delta T_{MAX} = 3,8^{\circ}C$



- $ERR_{MAX} = 5,4\%$
- $\Delta T_{MAX} = 2,4^{\circ}C$



$$ERR_{MAX} = 5,8\%$$

$$\Delta T_{MAX} = 3,1^{\circ}C$$

As shown by the comparisons graphs, each element analysed has a thermal response similar to that of the real element during the test in a vacuum chamber. Furthermore, it appears that all of them comply with the specification dictated by the ECSS-E-HB-31-03A regarding a maximum uncertainty of $\pm 5K$ after the thermal test. Furthermore, in almost all the elements analyzed, the firing phase of the test is the one in which there are the minor differences between the two curves, especially as regards the trends. This is a positive aspect as it is extremely important to be able to simulate the CTP firing mode as accurately as possible. In particular, the accuracy of the model relating to the HPMS avionics board and that of the thermal control system, which are decisive for the validity of the thermal model, is satisfactory. The major delta T's are found in the graphics of the COMSYS electronic board and of the Bulkhead. In the first case the biggest difference occurs in the initial phase of the test, while in the second during the final cooling phase. However, both values fall within the validity ranges considered. A possible improvement of the model could foresee an improved accuracy for these two elements.

Once the validity of the thermal model was assessed by comparing it with data resulting from the physical test performed in a vacuum chamber, the study proceeded with the simulation of a mission characterized by a burst phase lasting two hours, that is, as explained in the previous sections, the case of greater thermal stress for the CTP. The results related to the avionics module are presented below. The heat map shown in the figures relates to the final instant of the simulation, while the graphs shows the temperature trend on the HPMS board and Thermal strap during the two hours of burst mode.

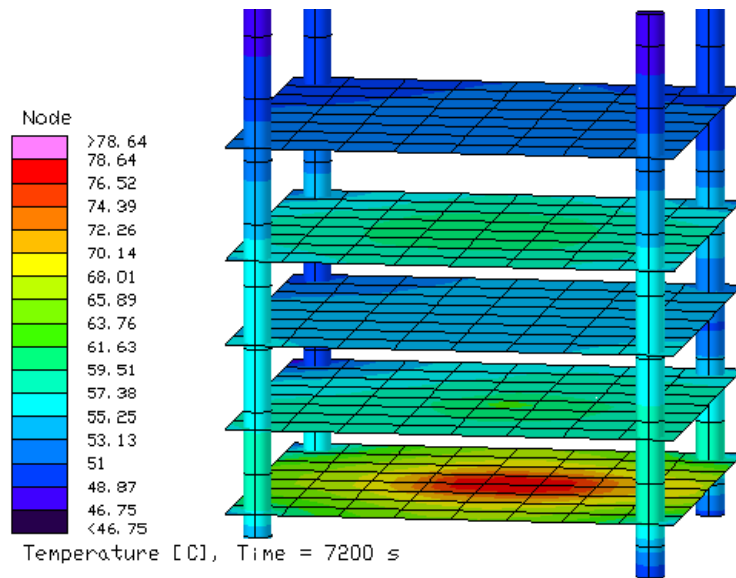


Figure 41: Thermal Desktop simulation of worst-case mission

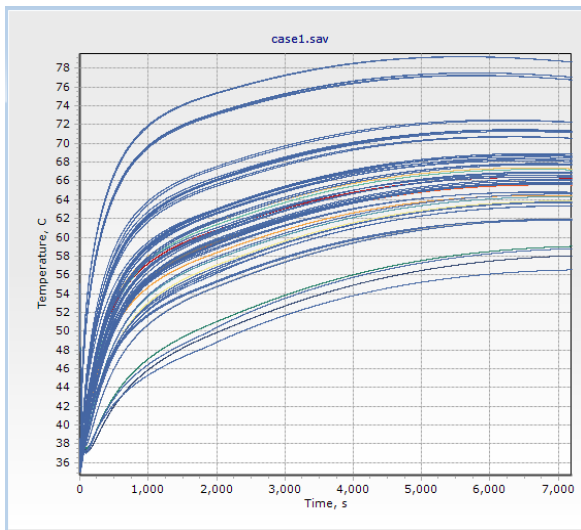


Figure 40: HPMS nodes temperature

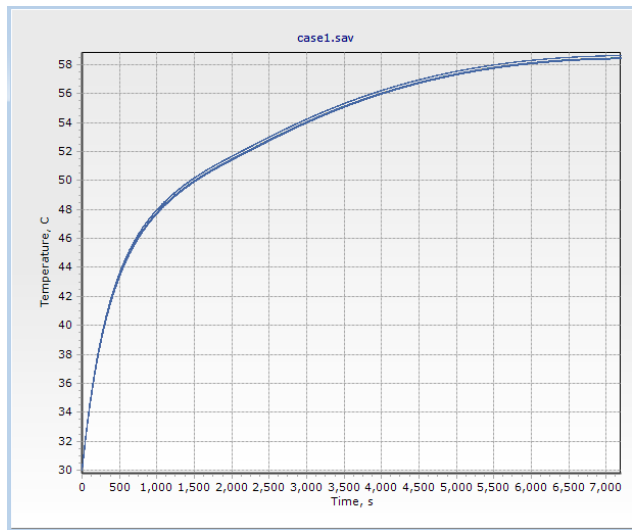


Figure 422: Thermal Strap nodes temperature

The results obtained with the simulations demonstrate the effectiveness of the thermal control system in keeping the most critical element of the CTP avionics module within the operating temperature range.

6. Case study 2 - ESAuProp-3 TCS Design

The ESA-uProp project 3 is about the design, development and verification of a 12U CubeSat test platform (CTP) which host a miniaturized electric propulsion system.

The project is based on the results obtained with version 2 of the ESA-uProp project, and starting from these, it aims to develop a CubeSat platform prepared for the integration of different electric propulsion systems, with the possibility of achieving higher performance and propulsive power. In addition to verifying the performance of different ePS, the other main objective of the CTP mission is to evaluate the mutual interaction between the electric propulsion systems and the platform that hosts them.

Main drivers for the platform design are: flexibility / adaptability of interfaces (mechanical, electrical, and data) towards propulsion system, accessibility, simple manufacturing and assembly, low-cost development.

Compared to the previous version of the project, in ESA-uProp 3 the goal is to get to test electric propulsion systems that reach firing powers up to 100W. To be able to manage such high powers, it was decided to develop a 12U platform (double compared to the previous version) to have the space necessary to accommodate different ePS, together with the avionics and battery packs that make up the service module. In this way the space dedicated to a propulsion system can reach up to 8U, with a consequent minimum volume for the service module of 4U.

One of the major problems in implementing electric propulsion systems, with relatively high powers for CubeSat missions, is given by the management of the electric power on board the spacecraft, and consequently to the management of the heat dissipated both by the engine itself during the burst phases, and both from avionics and from the batteries on board the CTP.

This chapter, and a large part of the thesis work, is dedicated to the study, analysis and implementation of virtual models for the resolution of the thermal problem on board the CubeSat. The main objective of this work is, once a solid thermal model of the test platform has been developed, the design and analysis of a thermal control system for the ESA-uProp 3 project.

6.1 Thermal model definition

The definition of the thermal model of the CTP for the ESA-uProp 3 project took place in parallel with the platform design process. The study of the thermal performance of the CubeSat through the analysis performed in Thermal Desktop allowed defining the characteristics and specifications of the CTP, optimizing the design process. However, the still advanced level of definition has led to greater uncertainty in the results of thermal analysis, requiring the study of variable configurations and performances, in order to obtain a wider spectrum of possible solutions.

A good experience, deriving from the development and verification of the thermal model of the CTP previous version, has made it possible to exploit the peculiarities in the evolution of the project, defining a presumably effective thermal model as regards the thermal simulation of the critical components on board.

As for the geometric dimensions, so also the powers managed by the subsystems of the CTP have increased compared to those that characterized ESA-uProp 2. Therefore, although the range of variability of the thermal flows produced during the operation of the platform was not yet precisely defined, the configuration of the model was marked with the aim of studying the worst cases, particularly critical from a thermal point of view, ensuring a high degree of accessibility and modification for the implementation of different thermal control solutions.

6.1.1 CTP environment, thermophysical and optical properties definition

As for version 2 of the CTP, also in this case the operational life of the platform includes a test campaign to be carried out in a relevant environment that simulates the vacuum conditions found outside the earth's atmosphere. The tests on the performance of electric thrusters and their interaction with the spacecraft that hosts them represent the missions of the CTP, and will be performed in the Small Plasma Facility vacuum chamber at the ESA-ESTEC laboratories in Noordwijk, the Netherlands.

Therefore, the operating environment of the CTP, unchanged between the two versions, made it possible to exploit the environmental model previously built with Thermal Desktop, as a basis for the development of the new thermal model of the platform.

Again, a parameterized virtual vacuum chamber was modelled. This allows you to vary, with extreme ease and in a short time, the geometric and physical characteristics, so as to be able to simulate different facilities, or the same operating in different ways, without the need to restart the construction of the thermal model each time.

The ten boundary nodes that divide the cylindrical structure of the thin shell type, allow to set an invariable temperature, as if the walls of the chamber had infinite thermal inertia. This characteristic is found in reality when using a vacuum chamber with cooled walls, which simulate a radiative environment, external to the spacecraft, almost as cold as the space one (80-100 K against the 3-4 K of deep space). The liquid cooling system of the chamber allows keeping the walls at a constant temperature, regardless of the thermal loads radiated from the inside. In the case that the walls of the vacuum chamber are not cooled, but are at room temperature, the heat flow generated by the spacecraft can lead to an increase in the temperatures of the internal walls.

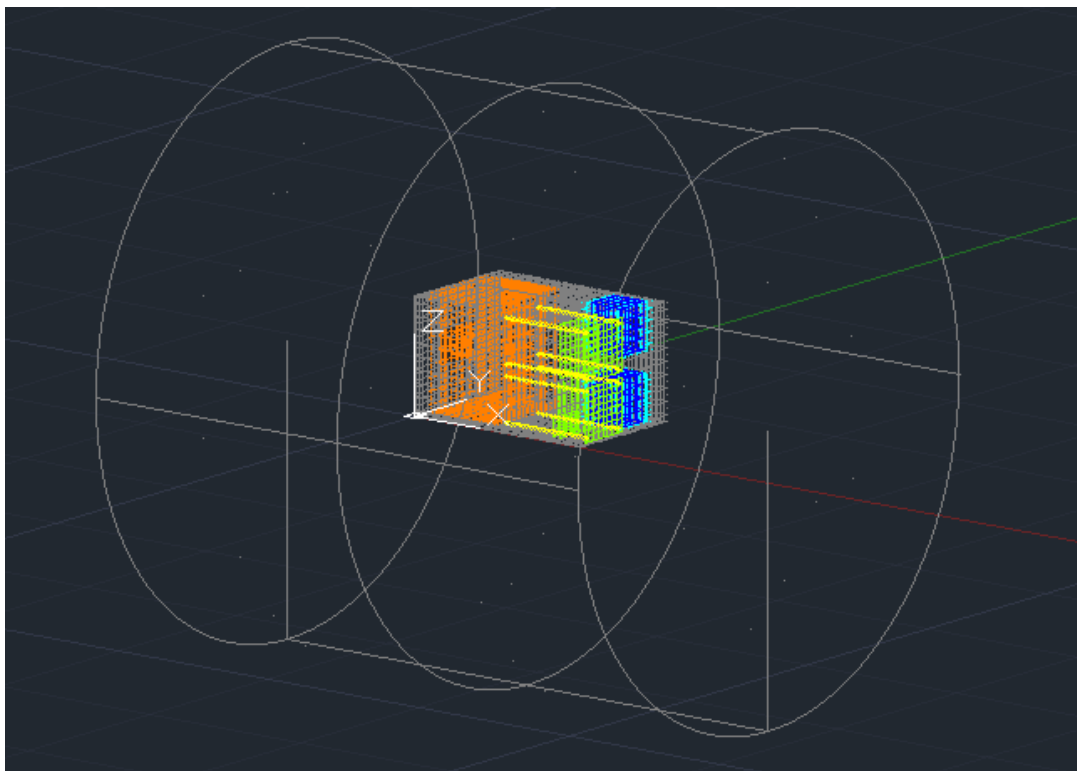


Figure 43: Vacuum chamber containing CTP in Thermal Desktop

The model does not consider the mechanical interface between the CubeSat and the vacuum chamber. However, the integration of the platform within the test facility requires the CTP to be supported on a four-legged structure, or by brackets, which maintain its position according to the evaluation of the performance of the PS, through the integration with the Thrust Balance. This aspect represents an open point, from which the model can be modified to take into account these contacts with external structural and measuring elements, through which conductive heat exchanges can occur. Although the modelling of these elements, external to the platform but in contact with it and internal to the chamber, can lead to greater accuracy in the

temperature trends resulting from the simulations made with the model, it has been neglected to limit the development time of the model, and reduce its complexity. It was estimated that inserting only the CTP in the centre of the vacuum chamber did not involve a significant loss of accuracy, based on the data collected for the verification of the ESA-uProp 2 thermal model. Furthermore, not considering these conductive heat exchange phenomena, presumably with thermal flows from the CTP towards the walls of the vacuum chamber, the temperatures of the CubeSat are overestimated, without risking the underestimation of the thermal criticality during the propulsive tests.

As for the environmental properties in which the CTP operates, also as regards the thermophysical and optical properties of the materials implemented in the system, and therefore in the model, no major changes have been made. For the structural elements, despite the variation in size from the CubeSat 6U to the 12U one, the same physical and optical properties were maintained. By default, the materials used to model the panels, which include the primary and secondary external structures, were the same as those used in the previously developed thermal model. The combination of aluminium alloy elements Al5005 and Al6082 was also deemed suitable for the new platform. The Al6082 is used also for battery packs drawer and for the bulkhead, as in the previous version. However, later, during the analysis process that accompanied the definition of the thermal control system, different solutions were implemented, which include the use of specific materials for passive thermal control techniques, such as surface treatments and external coatings for the structural panels.

As for the avionic boards, the study of the thermal control system required to carry out analysis with electronic boards of different materials and sizes, also considering the implementation of paints and coatings dedicated to the thermal protection of critical circuits.

The batteries maintain the thermophysical properties of lithium-ion accumulators, despite varying their size and mass, and the solder mask blue coating already used in the previous version has been considered.

The following tables list the optical and thermophysical properties of the materials used during the analyses, in order to define a thermal control system suitable for the platform.

Thermophysical properties			
Material	Conductivity $\frac{W}{m K}$	Density $\frac{kg}{m^3}$	Specific Heat $\frac{J}{K m^3}$
Al5005	201	2700	900
Al6082	17	2700	900
Aluminium board	205	2700	900
Batteries	65,8	2118	795
FR4 board	17,5	3937	1192
Copper	39,8	8930	385
Stainless steel	16,2	8000	500
Gap Filler 707-4597	1,6	2000	100
Generic Gap Filler	<i>Variable</i>	2000	100
Chamber	34,3	9000	850

Table 8:ESA-uProp 3 model - Thermophysical properties

Optical properties		
Material	Solar Absorptivity	IR Emissivity
Aluminium	0,25	0,10
Aluminium anodized	0,25	0,77
Aluminium Alodine	0,45	0,15
FR4	0,49	0,88

Copper	0,64	0,15
Solder mask blue	0,7	0,88
Steel	1	0,70

Table 9: ESA-uProp 3 model - Optical properties

During the study of the possible solutions for the thermal protection of the critical systems of the platform, components with materials different from those used in the previous version of the project were used in the analysis. The innovations concern the electronic boards in aluminium, which have been the subject of study as they are characterized by a better heat conductivity, and therefore greater ease of heat dissipation compared to the classic FR4 avionic boards. The other novelty was the use of thermal pads with the gap filler function that allows to fill the air gap between uneven surfaces. Thermal gap pads provide a thermal interface between heatsinks and electronic devices. As can be seen from the table of thermophysical properties, the performances of the Gap Filler 707-4597 were analysed, as it is already available in the laboratory, and a generic gap filler, to which the parameters of thermal conductivity and thickness were changed during the various simulations, in order to simulate the different thermal pad solutions on the market. There are no optical properties of the gap fillers as they are located in the centre of a sandwich structure between the electronic boards and the panels of the structure.

6.1.1 Thermal Desktop model

Starting from the already defined and consolidated elements of the thermal model verified for version 2 of the project (6U CTP), the geometry of the external structure was initially defined, dictated by the CubeSat standard for 12-unit platforms.

The electric propulsion system was inserted as the first element inside the structure. Given that the various ePSs that will be tested on the platform have not yet been precisely defined, it was decided to integrate a propulsion system with thermal and configurational characteristics similar to those of REGULUS, already implemented in the previous version of the model. However, it was decided to increase its original size, in order to simulate larger thrusters, suitable for implementation on CubeSat 12U platforms. The dimensions of the propulsion system currently implemented in the model are: $346\text{ mm} \times 226\text{ mm} \times 200\text{ mm}$ (x, y, z). Regarding the thermal dissipation of the ePS, the thermal efficiency considered is about 70%. This value derives both from the data obtained through the checks on the ePS REGULUS in the vacuum chamber (which had lower efficiency for non-maximum burst powers), and from the

data collected regarding other ePS models, even if often not very detailed. Furthermore, it is considered that reaching high propulsive powers should increase the efficiency of the propulsion systems, therefore the efficiency value considered is a conservative estimate downwards of those actually found on the ePS that will be tested.

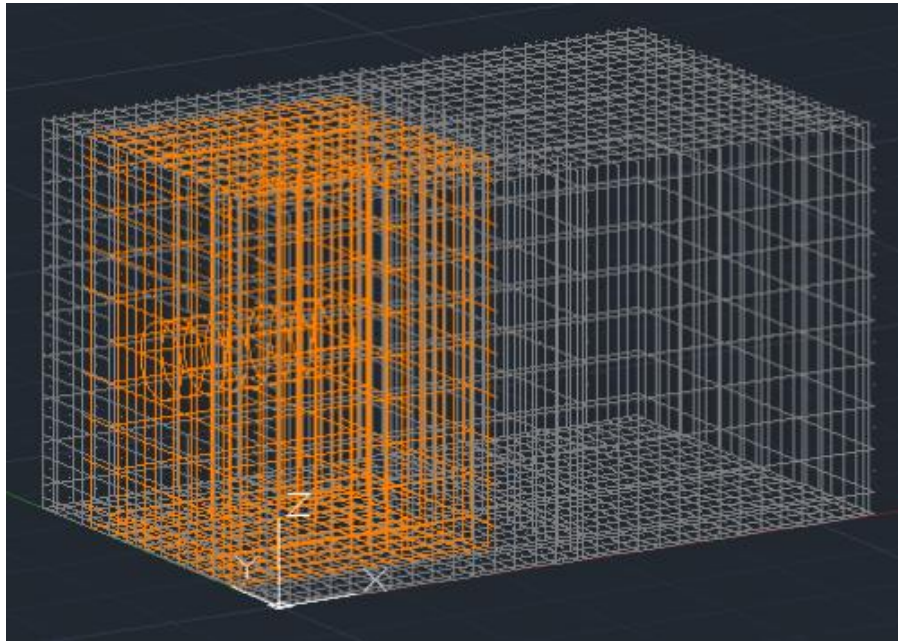


Figure 44: ePS integrated in CTP structure

Subsequently, the two battery packs of the CTP were integrated with the propulsion system, including their respective battery drawers. The modelling of these components was based on those already implemented on the 6U platform. In fact, in terms of size, each battery pack is similar to that present in the previous version of the model. They are assembled on the + X and + Y sides of the service module, one connected to the + Z panel and the other to the -Z one. Compared to version 2 of ESA-uProp, therefore, the battery packs have been doubled, effectively doubling the availability of electricity that can be stored on board, and both use the same type of batteries. Since the performance of the latter has not yet been defined, during the thermal analyses the thermal power dissipated by the batteries will be a variable parameter.

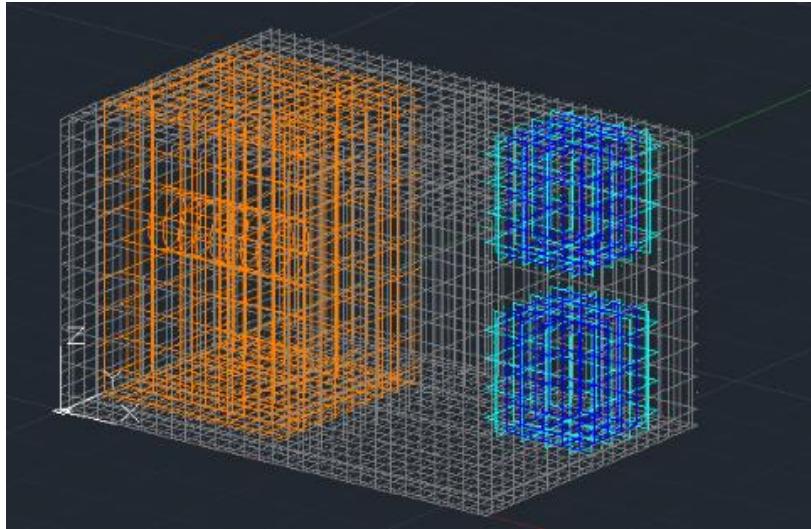


Figure 45: integration of battery packs on-board CTP

Finally, the avionics module of the CTP was modelled, including a volume of 2U. Compared to the previous version of the platform, this is the part that has undergone the most changes. The electronic boards are no longer assembled vertically one above the other to occupy 1U of volume, but are divided into two distinct series, and arranged horizontally between them. To model the structural support that holds them in place, the cylindrical solid element was again used, already used in the previous model to model the four support bars for avionics. These supporting structural elements have been connected at one end to the structural panel + X, and at the other to the bulkhead that separates the service module from the propulsion module.

The two electronic boards positioned in + Z and in series with each other are those belonging to the EPIS system, and are respectively the EPIS power and the Data Logger. The first has the function of power interface towards the propulsion system, regulating the input voltage to the ePS through the DCDC step-up circuit component, while the DL is responsible for the communication, data and command interface towards the ePS.

Three electronic boards are positioned in series on the -Z side: EPS, CDH and COMSYS. The first manages the electrical energy on board, acting as an interface with the batteries, with external energy sources and with the EPIS power system. It also supplies electricity to the other CDH and COMSYS avionics boards via the 5V and 3.3V power buses. The CDH and COMSYS boards with regard to thermal modelling are similar to the respective ones implemented in the 6U model of ESA-uProp 2.

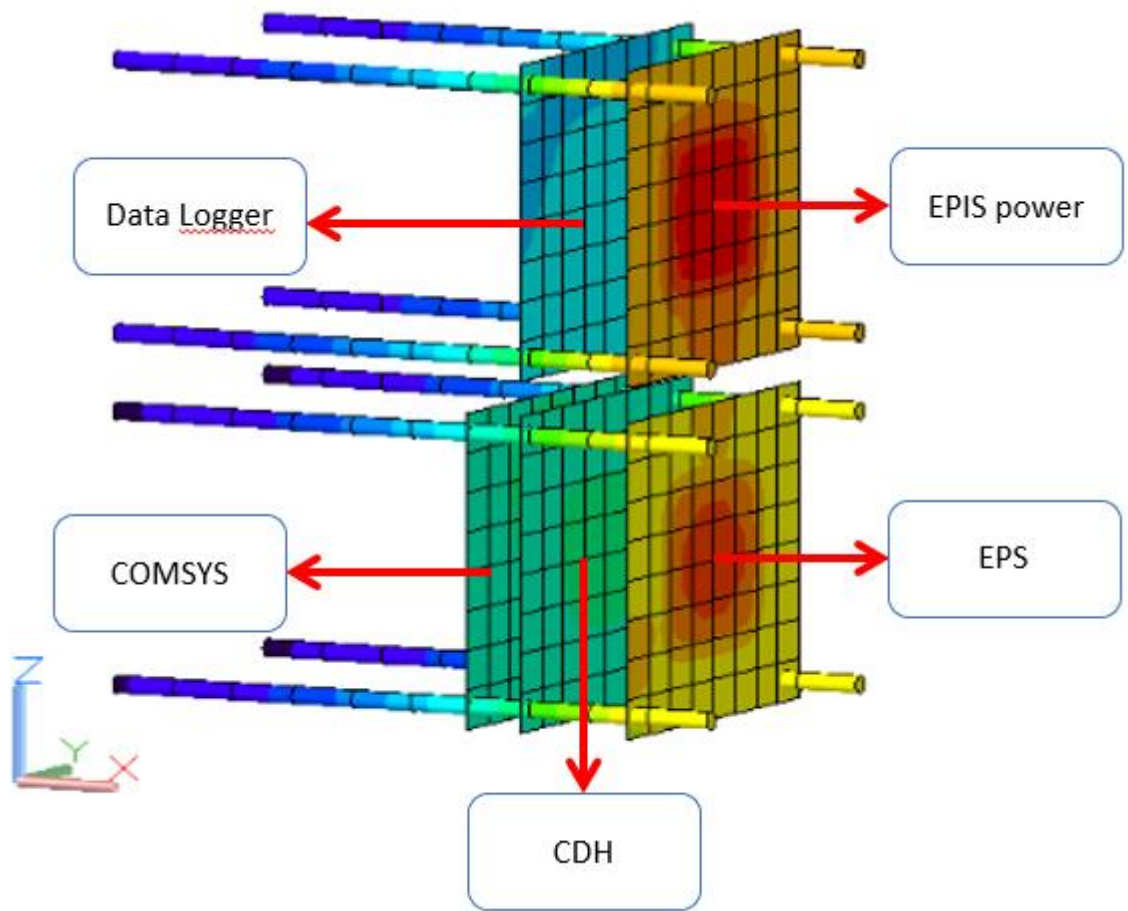


Figure 46: Avionics boards disposition

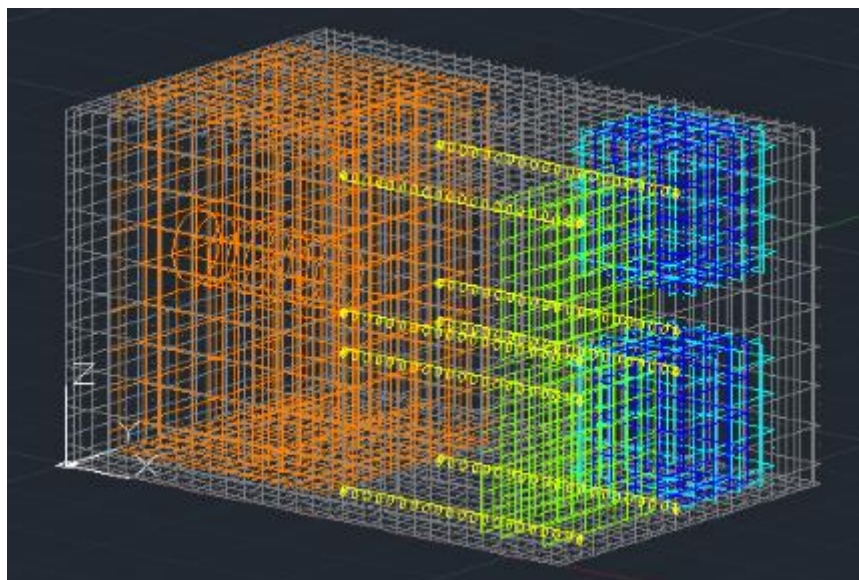


Figure 47: Avionics module integration

As explained in detail below, the configuration of the avionics module is not uniquely defined, but is changed during the thermal analysis campaign.

In the next sections dedicated to thermal analysis and the design of the thermal control system, the boards responsible for the electrical management on board the CTP will be of particular interest: EPS and EPIS power.

These two electronic components, due to the high electrical power required for the operation of the ePS and the other electronic elements, are responsible, together with the ePS itself and the batteries, for the greatest heat dissipation on board the CTP. Therefore, their modelling requires high detail and precision, in order to study their thermal performance as accurately as possible, and how to adequately protect them from the high temperatures reached by their components.

6.2 Thermal control system design

The construction of a first thermal model of the ESA-uProp 3 CTP in Thermal Desktop was necessary to study the thermal behaviour of the CTP through the early thermal analyses.

Taking into account an early configuration, but representative of the possible internal architecture of the CTP, and considering the operating environment, the goal is to predict equipment and structural temperatures with adequate uncertainty margins, due to still undefined design choices, for critical phases of the mission and compare with allowed limits.

Following a series of initial thermal analysis, once the thermal criticalities that occur during the CubeSat missions have been identified, TCS design proceed with the study of possible thermal control strategies that allow the mitigation of overheating problems.

Through new thermal analysis campaign carried out with Thermal Desktop, the goal is to find suitable solutions to ensure that equipment and structural temperatures are in the allowable ranges.

In order to broadly study the thermal behaviour of the CTP in different situations, due to specifications of the on-board systems not yet defined, in addition to the study of the worst operating conditions from the point of view of thermal stress, a parametric analysis campaign was undertaken, to simulate a wide range of possibilities and their interaction.

6.2.1 Thermal parametric analysis

Variable parameters

In order to consider the greatest number of different final configurations of the platform to evaluate its thermal behaviour, a study was made of the possible categories of undefined and therefore variable parameters. The classification of these parameters, which ranges of variation were considered, and the main reasons for these variations are presented below.

1. Configurations: this category includes the different solutions adopted for the two on-board electrical power management boards (EPS and EPIS power), both in terms of materials used for the boards and in terms of the connection method between the two. In fact, the analyses were carried out for the cases in which the electronic boards are made of FR4 (as in the previous versions of the project), of aluminium for the greater thermal conductivity, or of a double layer: one in FR4 and the other in aluminium to facilitate the transport of dissipated heat. Furthermore, it has been simulated the case in which the two electric power boards are separated (90x96 mm each), and are connected by a power cable joined to two connectors present on the boards, and the case in which they form a board single size 190x96 mm.

The other possible configurations explored during the analysis campaign on Thermal Desktop concern the physical distance between the power management boards and the two boards close to them: Data Logger (in series with EPIS power), and CDH (in series with EPS). The study conducted allowed to assess how moving away Data Logger and CDH boards from the sources of radiated heat (EPS and EPIS power) helps to reduce the temperatures on the boards.

2. Efficiencies: the electronic components of the various devices that manage/use the on-board electrical power have different and variable electrical efficiencies. Their value can depend on several factors and can change during the operation of the CTP. Since the thermal analysis were carried out when the electronic components and therefore their efficiencies had not yet been defined in detail, it was decided to use them as variable parameters to analyse different possibilities. The study of the variation in the efficiency of three components was considered essentially relevant:
 - EPS-HUB: The component on the EPS electronic board, dedicated to the distribution of electrical power from the EPS to the EPIS power.
 - EPIS power – DCDC: Dedicated to regulating the voltage from the CTP, in input to the ePS.

- Batteries: for a fixed output power, the current will vary depending on the voltage required at the output of the battery packs. For relatively high currents the heat dissipation will increase, while for low currents the negative effect is attenuated.

Another component that manages a large electrical power is the Battery Charge Regulator (BCR), present on the EPS electronic board, but since this component typically achieves particularly high efficiencies, it was decided to consider its constant efficiency.

3. Power loads: the last category of variable parameters for thermal simulations is that of power loads. In fact, the specification of the maximum electrical power of 120W used by the propulsion system during the firing phase was known, since the ePS models that will be integrated with the CTP are not known, the voltage and current requirements required in input by the propulsion system. Therefore, according to the Joule effect, it depends on the current intensity (and therefore on the required voltage) how much electrical power is dissipated in heat. The same principle is valid for the thermal load dissipated by the batteries, as already mentioned above. For this reason, the different combinations of voltage and current, in input for the ePS and output from the batteries, have been chosen as variable parameters for the analysis. They affect the efficiencies of the different electronic components.

VARIABLE PARAMETERS			
CONFIGURATION	EPS and EPIS power boards	a)	EPS Aluminium board EPIS FR4 board
		b)	EPS and EPIS power Aluminium boards
		c)	EPS and EPIS power FR4 boards
		d)	EPS and EPIS power: 2-layer Al/FR4 boards
		e)	Single Power Management System Aluminium board
		EPS-CDH	[1,5-5] cm

	distances between boards	EPIS power-DL	[2,5-7,5] cm
EFFICIENCIES	EPS	BCR	[0,98-0,99]
		HUB	[0,90-0,95]
	EPIS power	DCDC	[0,85-0,95]
	BATTERIES		[0,92-0,97]
POWER LOADS	ePS		[12V-10A; 16V-7A; 24V-5A; 28V-4A]
	BATTERIES		[12V-11.6A; 14.8V-9/10A; 16V-8.7A]

Table 10: Variable parameters

6.2.2 CTP thermal assessment

Once the variable parameters and their range of variation have been defined, a simulation relating to a 30-minute burst phase has been set using the Thermal Desktop Case Manager tool. In this way, for each case analysed, it was possible to evaluate the temperature trend and therefore the temperature at the end of the 30-minute burst.

From the analysis carried out on the results, reported below, it was found that the implementation of thermal control techniques and systems is necessary in order to keep temperatures below their operating limits.

6.2.2.1 Configuration

The first study carried out concerns the comparison in the choice of material that makes up the two power boards of the CTP, and the case in which the two boards were joined to form a single power board. The remaining parameters were set as follows:

- EPS-CDH distance: 2,5 cm
- EPIS power – DL distance: 5 cm
- $eff_{HUB} = 0.95$, $eff_{DCDC} = 0.90$, $eff_{BATT} = 0.95$, $eff_{BCR} = 0.98$
- ePS input: 25V 5A
- Batteries output: 14.8V 9.5A

Three relevant cases are shown below.

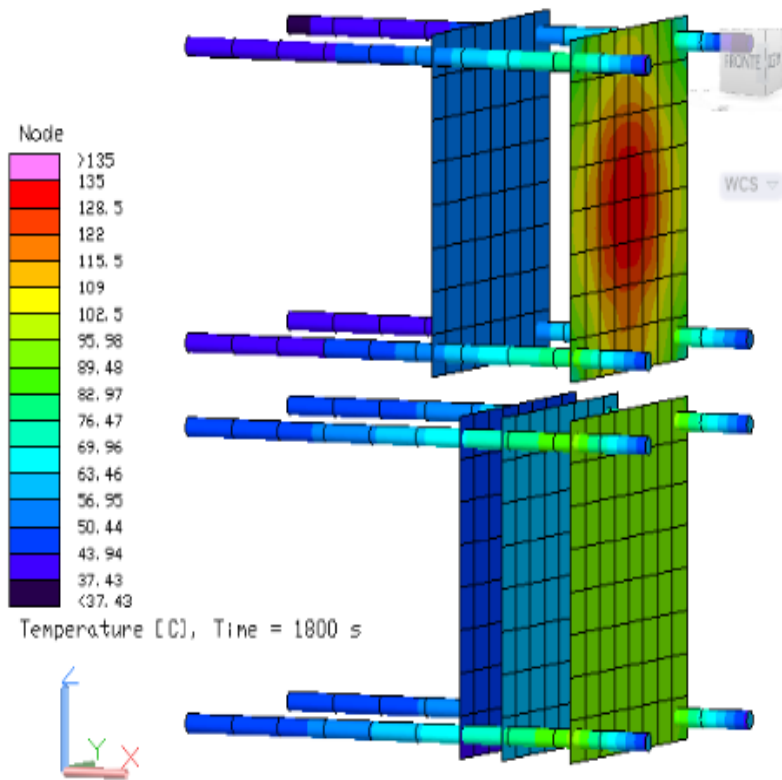


Figure 48: EPIS power in FR4, EPS in Aluminium

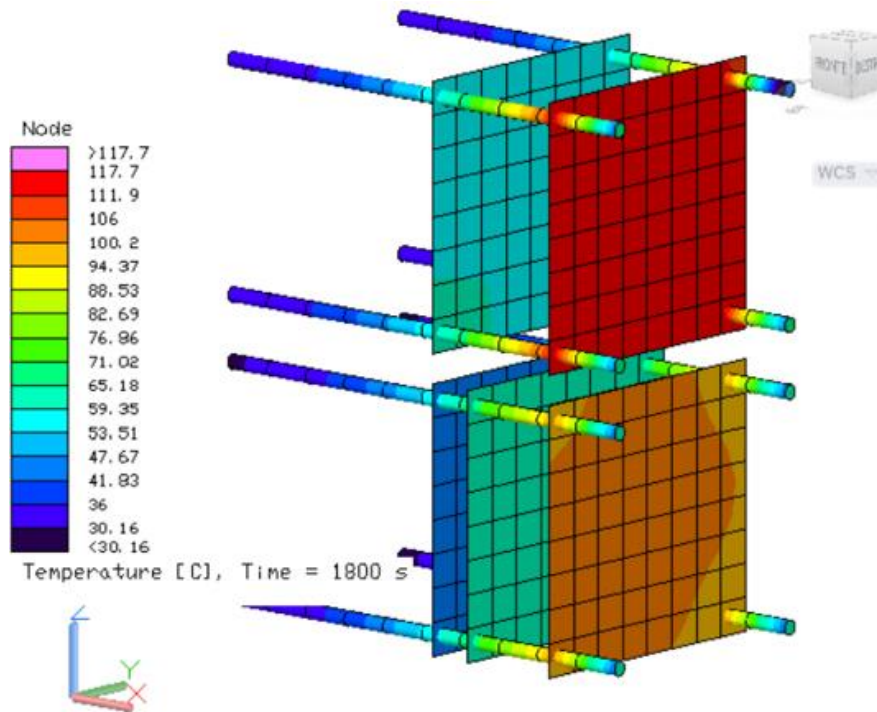


Figure 49: Two-layers Aluminium/FR4 EPS and EPIS power boards

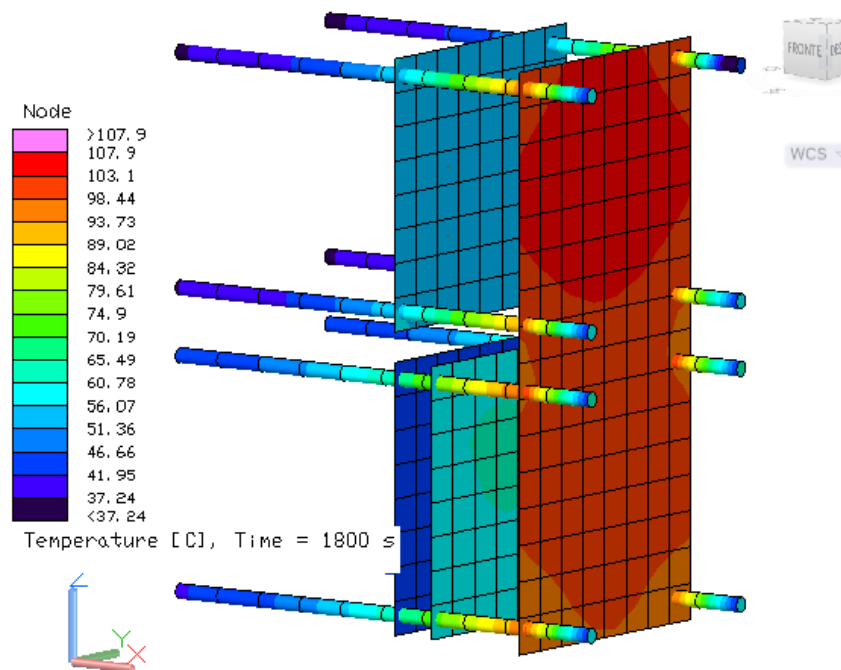


Figure 50: Single Aluminium power board

In the first case, in which the two power boards are of different materials, it is possible to find that in the EPIS power the dissipated heat is transported with relative difficulty, generating very high temperatures in the areas where dissipations occur. Conversely, on the EPS board, the temperature is homogeneous, as aluminium is a better conductor of heat than the FR4. Temperatures beyond the operating limits are reached on both boards, and also on adjacent boards (DL and CDH), due to the strong radiative component generated by the power boards, the temperature exceeds the limits.

In the second case, both power boards are made up of two layers: one in FR4 on which the thermal loads are applied, and the other in aluminium dedicated to the distribution and transport of heat. As can be seen, the peak temperatures are reduced, but without a system dedicated to transporting the heat from the electronic boards to a heat sink, the temperatures remain excessively high.

The third case concerns the solution with a single power board composed of aluminium. This solution generates an even better heat distribution, with a consequent decrease in the maximum temperature. Even in this case, however, the temperatures exceed the maximum limit, and the overheating of the DL and CDH boards is still too high.

The other case study regarding the internal configuration of the avionics box concerned the distance between the power management boards (EPS and EPIS power) and the related electronic boards in series with them: the CHD close to the EPS, and

the Data Logger close to EPIS power. The analysis was done by keeping the position of the power boards fixed, and gradually moving the other boards away from them. To verify the effect of this removal from the main heat sources, the significant data was the maximum temperature reached on the CDH and DL boards following the 30-minute firing phase. The remaining parameters were set as follows:

- $eff_{HUB} = 0.95$, $eff_{DCDC} = 0.90$, $eff_{BATT} = 0.95$, $eff_{BCR} = 0.98$
- ePS input: 25V 5A
- Batteries output: 14.8V 9.5A
- EPS: aluminium board
- EPIS power: FR4 board

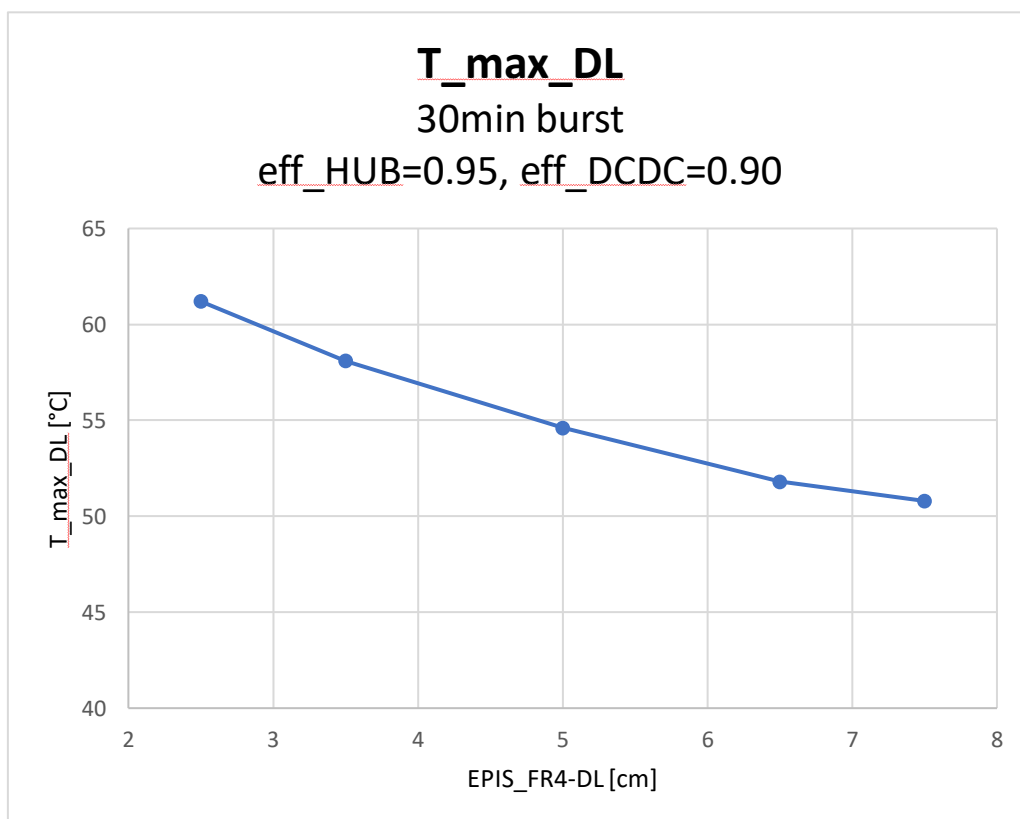


Figure 51: Temperature trend of the DL board as the distance from EPIS power varies

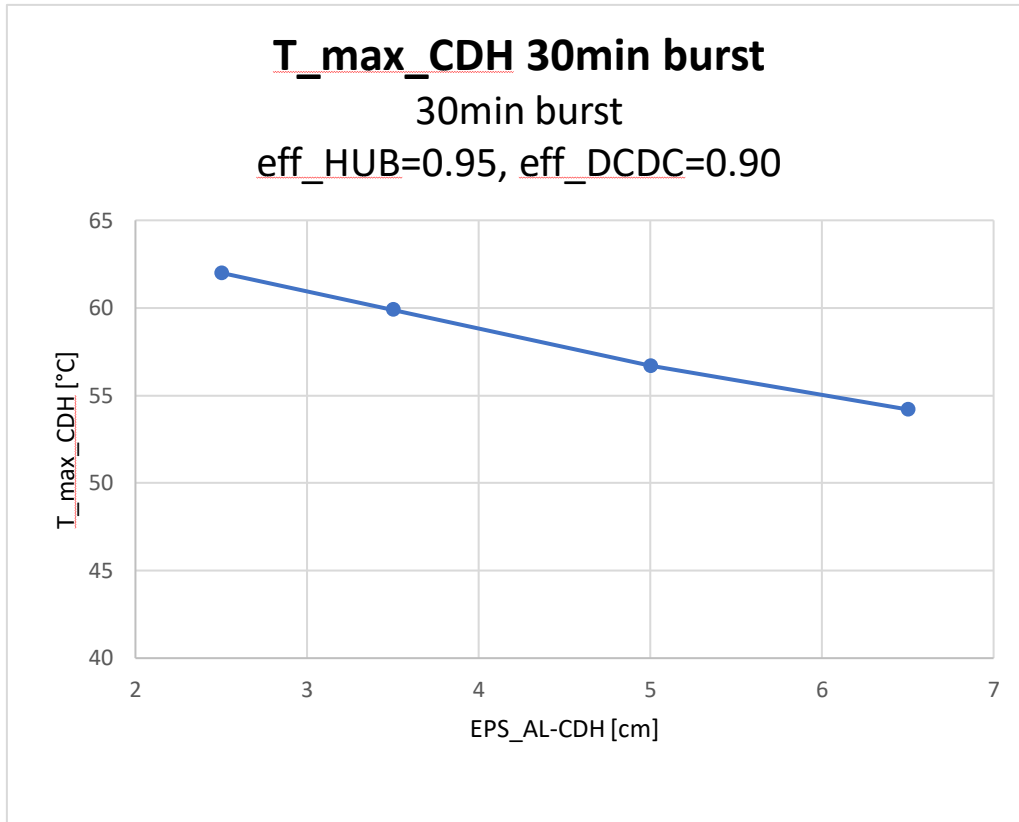


Figure 52: Temperature trend of the CDH board as the distance from EPS varies

From the graphs of the maximum temperatures on the two avionics boards, as the distance from the power boards varies, it can be deduced that for every centimetre of the increase in the distance of the Data Logger from the EPIS power, the maximum temperature of the board decreases by about 5%: more than 10 ° C with a distance of 5 cm from the starting position. As for the CDH, its maximum temperature decreases less sharply: about 3.5% less for each additional centimetre of distance. This is due to the fact that the EPS board is at a lower temperature than the EPIS, and therefore radiates less heat to surrounding components.

Despite the proven beneficial effect of increasing the distance from the main heat sources of the avionics box, the space inside this module is limited, as it cannot exceed 10 cm (one unit dimension) from the wall of the structure + X to the last electronic board in the direction -X. This limitation is due to the fact that the remaining two units in the -X direction are to be left to accommodate the electric propulsion system.

6.2.2.2 Efficiencies

The study of the variation in the efficiency of electrical devices concerns the three components with the greatest dissipation of the avionic module: HUB of EPS board, DCDC step-up circuit of the EPIS power board, and the two battery packs. In fact, in addition to these components, there are many others on board the CubeSat on which a study on the effects of variation of their thermal efficiency can be carried out. First of all, the electric propulsion system: since different ePS models can be integrated, the thermal efficiency of each of them is not yet known. Therefore, the REGULUS PS, already analysed and tested in the previous version of the project, was considered for the thermal analysis in the development phase. In this way, the efficiency values and the thermal loads dissipated by the propulsion system were already known. Other components, not considered in this study, are the other electronic boards on board. Even for these, however, the dissipated heat data were already known, derived from the test and analysis sessions carried out in version 2 of ESA-uProp. For the efficiency data of components with not well-defined thermal behaviour, which however produce relatively low dissipated heat fluxes compared to those analysed, an average efficiency value reflecting their behaviour was considered, according to the data collected through datasheets and reviews of design.

The analysis was done by varying the efficiencies of the HUB and the DCDC in the ranges described in table 10. Also, in this case, the result extrapolated from the simulations is the maximum temperature, reached after a burst phase of 30 minutes, of the pairs of electronic boards: EPS-CDH and EPIS power-DL. Subsequently, from the

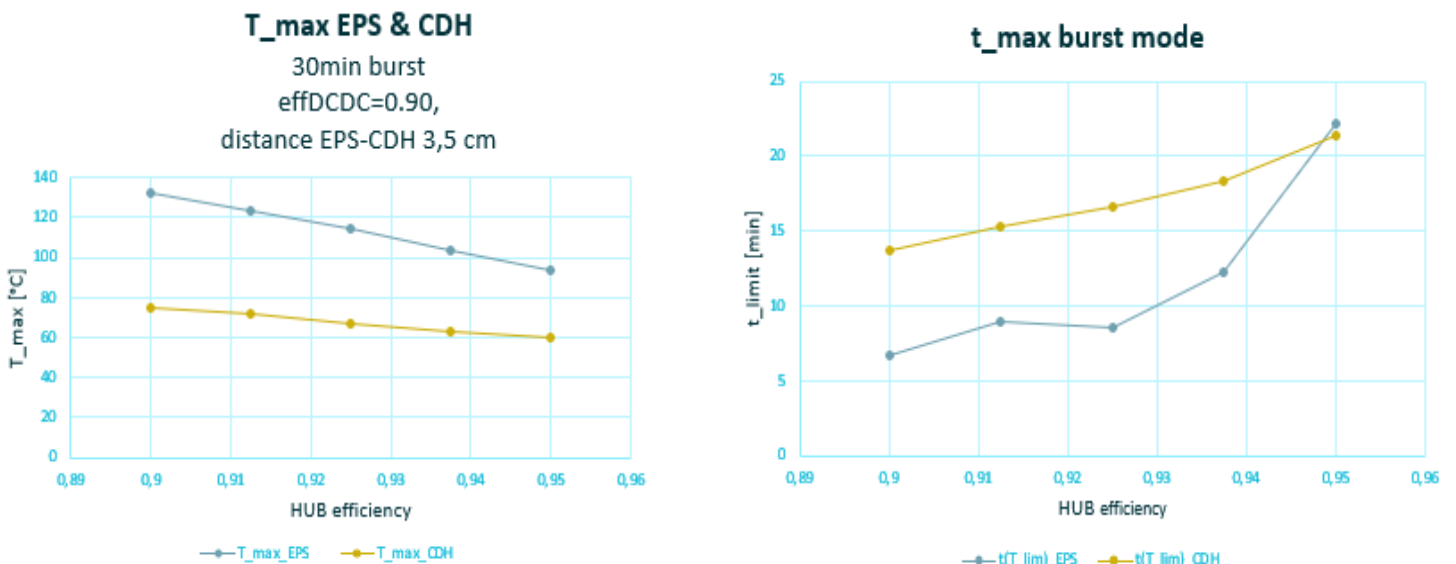


Figure 53: EPS HUB efficiency variation

data on the temperature trend of the various cases analysed, the maximum burst time that the electronic boards can tolerate under the defined conditions was obtained.

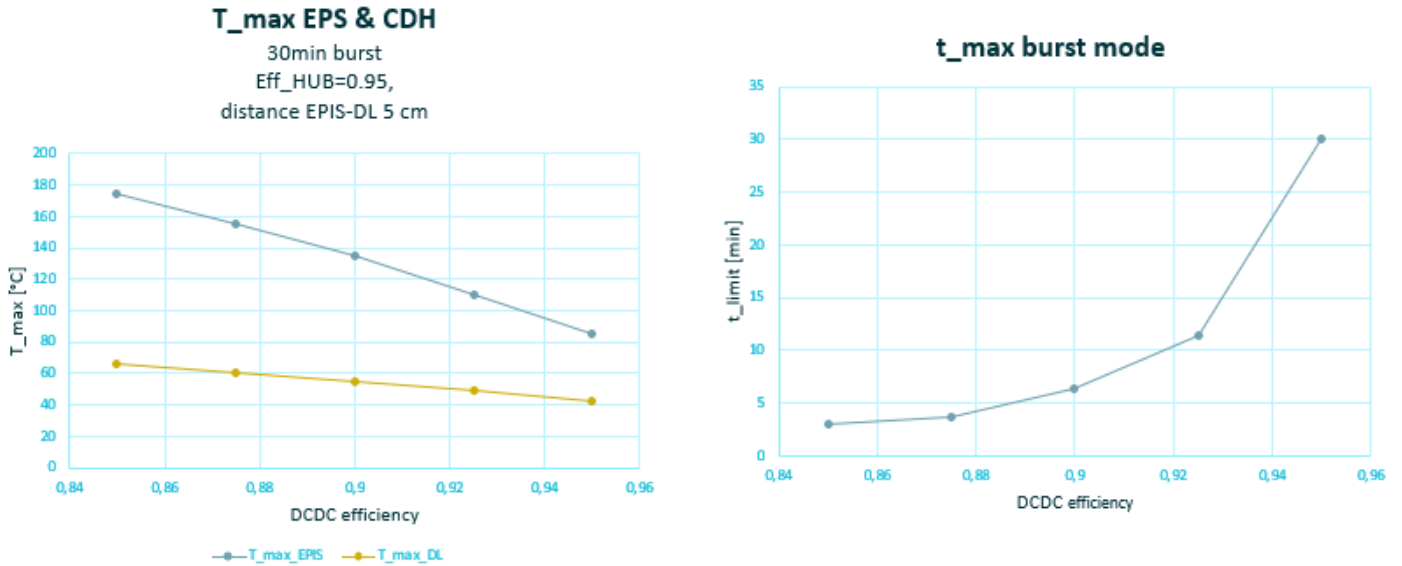


Figure 54: EPIS power DCDC efficiency variation

It can be deduced that higher thermal efficiency values allow a significantly longer duration of the burst phase. This treatment was made considering the following temperature limits of the electronic boards analysed:

- EPIS power and EPS: 90°C
- CDH and Data Logger: 50°C

However, from the previous graphs it can be deduced that high thermal efficiency values are not sufficient to guarantee a thermal response to the burst phase such as to ensure that the components do not exceed their upper operating temperature limits. This is due to the high thermal loads that are dissipated even when the efficiencies are high.

The parametric analysis carried out by studying the variation in the efficiency of the batteries is intrinsically linked to the variation in the mode of supply of electrical power by the batteries. Initially, based on the data obtained from the simulations performed on the model of the ESA-uProp 2 batteries, and from those obtained during the tests in the vacuum chamber, a constant average efficiency value of the batteries was set equal to 0.95.

However, this value was referred to the case in which the battery packs provided an average voltage of 14.8V and a maximum current of about 9.5A. With the same electrical power supplied, as previously described, cases have been considered in

which the average output voltage varies in the range [12-16] V with a consequent variation of the maximum current in the range [11.6-8.7] A. A greater current flow involves, due to the Joule effect, an increase in heat dissipation of the electrical power, and therefore a decrease in efficiency. Therefore, the parametric analysis also involved the study of the efficiency of the batteries in the interval [0.92-0.97].

The following figures show the trend of the nodal temperatures of the battery packs, for a burst phase lasting 2000 seconds. The first refers to the thermally best case, in which the batteries supply an output voltage of 16V at a maximum current of 8.7A, and therefore with an efficiency of 0.97 each battery pack dissipates 2.1W of thermal power. The second image refers to the thermally worst case, in which 12V with 11.6A maximum are supplied. In this case, an efficiency of 0.92 is considered, with a thermal dissipation of 5.5W for each battery pack.

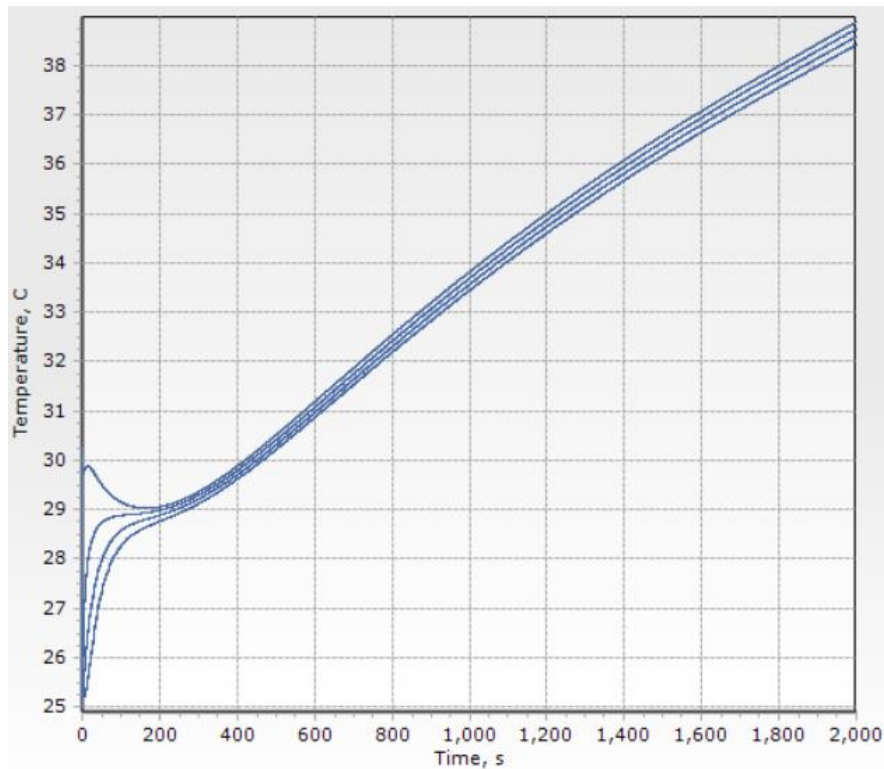


Figure 55: battery packs temperatures in best thermally case

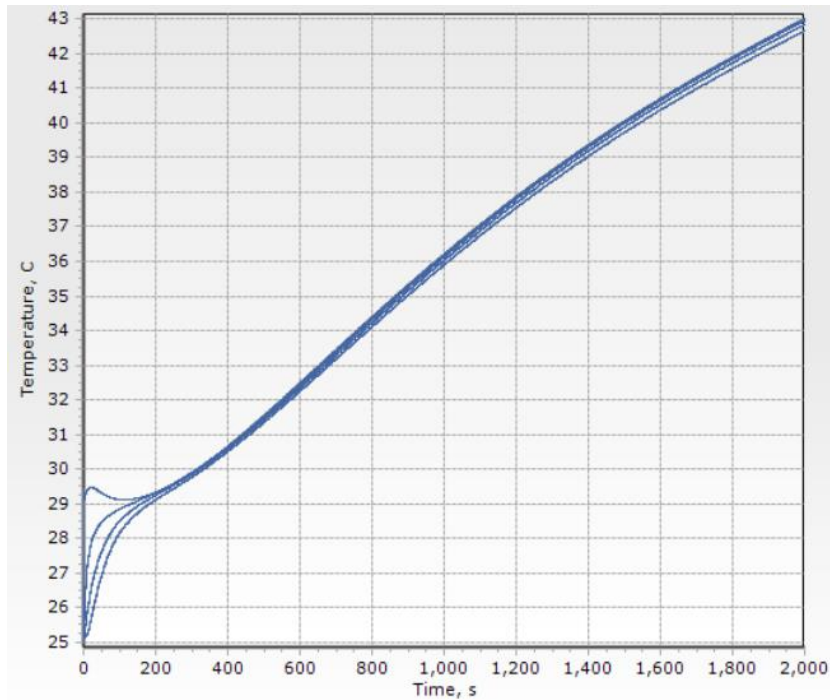


Figure 56: battery packs temperatures in worst thermally case

The worst case is of particular interest, since from the temperature trend it can be deduced that the operating limits of the specific component are not reached and exceeded.

The first parametric analysis campaign, the results of which have been presented in this section, demonstrated that: although it is possible to implement particular geometric configurations, specific materials favourable to heat dissipation, and electronic components with high thermal efficiencies, without the use of additional on-board thermal control systems it is almost impossible to keep the CTP running for considerable durations during the burst phase, without its internal devices being damaged by high temperatures.

For this reason, apart from the parametric study done on the thermal performance of the battery packs, the variation of the currents in the supply of electrical power between the different on-board systems, and in particular the worst cases with the highest current intensities, was analysed in the subsequent thermal analysis phase, together with the study of the implementation of thermal control systems for maintaining on-board temperatures within the operating ranges.

6.2.3 Thermal control system analysis

A number of problems emerged from the previous thermal parametric analysis:

- For medium-long duration burst phases, the electronic power boards, in the various configurations seen, reach temperatures above their operational limits.
- DL and CDH boards are affected by the high temperatures of EPIS and EPS, and must be spaced properly from them, taking into account the limited space for the avionics module.
- For the analysed cases, the limit temperatures of EPS and EPIS are reached too quickly, unless their components are highly efficient. Even in these cases, however, the risk of reaching the limit temperatures is too high.
- Even in the case of using aluminium alloys for the electrical power boards, which allow a more homogeneous distribution of thermal loads and therefore of the temperature, the absence of devices dedicated to transporting heat to heat sink does not allow to manage the temperatures of the most critical components adequately.

To solve these thermal problems, and to allow safe operation of the platform during the most critical mission phases, despite the high thermal loads dissipated by the electronic components and the propulsion system on-board the CTP, a study was carried out on the implementation of thermal control systems through an analysis campaign on the model built in Thermal Desktop.

The study focused on the solutions for thermal control on-board CubeSat type nanosatellites presented in chapter 3, those belonging to the category of passive thermal control systems. The reason these types of systems were first studied is that generally they are characterized by simplicity, and therefore their use leads to a containment of the weight, volume, and cost of the TCS. This simplicity of design, coupled with the absence of complex power lines, implies high reliability.

The two main solutions analysed through simulations with Thermal Desktop are detailed below. They have been combined with a series of other thermal control solutions, starting with specific geometric configurations, materials used, and coatings dedicated to thermal control.

6.2.3.1 Thermal strap solution

The use of a thermal strap system for thermal control was the first solution analysed. The reason for this choice was that this type of thermal control system had already been used on-board version two of the CTP, guaranteeing satisfactory performance regarding the protection of the most critical systems from the thermal point of view (High Power Management System). The experience gained and the know-how generated by the implementation, assembly, and use of this system, with the related data collection, were the reasons why it was first used in the analysis.

Initially, the "default" version of the model was considered, that is the one mostly used for the parametric analysis described in the previous version. In this way, it was possible to evaluate the impact of the thermal straps on the thermal behaviour of the CTP, and in particular of the electronic power boards.

The model version is characterized by:

- EPS-CDH distance: 3,5 cm
- EPIS power – DL distance: 5 cm
- $eff_{HUB} = 0.95$, $eff_{DCDC} = 0.90$, $eff_{BATT} = 0.95$, $eff_{BCR} = 0.98$
- ePS input: 25V 5A
- Batteries output: 14.8V 9.5A
- EPS: aluminium board
- EPIS power: FR4 board

Two copper thermal straps have been applied to the two electronic power boards. The two systems, identical to each other, are connected through contactors, which simulate copper cables, to the most critical components of the two electronic boards. The copper cables carry the excess heat to two copper plates in contact with the panel of the +X structure, which acts as a heat sink.

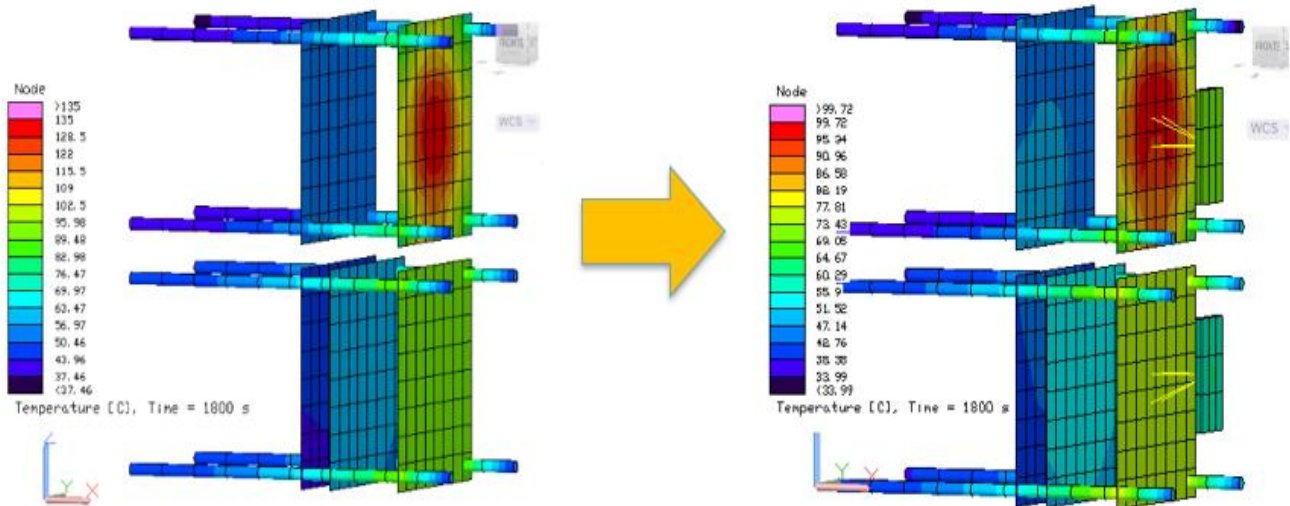


Figure 57: Comparison of simulation results: CTP without TSs vs. CTP with TSs

The result of applying the thermal straps shows a sharp drop in the maximum temperatures reached by the two power boards (EPS and EPIS power). On the EPIS power board, the one subjected to the greatest thermal loads, there is a decrease in maximum temperature after a firing phase of 30 minutes of about 35°C. From the analysis of the data, it results the improvement of thermal conditions of CDH and DL

boards as well, given by the decrease of the temperatures on EPS and EPIS power, and therefore a reduction of the radiated thermal power.

While recognizing a clear improvement in the thermal conditions of the CTP at the end of the burst phase, it is still evident that the temperatures reached on the electronic boards are excessively high.

To improve the thermal conduction of critical devices, two-layer power boards are implemented. This type of electronic board is characterized by the presence of components that generate heat dissipation on the side of the board in FR4, while the other layer of the board is in aluminium, and allows to manage heat more uniformly and transport its flows. In the analysed case, the FR4 side is in the -X direction, while the aluminium layer is in the + X position near the structure panel.

the aluminium layer favours heat transport with the thermal strap, and increases the dissipation of excess heat to the heat sink, improving thermal performance. This effect was already evident in the previous case with the aluminium EPS board, while now it is also observed on the EPIS power board, whose maximum temperature decreases by about 10°C.

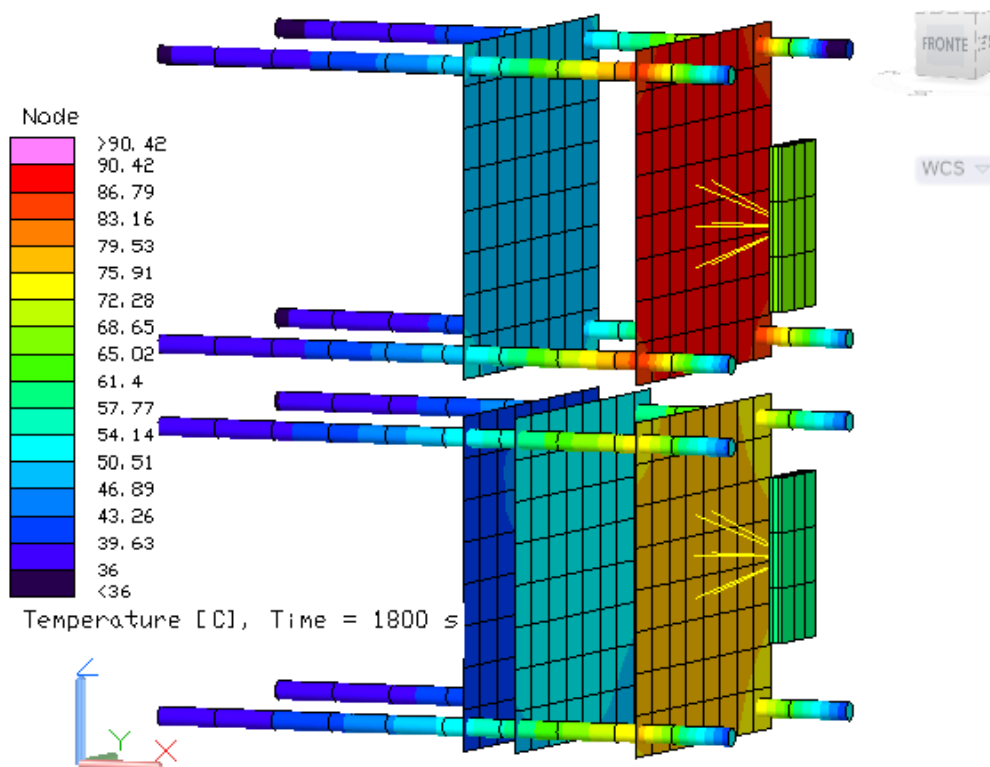


Figure 58: two-layers power boards with thermal strap systems

Once in "standard" conditions, i.e., with average current values and therefore average efficiencies, have been reached conditions such that the maximum temperatures measured at the end of the burst phase fall within the expected operating ranges, or are at the limit of them, analysis of the worst heat dissipation conditions are carried out. Worst condition is when the intensity of the current flowing in the electrical circuits of the CTP is maximum.

The worst load case analysed is characterized by:

- EPS-CDH distance: 3,5 cm
- EPIS power – DL distance: 5 cm
- $eff_{HUB} = 0.90$, $eff_{DCDC} = 0.85$, $eff_{BATT} = 0.92$, $eff_{BCR} = 0.98$
- ePS input: 12V 10A
- Batteries output: 12V 11.6A
- EPS: FR4/Aluminium board
- EPIS power: FR4/Aluminium board

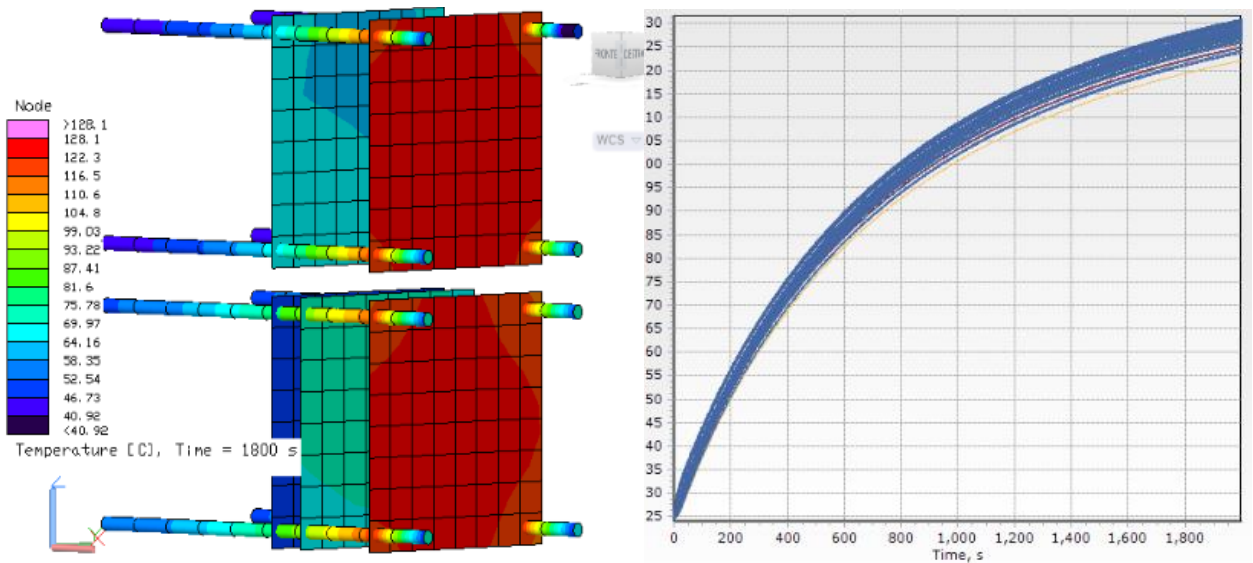


Figure 59: Worst heat load condition - EPIS power temperature trend

From this analysed condition, it results that the solution characterised by the implementation of two thermal straps in contact with the aluminium layer of the EPS and EPIS power boards, is inadequate, and is not able to meet the temperature requirements of the CTP and of its critical components in the worst thermal case, with large heat dissipations.

The biggest limitation of this thermal control system is the poor efficiency in transporting heat through conductive copper braids. In fact, when the thermal loads

dissipated by the electronic boards reach very high values, the limited contact area of the thermal strap, and in particular, the limited area/length ratio of the copper braids, allows only a reduced part of the dissipated thermal power to be transported towards the plate in contact with the structure. As a result, the critical devices, on which dissipations occur, reach extremely high temperatures.

To make the transport of thermal power from critical components to heat sinks more effective, it was necessary to abandon the solution of a thermal control system with thermal straps, and adopt a solution characterized by a better Area/length ratio.

6.2.3.2 *Thermal gap filler pad solution*

The first solution analysed to improve the transport of heat, from the electronic power boards to the panel of the structure, which has the function of a heat sink, is the one that foreseen for the two power boards for the EPS and EPIS power systems made by double-layer FR4 / Aluminium. Being able to exploit the space available to the avionics module, the two power boards have been moved from their initial position, placing them directly in contact with the structure panel. The side of the boards in contact with the structure is the aluminium one, while on the other side of the FR4 board there are the electronic components responsible for heat dissipation. In this way, the heat is transmitted directly from the electronic boards to the structure, without the need to use an intermediate thermal strap system. The advantage of this solution is that it allows obtaining a wider contact area, with a resolutely reduced length of the transport medium (aluminium) of the thermal loads: length equal to the thickness of the aluminium layer of the board, about 1.5 mm.

In this way it is possible to obtain a greater distance between the EPS and EPIS power systems, sources of radiated heat, and the CDH and DL electronic boards. The disadvantage of this configuration is that the dissipative components of the power boards are all located on the -X face in FR4 of the two boards, in direct line of sight with the CDH and DL boards. This leads to an increase in the heat component radiated towards the two boards.

Performing a thermal simulation in Thermal Desktop with this configuration gives the following result.

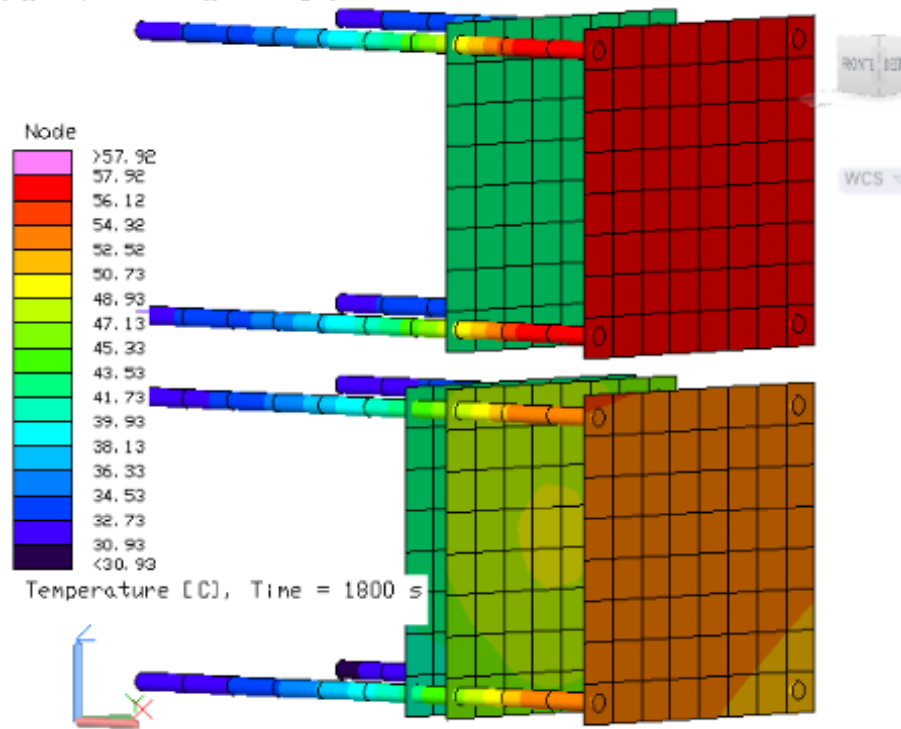


Figure 60: electronics power boards EPS and EPIS power in contact with structure panel

Compared to the solutions analysed previously, for the worst thermal loads case, this configuration allows to obtain significantly reduced maximum temperatures on the EPS and EPIS power boards. However, the temperatures reached by the two adjacent electronic boards, CDH and DL, are still close to the operating limit of 50°C .

The significant decrease in the temperatures reached by the EPS and EPIS power boards implies that the +X panel of the structure is subject to a large heat flow generated by the thermally critical components of the boards. Although the structure, built in aluminium alloys, has significantly higher operating temperature limits than those of the various on-board equipment, we want to avoid that the heat absorbed on the heat sink face is redistributed through conduction in other areas of the CTP, going inevitably to heat other components on board the platform. To minimize this inconvenience, and to allow the external surface to dissipate the greatest possible amount of thermal energy by radiation, a radiative thermal control system is implemented which includes the construction of the panel of the face +X of the structure in anodized aluminium, with the external application of a black paint in order to increase the IR emissivity and facilitate the dissipation of heat. From this point forward, the analysis results presented include this type of solution, with the structural panel +X as a radiator.

In order to maintain a high Area/length ratio for the transport of heat from the dissipative sources to the heat sink, thermal gap filler pads have been implemented in the thermal model to connect power boards to the structure panel.

These thermal protection devices are composed of silicone-based materials. their flexible design allows them to fill the air gap between uneven surfaces. Thermal gap pads provide a thermal interface between heatsinks and electronic devices.

These components characterized by:

- Good thermal conductivity
- Soft and high compressibility
- Easy to assemble
- Good insulator
- Shoch and vibration absorber

They are manufactured in a variety of standard thicknesses and dimensions but can also be custom fabricated to fit various applications. Their thermal conductivity can vary depending on the type of material that composes them.



Figure 61: Thermal gap filler pads

The parameters characterizing the gap filler devices are: the contact area, the thickness, and the thermal conductivity. As already highlighted, it is necessary to have an area/thickness ratio as high as possible, combined with a high thermal conductivity that facilitates the heat transmission.

The first solution analysed includes:

- EPS and EPIS power in FR4
- Two thermal gap filler pad: $80 \times 80 \text{ mm}$ area, 3 mm thickness, 1.6 W/mK conductivity in contact with EPS, EPIS power and structure panel
- EPS-CDH distance: 5 cm
- EPIS power – DL distance: 5 cm
- $eff_{HUB} = 0.95$, $eff_{DCDC} = 0.90$, $eff_{BATT} = 0.95$, $eff_{BCR} = 0.98$
- ePS input: $24 \text{ V } 5 \text{ A}$
- Batteries output: $14.8 \text{ V } 9.5 \text{ A}$

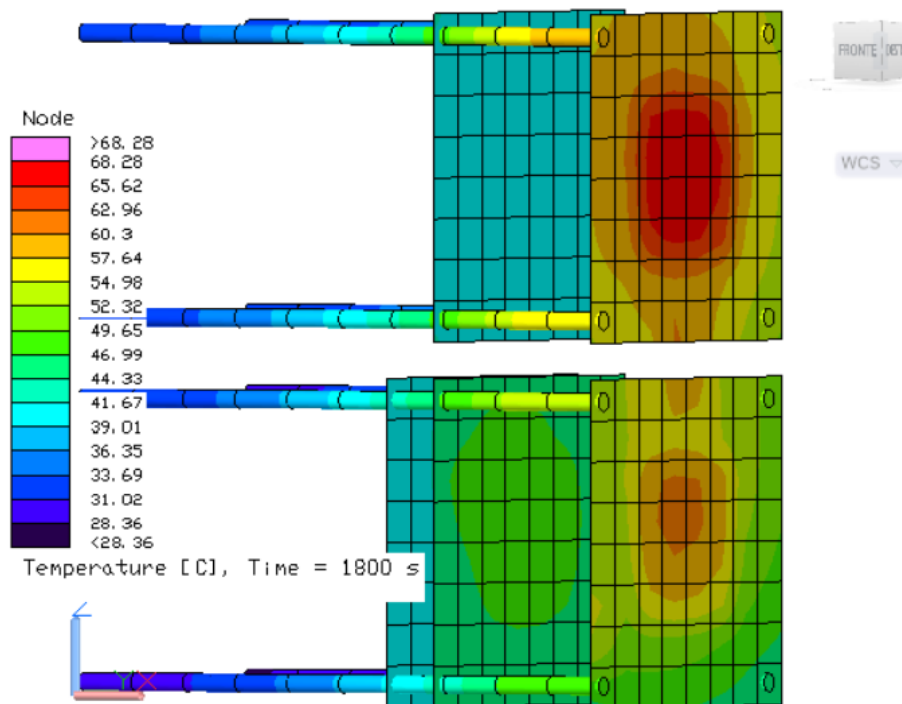


Figure 62: Avionics boards temperatures with thermal pads implementation

The results obtained meet the temperature requirements of the different on-board avionics systems. The specifications of the thermal gap filler pad system used refer to the component already available in the StarLab laboratory at the Politecnico di Torino.

By carrying out various simulations on this thermal model, which implements the described thermal gap filler pad, it appears that if the electrical current values are the ones of the worst thermal load situation, the temperature trend during the burst phase worsens, obtaining temperatures that are too close to the operating limits of the devices, and therefore not safe considering the uncertainty margins typical of thermal simulations. Therefore, although this specific thermal gap filler is already available and ready to be assembled and used on-board the CTP, it is necessary to

consider other models with better performances, which guarantee thermal control even in the worst operating conditions.

After a parametric analysis of the thickness and conductivity of the thermal gap filler, it has been found the best cost-effective solution is the employment of two 80×80 mm thermal gap filler pads, with a thickness of 1.5 mm, and a thermal conductivity of 1.6 W / mK .

6.3 Results and discussion

By implementing the solution with thermal gap filler pad just described, the following results are obtained.

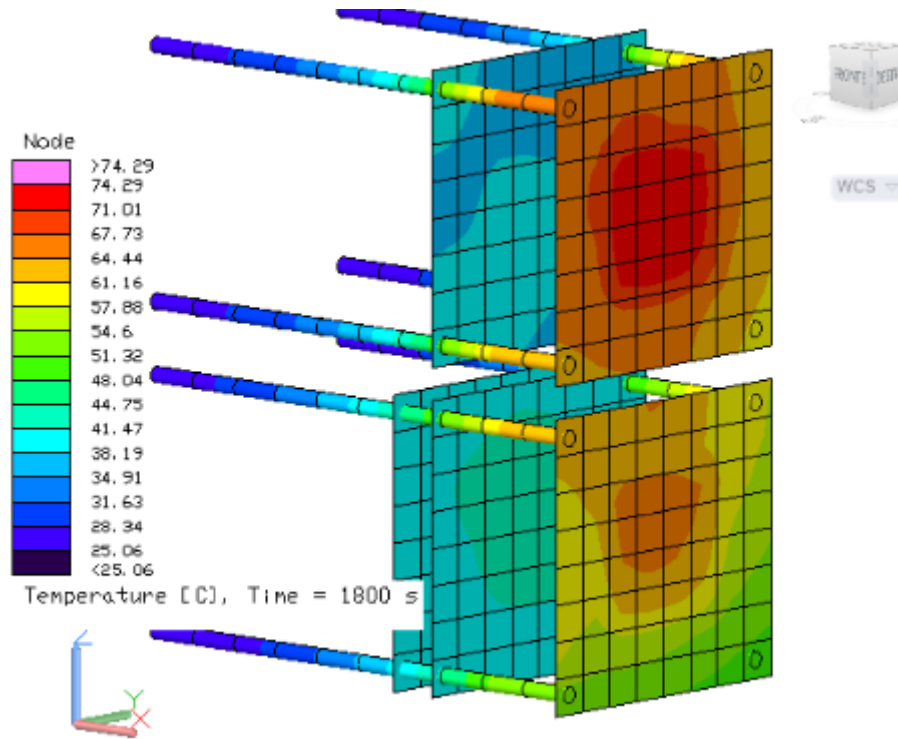


Figure 63: worst case scenario with 80x80mm, 1.5mm, 1.6W/mK gap filler

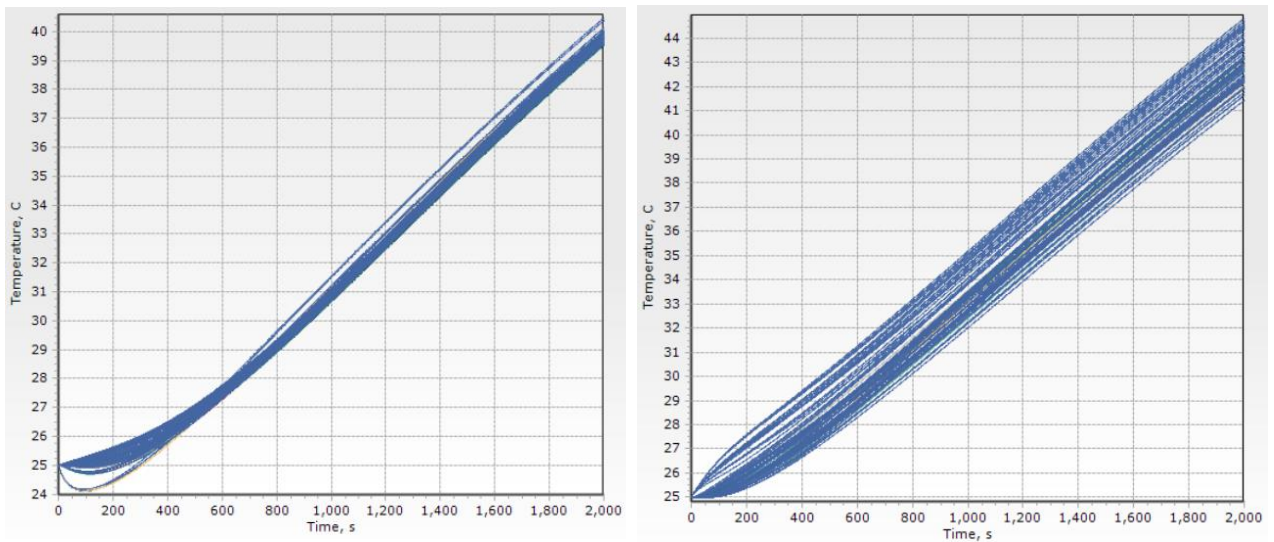


Figure 64: Data Logger and Command and Data Handling boards temperature trends

It appears that this solution, even in the worst thermal scenario due to the high thermal power dissipated by the electrical devices, guarantees adequate thermal control, and allows temperatures to be kept within the operative ranges defined by the system requirements.

Although other solutions analysed made it possible to comply with the thermal requirements of the different components of the CTP, such as the solution characterized by two FR4 / aluminium double-layer power boards directly in contact with the structure, the use of the gap filler system is more advantageous from several points of view.

As far as the cost of the system is concerned, the solution with double-layer electronic boards requires higher development and production costs than using entirely FR4 boards. Furthermore, development times are also reduced by using single-layer electronic boards. The use of thermal gap filler systems does not involve particular increases in cost and raise of project development times, since, even if thermal pads with the characteristics described above are purchased, instead of using those already available, the cost of this solution is relatively low compared to those of the other devices on board the CTP.

From the point of view of the performance of the thermal control system, using only FR4 boards, it is possible to mount the electronic components on both sides of the boards. Therefore, this allows assembling on the + X side (towards the structure) of the boards the most dissipative components (HUB and DCDC step-up) reducing the radiation of heat towards the DL and CDH boards, and directly taking the excess heat through the gap filler.

The solution implemented in the thermal model involves the application of two thermal gap filler pads with dimensions of $80 \times 80 \text{ mm}$. The two electronic boards on which they are applied have an area of $96 \times 90 \text{ mm}$. Therefore, the thermal pad remains in contact with the central portion of the board area, leaving the ends uncovered. In this way, it is possible to fix, with the necessary screw systems, the four corners of the boards to the +X face of the structure, connected in the middle by the gap filler pad. The strong and sudden variations in temperature lead to variations in the thickness and deformation of the gap filler. This phenomenon could lead to a partial or total lack of contact with the relative electronic board and the CubeSat structure in particular operating conditions of the CTP. If the contact area is reduced, the excess heat is dissipated in a reduced way, generating dangerous overheating of the critical components of the electronic board.

To reduce the risk of unexpected deformations of the thermal gap filler pad, and to avoid imperfect contacts between the heat source (electronic board), the heat carrier medium (gap filler), and the heat sink (structure), it was also analysed the solution that

involves the use of an aluminium plate that guarantees the contact between the various elements of the system listed. The aluminium plate would be built with the additive manufacturing technique, so as to be shaped according to the geometry of the surface of the electronic board and its components. Therefore, it would have the function of guaranteeing contact between the electronic board and the gap filler on one side, while on the other hand, it would ensure contact with the structural panel through a smooth face fixed by screws to the structure. The area of these conductive aluminium plates would be equal to those of the two electronic boards to which they would be applied, while the thickness would be 2 mm.

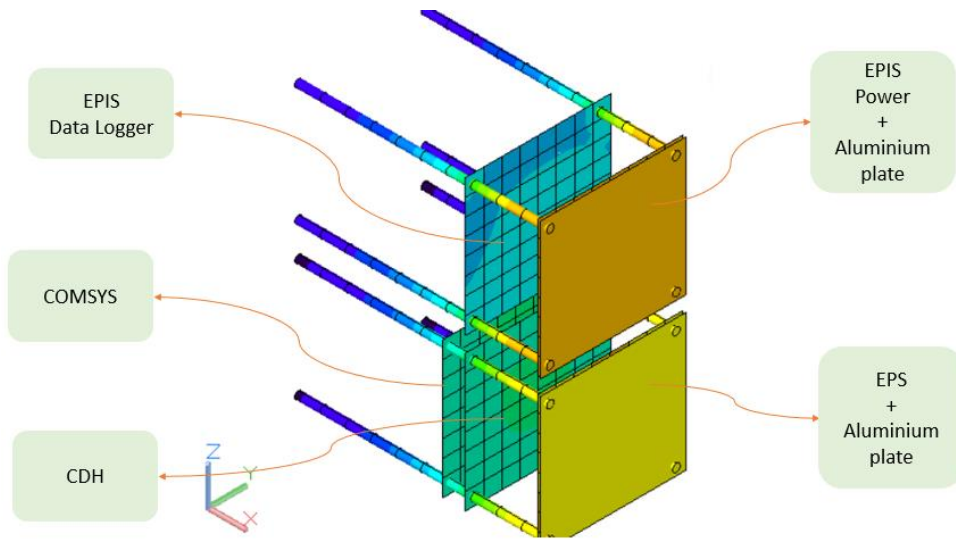


Figure 65: Avionics module configuration with Aluminium plate implementation

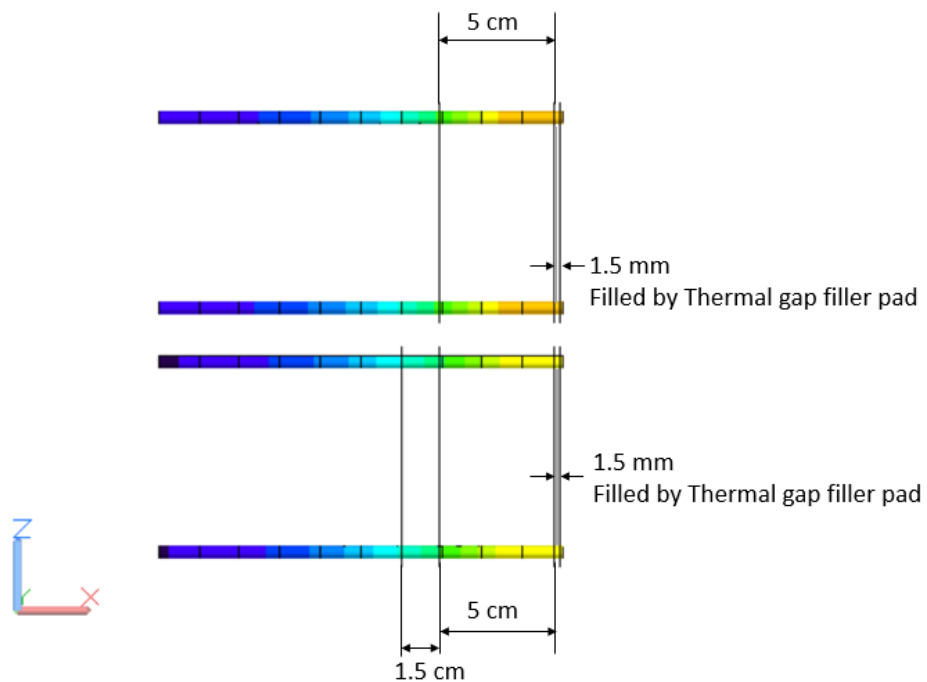


Figure 66: avionics module - boards distances

7. CONCLUSION

The significant reduction in cost and development times of the CubeSat platforms compared to more traditional spacecraft, are the main reasons that today are leading to increasingly wider use of these small systems, and that in the future will make them protagonists or in support some of the most significant space missions.

This ambitious path started almost twenty years ago with the first 1U systems, would not be possible without a continuous research process aimed at making this category of nanosatellites capable of fulfilling tasks often considered unachievable. The study for the miniaturization of technologies already in use in conventional space systems, or the invention of new ones, is the engine that pushes the advent of CubeSats day by day, capturing the interest of public agencies and private companies.

The thesis work presented in this document is placed in this research area for the integration of miniaturized technologies: the use of electric micro-propulsion system onboard CubeSat.

Using information on the CubeSats state of the art as a starting point, and more specifically considering the SoA of thermal control systems for small satellites and electric thrusters dedicated to being employed on these platforms, the research focused on how to make the design of a thermal control system effective from a performance, economic and time point of view.

The main stages of this work were:

- the refinement of a CubeSat 6U thermal model of a platform in an advanced design phase, and the relative validation of the thermal results of the model through a test campaign conducted in a thermal environment relevant to the study of the interaction between the ePS and the host spacecraft.
- The definition, starting from the data collected experimentally through the previous model, of a new thermal model for a CubeSat 12U test platform.
- The use of the above model for the parametric analysis suitable for the study of possible alternative architectures of the thermal control system necessary for the protection of the on-board subsystems of the platform.
- Finally, following trade-off analysis and cost-benefit evaluation, the definition of the TCS to be used for the management of the on-board thermal environment.

One of the most relevant results deriving from the various analyses performed, and was also confirmed by the test campaign carried out in the laboratories of the

Polytechnic of Turin, in that of the T4i company and the University of Padua, and the EPL of ESA -ESTEC, is that the thermal impact deriving from the implementation of an ePS on a CubeSat platform is very troublesome, it must be addressed with extreme importance, but nevertheless, it is not unsustainable.

The end of this thesis work does not coincide with the end of the ESA-uProp project, but on the contrary, after a preliminary design phase and subsequently a detailed one, the project is preparing to enter the phases of greatest interest for the study of interaction between the CTP and the ePS. The test plan of the third version of the platform, taking up the structure and the stages of the one developed for the second version of the CTP, will allow verifying the project requirements defined so far by carrying out tests in the respective environments depending on the considered stage of verification. More specifically, the work done on the TCS and the respective thermal model described in this thesis will be carried out in the coming months. After an initial evaluation of the performance of the TCS through tests performed in the laboratory of the Politecnico di Torino, the integration of the complete CTP with the ePS will allow the tests to be carried out in vacuum chambers. The data obtained from these tests will be necessary for the validation of the thermal model and its improvement. Later this analysis tool will be used for detailed perform test and mission predictions.

8. REFERENCIAS

- [1] Stesina F. Validation of a Test Platform to Qualify Miniaturized Electric Propulsion Systems. *Aerospace*. 2019; 6(9):99.
- [2] Walker R. et al. Deep-space CubeSats: thinking inside the box. *Astron. Geophys.*, vol. 59
- [3] Zanola S. ASSESSMENT OF THE IMPACT OF MINIATURIZED ELECTRIC PROPULSION SYSTEMS ON SMALL SATELLITES TECHNOLOGY. Politecnico di Torino, 2019.
- [4] Corpino S. et al. Thermal design and analysis of a nanosatellite in low earth orbit. *Acta Astronautica*, vol. 115, n. 13.
- [5] Larson W. J., and Wertz J. R. Space Mission Analysis and Design. Space Technology Library, 1991.
- [6] Meseguer J., Pérez-Grasa I., Sanz-Andrés A, and Alonso G. Spacecraft Thermal Control. Elsevier Science & Technology, 2012.
- [7] Small Spacecraft State of the Art Report 2015. NASA Technical Memorandum.
- [8] Marraffa G. THERMAL ANALYSIS OF CUBESAT. Politecnico di Torino, 2019.
- [9] Langer M. et al. Thermal control of High-Power Application on CubeSats. IAC 2018.
- [10] ECSS-E-HB-31-03A "Thermal analysis handbook". 15 November 2016.
- [11] Gilmore David G. Spacecraft Thermal Control Handbook, Vol. 1, Aerospace Press, 2002.
- [12] Ring S. G., Johnson D., Cullimore B. A., SINDA/FLUINT User's Manual, C&R Technologies, Inc., 2015.
- [13] Manente M., Trezzolani F., Magarotto M., Fantino E., Selmo A., Bellomo N., Toson E., Pavarin D., REGULUS: A propulsion platform to boost small satellite missions, *Acta Astronautica*, Volume 157, 2019, p. 241-249.
- [14] ECSS-E-ST-31C "Thermal control general requirements". 15 November 2008.